NTNU – Trondheim
Norwegian University of
Science and Technology

Octabuoy Concept and Spar Buoys: Non Linear Effects and Analysis

Line J.C. Haakenaasen Dahl

Marine Technology
Submission date: June 2012
Supervisor: Marilena Greco, IMT

Norwegian University of Science and Technology
Department of Marine Technology

NTNU Trondheim
Norwegian University of Science and Technology
Faculty of Engineering Science and Technology
Department of MarineTechnology

MASTER THESIS IN MARINE TECHNOLOGY

SPRING 2012

FOR

Line J.C.H. Dahl

Octabuoy concept and Spar Buoys: non linear effects and analysis

(Octabuoy konseptet og Sparbøyer: ikke-lineære effekter og analyse)

The Octabuoy is a semisubmersible drilling and production platform specially shaped to improve the behavior in harsh conditions, as in North Sea, relative to to other deep draught floaters (semis and spars). The design consists of an octagonal ring pontoon supporting four columns, with limited waterplane area, and the topside facility. A set of risers is used for pumping the oil and a mooring system takes care of the configuration and horizontal motion control. This concept represents an alternative floating production system to spars, tension leg platforms and traditional semisubmersibles, especially for deep and ultra-deep water oil explorations. The dynamic response of the platform depends on its coupling with the risers and mooring lines. The latter is expected to be increasingly significant going toward deeper waters. The platform should be able to withstand the nonlinear-wave loads in extreme sea conditions and the viscous effects due to interaction with current, wind and waves. In this framework it is crucial to identify prediction tools able to handle the relevant phenomena and to provide reliable predictions in feasible time. This is especially true when dealing with statistical analyses.

Objective

The aim of the thesis is to improve the knowledge about the Octabuoy concept with focus on quantifying the relevance of nonlinear-wave loads and viscous effects in operational conditions. Existing simulation tools based on potential-flow theory and real viscous-flow conditions will be examined and applied in a comparative and combined way to estimate the loads. Existing experimental studies on Spar Buoys will be used to assess the developed solution strategy for the loads prediction.

The work should be carried out in steps as follows:

1. Give an overview of previous work, with main focus on state-of-the-art solvers used to estimate the nonlinear effects. Topics that have been discussed in the project thesis need not to be repeated in the master thesis report unless found useful for the discussion.
2. Compare different alternative methods for the estimate of the loads and identify a suitable numerical-solution strategy able to estimate nonlinear effects for a deep floating platform as an Octabuoy or a Spar Buoy and then to analyse its response.
3. Use existing experiments on Spar Buoys to assess the use of the identified solution strategy in terms loads/motions. Examine the numerical convergence and accuracy of the involved solvers.
4. Apply the solution strategy to the Octabuoy concept using also what has been learnt from the project thesis and examine the relative importance of nonlinear effects on the response.

The work may show to be more extensive than anticipated. Some topics may therefore be left out after discussion with the supervisor without any negative influence on the grading.

The candidate should in her report give a personal contribution to the solution of the problem formulated in this text. All assumptions and conclusions must be supported by mathematical models and/or references to physical effects in a logical manner.

The candidate should apply all available sources to find relevant literature and information on the actual problem.

The thesis should be organised in a rational manner to give a clear presentation of the work in terms of exposition of results, assessments, and conclusions. It is important that the text is well written and that tables and figures are used to support the verbal presentation. The thesis should be complete, but still as short as possible. In particular, the text should be brief and to the point, with a clear language. Telegraphic language should be avoided.

The thesis must contain the following elements: the text defining the scope (i.e. this text), preface (outlining project-work steps and acknowledgements), abstract (providing the summary), table of contents, main body of thesis, conclusions with recommendations for further work, list of symbols and acronyms, references and (optional) appendices. All figures, tables and equations shall be numerated.

The supervisor may require that the candidate, in an early stage of the work, present a written plan for the completion of the work. The plan should include budget for the use of computer and laboratory resources that will be charged to the department. Overruns shall be reported to the supervisor.

From the thesis it should be possible to identify the work carried out by the candidate and what has been found in the available literature. It is important to give references to the original source for theories and experimental results.

The thesis shall be submitted in two copies:
- The copies must be signed by the candidate.
- This text, defining the scope, must be included.
- The report must appear in a bound volume or a binder.
- Drawings and/or computer prints that cannot be included in the main volume should be organised in a separate folder.
- The bound volume shall be accompanied by a CD or DVD containing the written thesis in World or PDF format. In case computer programs have been made as part of the thesis work, the source codes shall be included. In case of experimental work, the experimental results shall be included in a suitable electronic format.

Supervisor :Marilena Greco
Submitted :16 January 2012
Deadline :15 June 2012

Marilena Greco
Supervisor

Summary

The age of the easy accessible hydrocarbon goes towards the end and new more challenging fields is the future of the oil industry. This is often synonymous with large depths where sea bed mounted platforms are highly uneconomical options. Floating platforms are therefore commonly chosen solutions.

In this thesis two types of deep floating platforms are investigated; The spar buoy, a well known, well documented concept and the Octabuoy, a newly developed concept. Both platforms are analysed in two DNV programs, Wasim and Waqum. Wasim is a non linear time domain hydrodynamic program and Waqum is an impulse response function operator with the possibility of adding non linear effects. The spar bouy concept is used as a pilot test in the softwares. A recreation of the experimental results from H.A. Haslum's doctoral thesis from 2000 is attempted. The impact of non linear effects and mooring on both platforms is discussed. The subject of viscous damping is also approached.

As has previously been confirmed by many researchers, the spar buoy is susceptible to non linear effects. The triggering of the Mathieu effect is shown in the Wasim analyses. Discussion is also made as to whether the spar might also be susceptible to large excitations due to second order difference frequency interactions between surface waves and body motions. Both these effects happen at low frequencies where radiation damping is low. Viscous damping is therefore of importance. From previous research mooring is found to be important to avoid the Mathieu effect by increasing the damping and moving pitch periods out of the danger zones.

After analysing the spar buoy, the Octabuoy's motion characteristics are tested in mild to severe sea states in both softwares. Non linear effects are found to be significant in the vertical rotational degrees of freedom. The heave motion however seems relatively unaffected by non linear effects. Since Wasim models the free surface linearly, what makes the pitch/roll motion affected by non linearities is found to be either non linear hydro statics or non linear Froude-Krylov forces. The Octabuoy is designed to avoid the variation on hydrostatic stiffness. However, the deadrise angle is 10 degrees larger than the ideal angle. Whether this is what leads to non linear pitch/roll motion is not known at this stage.

Two softwares are used in the thesis. Wasim has very long CPU time but calculates accurately and detailed information is easily accessed with for instance the Wasim application ForceInspector. Waqum is very quick, with CPU time in the order of minutes. The program requires an experienced user who knows what must be included for a complete analysis. There are uncertainties about the results from Waqum analysis and more verification is needed for the author to feel confident about the software.

To conclude, the programs might work well together. Much can be tested quickly in Waqum, and then final configurations can be run more thoroughly in Wasim. It is the experience of the author that at least until the new version of HydroD is finished, running time domain analysis in Wasim should be done through scripting. This gives a larger control over the actual input and might decrease the chance for error.

Keywords: Octabuoy, Spar Buoy, Non Linear Effects, Mooring, Wasim, Waqum.

Sammendrag

Tiden med enkelt tilgjengelig hydrokarbon går mot slutten og nye, mer utfordrende felt, er framtiden for oljeindustrien. Dette er ofte synonymt med store dybder der plattformer montert havbunnen er svært uøkonomisk alternativer. Flytende plattformer er derfor ofte valgte løsninger

I denne avhandlingen blir to typer dyptflytende plattformer undersøkt; Sparbøyen, et velkjent og godt dokumentert konsept og Octabuoy, et nyutviklet konsept. Begge plattformene er analysert i to DNV programmer, Wasim og Waqum. Wasim er et ikkelineært hydrodynamisk tidsdomene program og Waqum er en impulsrespons funksjons operator med mulighet for å legge til ikkelineære effekter. Sparbøye konseptet blir brukt som pilottest av programvarene. Forsøk på å gjenskape de numeriske og eksperimentelle resultatene fra H.A. Haslum doktoravhandling fra 2000 er blitt gjennomført. Effekten av ikkelineære effekter og forankring på begge plattformene er undersøkt. Effekten av viskøs demping er også diskutert.

Som tidligere bekreftet av mange forskere, er Sparbøyen påvirket av ikkelineære-effekter. Trigging av Mathieu effekten er vist gjennom analyse i Wasim. Det blir også diskutert hvorvidt sparbøyer kan stå i fare for store eksitasjoner grunnet andre ordens differanse frekvens interaksjoner mellom overflatebølger og platformens bevegelser. Begge disse effektene vil skje ved lave frekvenser der bølgedannelses dempningen er lav. Viskœs dempning er derfor av betydning. Fra tidligere forskning er det blitt bekreftet at ankerliner er viktig for å unngå Mathieu effekten. Ankerlinene øker dempingen og kan flytte stampperioden ut av faresonene.

Etter å ha analysert Sparbøyen ble Octabuoy testet i milde til alvorlige sjøtilstander i begge programmene. Resultatene indikerer at ikkelineære effekter er signifikante i de vertikale rotasjonsfrihetsgradene. Hivbevegelsen virker imidlertid relativt upåvirket. Da Wasim modellerer den frie overflaten lineært må den ikkelineære rull/stamp bevegelsen skyldes ikkelineær hydrostatikk eller ikkelineær radiasjon/diffraksjon. Octabuoyen er utformet for å unngå variasjon i den hydrostatiske stivheten. Imidlertid er deadrisevinkelen 10 grader større enn den ideelle vinkelen. Hvorvidt det er dette som fører til den ikkelineære rull/stamp bevegelse er ikke kjent.

To programmer er brukt i oppgaven. Wasim har svært lang CPU tid, men beregner nøyaktig og gir detaljert informasjon. Waqum opererer veldig rask, med en CPU-tid i en størrelsesorden påminutter. Programmet krever en erfaren bruker som vet hva som må inkluderes for en fullstendig analyse. Det er usikkerhet rundt resultatene fra Waqum analysene og mer verifikasjon er nødvendig for forfatteren å føle seg trygg på programvaren.

For å konkludere kan programmene fungerer godt sammen. Mye kan testes raskt i Waqum, og deretter kan endelig konfigurasjon kjøres mer grundig i Wasim. Det er forfatterens oppfattning at i alle fall inntil den nye versjonen av HydroD er ferdig, bør tidsdomene analyser i Wasim kjøres via script. Dette gir større kontroll over den faktiske innputen og kan redusere sjansen for feil.

Nøkkelord: Octabuoy, Sparbøye, Ikkelineære-effekter, Ankerliner, Wasim, Waqum.

Preface

This report constitutes the mandatory master thesis which is part of the masters degree program at Department of Marine Technology, Norwegian University of Science and Technology. The thesis represents the total work of one semester and builds on the work done in the project thesis from fall 2011.

My supervisor has been Professor Marilena Greco at Department of Marine Technology, Norwegian University of Science and Technology. I would like to thank her for all her help and encouragement throughout both project and master thesis. Despite geographical challenges she has been committed and interested in the entire duration of the work. Most of the work has been preformed at DNV Høvik where I have received much help and support from the entire Maritime Advisory Ship Hydrodynamics and Stability section. I would especially like to thank Håvard Nordtveit Austefjord, Tormod Landet, Olav Rognebakke and Jens Bloch Helmers for invaluable help and patience. Finally I would like to thank Moss Maritime AS for the opportunity to work with their exciting and interesting new platform concept.

.....
Line J.C. Haakenaasen Dahl

Contents

List of Figures

List of Tables

Nomenclature

Symbols used in the text are listed below. The symbols are sorted in the order of appearance.

∇_s	Submerged volume
$\overline{GM}$	Metacentric height
KB	Distance from keel to centre of buoyancy
KG	Distance from keel to centre of gravity
BM	Distance from centre of buoyancy to meta centre
η_i	Displacement in degree of freedom i
ρ	Density of salt water $\rho = 1025 \frac{kg}{m^3}$
g	Acceleration of gravity. $g = 9.81 \frac{m}{s^2}$
S_{11}	Second moment of the water plane area
z_B	Vertical centre of buoyancy
z_G	Vertical centre of gravity
C_{ii}	Restoring coefficient in degree of freedom ii
I_{ii}	Moment of inertia in degree of freedom ii
A_{ii}	Added mass coefficient in degree of freedom ii
B_{ii}	Damping coefficient in degree of freedom ii
ω	Wave circular frequency
$\omega_{n,i}$	Natural frequency in degree of freedom i
T	Wave period
$T_{n,i}$	Natural period in degree of freedom i
Φ	Velocity potential
ζ	Wave elevation
∇	Differential operator
p	Pressure
H_s	Significant wave height
T_p	Peak period
CPU-time	Time used by computer for processing instructions
COG	Center of gravity
GUI	Graphical User Interface
FFT	Fast Fourier Transform
RAO	Response Amplitude Operator
MPL	Most Probable Largest value
DNV	Det Norske Veritas

Chapter 1

Introduction

As the offshore industry depletes hydrocarbon reservoirs below the sea bed at small to moderate depths, it becomes a requirement to seek deeper waters for less accessible oil reservoirs. These are new conditions which often includes harsher weather conditions and complicated mooring configurations. With the increased water depth, sea bed mounted platforms become highly uneconomical. This leaves various types of floating platforms as the only viable option. To cope with the increasing depth and different weather conditions, innovation and development of new concepts is needed with regards to the floating platforms. The hydrodynamic interaction between these platforms with ocean waves, including the understanding and quantifying of the non linear components of the hydrodynamic loads, remains a continuous process.

A new floating platform concept, the Octabuoy, was investigated in the project work from fall 2011. Not much literature exists with regards to the concept. It was a desire to investigate it further as to how it is best analysed, how important non linear effects were and also more generally to look into non linear analysis. Since there is so little data concerning the Octabuoy platform, the spar buoy concept will work as a test of the solution scheme. Spar buoys will therefore be thoroughly explained to justify the comparison. Then a simple spar buoy will be analysed in two softwares, Waqum and Wasim and the results will be compared with the experimental data. Finally the Octabuoy will be analysed in the same softwares and the results discussed.

The objective of this study includes: (1)To give an overview over relevant previous work and theory;(2) compare alternative methods to estimate non linear and viscous loads;(3) assess the softwares by analysis of the well known spar buoy concept and comparing results with existing experimental data; (4) apply the softwares to the Octabuoy platform and assess the importance of non linear effects.

Chapter 2

Project

This master thesis continues the work which was started in the project thesis work preformed during the fall semester 2011. The project thesis consisted of two parts. The first was a literature study of an Octabuoy platform and its particularities compared to other competing platforms and then an introduction to softwares used in the second part. The second part consisted of a case study of the platform where it was analysed in the DNV software Wasim. Parts of the literature study which is considered relevant for this thesis will be repeated.

The analyses from the project work had errors and the thesis concluded that new analyses were needed in order to identify the errors. As Wasim would be extensively used in this master thesis a natural starting point became to understand the errors of the project thesis.

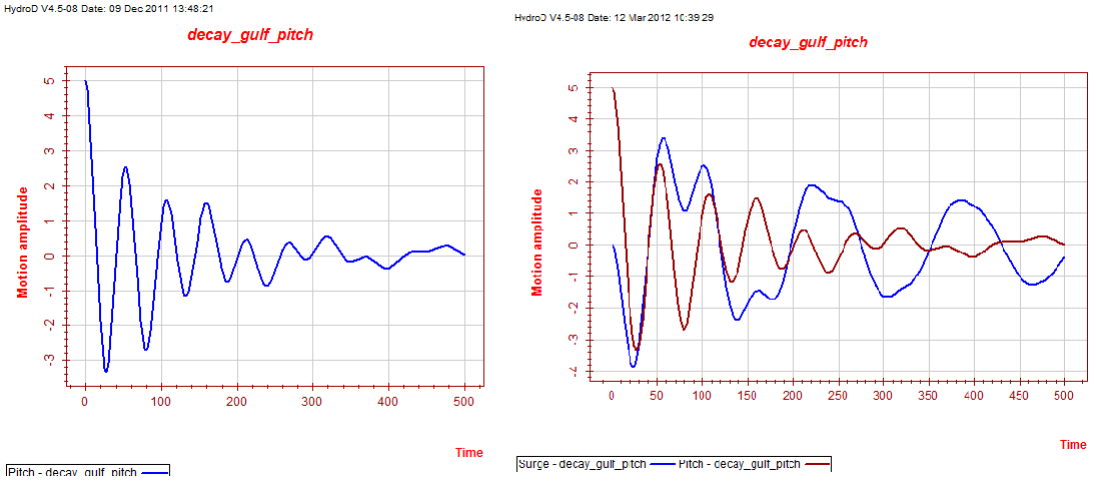

Figure 2.1: Pitch decay with additional stiffness matrix shown alone and together with the surge decay.

In the project thesis it was concluded that some of the decay tests appeared to be incorrect. The pitch and roll decay did not decay as the other degrees of freedom. Further inquiry has led to an acceptance of the decay and they are no longer considered to be incorrect. It is now believed that the reason for the irregular decays are coupling effects between surge/pitch and sway/roll.

This effect disappears when one removes the additional stiffness matrix so that the horizontal degrees of freedom have no added stiffness [1]. In figure 2.1 the pitch decay is shown together with the surge decay from the pitch decay test preformed in Wasim. The figures indicate that the reason for the irregular pitch decay is the coupling with the surge motion.

One of the more important problems with the project thesis were the results from the irregular spectrum tests. In these analyses the input spectra waves were defined with a spreading function and not as a long crested waves. The exponent in of the spreading function was 8 and it was assumed that this resulted in waves that were close to being long crested. The test results showed large motions perpendicular to the main heading of the waves (180° head sea). The same settings and the same spreading had been used for analysis in Orcaflex without giving the same perpendicular motion. Speculations were that perhaps the model contained some imbalance leading to large excitations perpendicular to the main motion due to only small perturbations. However the model is completely symmetric; the same stiffness was applied to surge/sway and roll/pitch and the mass model was symmetrical.

Regular wave tests were preformed to check whether the error reoccurred in simpler analyses. Two regular wave tests were carried out in head sea and two in beam sea. In each heading one analysis was run with additional stiffness matrix and one without. The regular wave tests did not show the same motion tendencies perpendicular to the wave direction as the irregular wave spectrum tests. Only small perturbations of an order of magnitude 10^{-4} was observed along the perpendicular axis. This means that the phenomena observed in the project, with motion perpendicular to the incoming waves did not occur with regular waves, with or without additional stiffness. It was therefore concluded that the additional stiffness matrix was not the cause of the motion.

New irregular wave spectrum analyses were preformed, with and with out the use of the spreading function.

Analysis number	head sea	beam sea	spreading function	long crested sea state
1	X	-	X	-
2	X	-	-	X
3	-	X	X	-
4	-	X	-	X

Table 2.1: Irregular wave spectrum analyses preformed in error search.

The long crested head sea wave test showed only small motion along the x-axis which coincided with results from Orcaflex and model trials. The same applied for the beam sea analyses. The results in beam and head sea gave the same results; short crested waves resulted in large motions perpendicular to the main wave propagation direction. Long crested waves gave only small perturbations in the perpendicular direction.

One of the spreading function analyses was rerun linearly which decreased the perpendicular motion significantly. This is interpreted as yet another confirmation of the errors from the short crested sea analyses. It was suspected that the number of wave components was affecting the results as it is known that a higher amount of wave components is often needed for a spectrum with spreading than the long crested spectrum to obtain accurate results. The errors surrounding the Wasim irregular spectrum will be further discussed in section 8.2

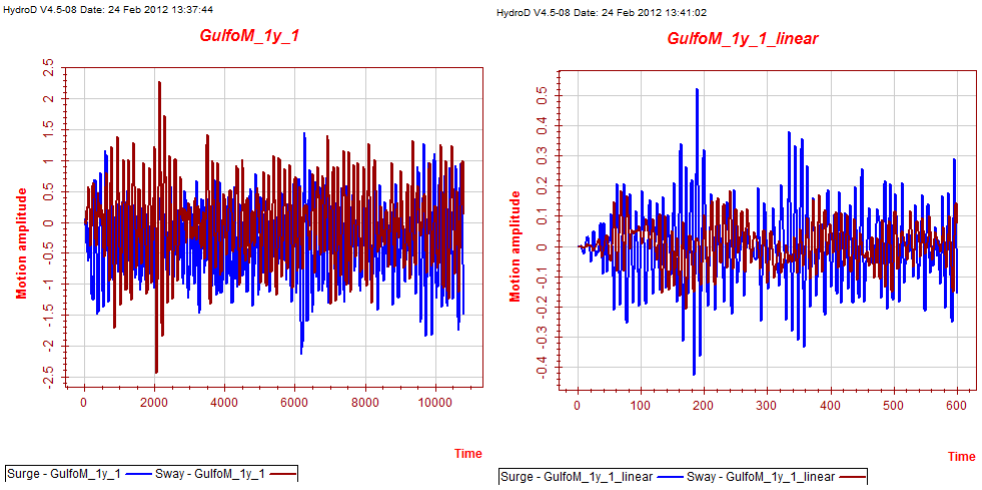

Figure 2.2: Surge and sway motions in head sea with spreading function. Left image shows the non linear run while the right is the linear.

2.1 Numerical inaccuracies

Another problem faced in the project work was that the restoring in pitch and roll were different even though the model was symmetrical and the input additional critical damping and restoring equal in the two degrees of freedom. This was discussed with Torgeir Vada from DNV Software and it turned out that the difference was due to a numerical inaccuracy in Wasim for the calculation of the metacentric height in roll.

Wasim calculates a 25 cm difference in the metacentric heights of pitch and roll, while Wadam only finds the difference to be 2.5 cm in the same panel model. It seems that it is primarily the roll which is incorrect as pitch has approximately the same value in Wadam and Wasim, and it seems to be an inaccuracy in Wasim and not in the model. The error corresponds to approximately 5% of the error in the calculation of the water plane moment of inertia. The error will be corrected.

Chapter 3

Theoretical Background

3.1 The Platform Concepts

The hydrodynamical analysis of two different platform concepts is the main focus of this master thesis. The spar buoy and the Octabuoy concept are both developed with similar purposes and can be viewed as competing concepts. They therefore have to deal with similar challenges and problems. Here follows a brief introduction explaining the two concepts. Parts of the explanation is also given in the project thesis.

3.1.1 The Spar Buoy

In the mid nineties a new type of floating platform became increasingly popular in the deep waters of the Gulf of Mexico area. This was the spar buoy concept and the first production spar buoy in the world was installed in 1997 at Viosca Knoll 826, Gulf of Mexico [4].

A typical spar buoy is shaped like a long cylinder. The cross-section is usually constant and the platform floats vertically. Spar platforms have large drafts, commonly in the order of 200 m. This is to minimize the vertical excitation which allows for the installation of rigid riser and dry well heads. There are many advantages with a spar; structural simplicity, low motions in moderate and extreme ocean waves because of their relatively long natural periods, good protection of riser connections to the sea bed, low cost and so on [4]. The combination of large drafts and small water plane areas gives the platform concept large natural periods away from the energetic wave period. Avoiding the first order vertical excitation is thus one of the most basic features of the spar design. However, this has the consequence that the 2^{nd} order effects becomes an important contribution to the total response. This can become especially critical since the platform concept has a very low level of damping.

Several experimental studies and numerical simulations have been preformed to obtain a better understanding of the response of spar buoys to ocean waves, wind and current. Research using numerical simulations has utilized both frequency domain and time domain approaches. Some of the frequency research may however be subject to errors due to linearisation of non linear terms. A linear wave frequency analysis does not capture all desired features of the spar motion [4].

From a physical aspect a linear damping assumption is for instance not a good approximation when large response amplitudes occur. Viscous drag effects dominate the damping at large responses and consequently the damping is quadratic. Spar buoys are therefore in many cases preferably analysed in the time domain. In cases where the damping is very low, like with the spar buoy, transient effects are important. In order to get reliable extreme values, long time series and sophisticated statistical methods are needed [5].

Early spar buoys were designed to withstand the sea state with the statistically largest significant wave height. This issue was discussed by Haslum and Faltinsen [6]. Their spectral analysis showed that there were large heave motions for sea states with periods longer than the period at the largest significant wave height. This showed how more thorough analyses at longer periods were needed in order to ensure safety of the spar buoys.

Spar buoys usually connect with the sea bottom through risers fastened to the platform through a moonpool. The moonpool affects the motions, but including it may be challenging. Drag effects on the exterior hull and drag effects from internal structures in the moonpool can be calculated by Morison drag elements. Interpreting a time series of the response may be troublesome. In DNVs Recommended Practice C205 it is stated that neglecting viscous damping in the moonpool will result in unrealistic large motions and free surface elevation in the moonpool close to resonance [7].

3.1.2 The Octabuoy

The Octabuoy platform is a concept designed by Moss Maritime as. It is a deep draft semi-submersible consisting of four columns with conical shape in the free surface zone. The design principles behind deep draft floaters is to reduce the 1^{st} order heave excitation, which allows for rigid risers and dry well heads. To ensure natural periods in heave, pitch and roll which are far from the range of the first order wave frequency excitation, the Octabuoy has a small water plane area and a large draft. The platform is kept in position by means of catenary mooring lines. These have small effect on the first order excitation, but have an important effect on the 2^{nd} order slow drift motions in horizontal direction [2].

The columns have a conical shape in the free surface zone to avoid a time varying pitch and roll restoring stiffness which can lead to the parametric motion effects discussed below. The Octabuoy has its name from the square shaped octagonal pontoon at the bottom of the structure. These contribute to the viscous damping.

With its deep draft, large columns and pontoons the Octabuoy also has a large storage capacity. The large underwater structure makes the platform sensitive to current, but wind force is also important. From model trials in the Ocean Basin at Marintek in Trondheim it has been found that helical strakes must be installed on parts of the columns to avoid vortex induced vibration [3].

Figure 3.1: Visualisation of the Octabuoy platform.

At the time this master thesis is written, the first Octabuoy is under construction. It is planned that the platform will be operating in at least two different fields during its life expectancy. Approximately 10 years in the North Sea at the Cheviot field before it is towed to the Gulf of Mexico. These two locations are quite different both in depth (150m and 1500m respectively) and weather condition, which is discussed further in the project thesis and is not of relevance in this thesis.

3.2 Hydrodynamic effects

Some non linear effects a deep floating platform might be subjected to will be looked into in the analyses of this thesis. These non linear effects will be explained in detail in the following section. In the project work the Mathieu effect was investigated. The analysis preformed in this thesis intended to trigger this effect on a simple spar buoy in two different softwares. Below follows an extended version of the study done on the phenomenon during the project work.

3.2.1 The Mathieu Effect and Spar Buoys

Parametric resonance is a phenomenon which may occur when a parameter in a mechanical system varies over time. The effect differs from forcing since the action appears as a time varying modification on a system parameter. It is different from ordinary resonance as it exhibits instability. Parametric resonance can affect ships and offshore structures which can lead to disasters at sea. A parametric instability concerning a coupling between heave and pitch/roll is known as the Mathieu effect. The effect is triggered by an oscillation hydrostatic stiffness in the vertical modes. It is possible to minimize the amplitude of the oscillating stiffness by varying the cross-sectional area in the free surface zone [8]. The main sources for the explanation of the

Mathieu effect on spar buoys and on the Octabuoy are sources [2] and [6] and can be assumed source when no other source is given.

The explanation of the Mathieu effect will first be done with a spar buoy as example. For this platform concept the pitch and roll motions may be considered similar and only pitch will be discussed here. The pitch restoring force in still water depends on only two parameters; the metacentric height ($\overline{GM}$) and the submerged volume (∇_s). In hydrostatic theory the metacentric height is defined as $\overline{GM} = KB+BM-KG$. If the restoring term is evaluated from the displaced position instead of the mean position both ∇_s and $\overline{GM}$ are functions of the heave motion. Pitch restoring force is defined as follows

$$C_{55} = \rho g S_{11} + \rho g \nabla_s (z_B - z_G) = \rho g \nabla_s \overline{GM} \tag{3.1}$$

$$\overline{GM} = \frac{S_{11}}{\nabla_s} + z_B - z_G \tag{3.2}$$

$$S_{11} = \int \int_y x^2 \, \mathrm{d}x\mathrm{d}y \tag{3.3}$$

Here z_B is the vertical centre of buoyancy and z_G the vertical centre of gravity. S is the waterplane area in the static condition. As the platform moves in heave, $\eta_3(t)$ the metacentric height and displaced volume changes with the vertical motion. With vertical sides the parameters change as follows

$$S_{11,new} = S_{11} \tag{3.4}$$

$$z_{B,new} = z_B + \frac{1}{2}\eta_3 \tag{3.5}$$

$$z_{G,new} = z_G + \eta_3 \tag{3.6}$$

$$\nabla_{s,new} = \nabla_s - S\eta_3 \tag{3.7}$$

These changed parameters leads to a varying restoring term in pitch

$$C_{55,new} = \rho g S_{11} + \rho g (\nabla_s - S\eta_3)(z_B - z_G - \frac{1}{2}) \tag{3.8}$$

$$= C_{55} - \frac{1}{2}\rho g [\nabla_s + 2S(z_B - z_G)]\eta_3 + \frac{1}{2}\rho g S \eta_3 \tag{3.9}$$

This equation shows the non linear coupling between the heave and pitch motion. One can also see how the pitch restoring is time dependent.

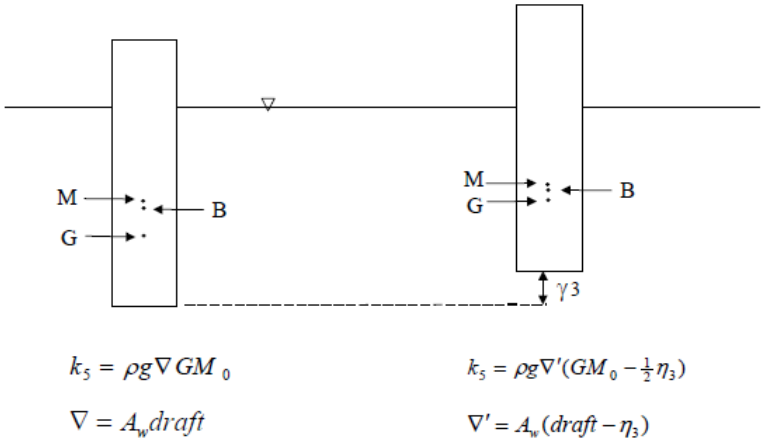

Figure 3.2: Variation in pitch restoring of regular spar at displaced positions [9].

Although pitch restoring is varying in time, this does not necessarily mean that an instability will occur. For this to happen other conditions must be fulfilled. These conditions are connected to the wave period in relation to the pitch natural period. To understand this, the Mathieu equation for a one degree of freedom system is investigated. The explanation of this can be found several places, among these in the project thesis from fall 2011. What is found by the explanation is that when the wave induced heave motion frequency ω is related to the natural period in pitch, $\omega_{n,5}$ by $\frac{\omega_{n,5}}{\omega} = \frac{n}{2\sqrt{a}}; n = 1, 2, 3, ...$ parametric excitation can occur. For small damping ratios this corresponds to wave periods given by

1. $T = \frac{1}{2}T_{n,5}$
2. $T = T_{n,5}$
3. $T = \frac{3}{2}T_{n,5}$

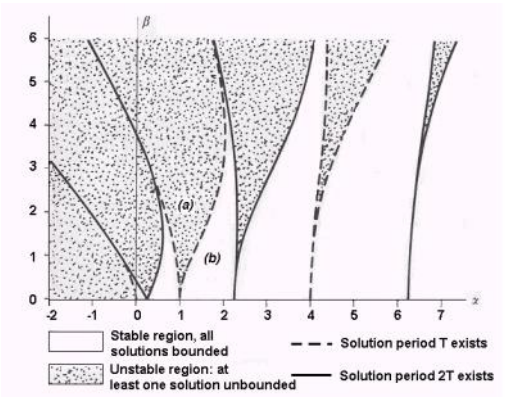

(a) Stability diagram for the Mathieu equation

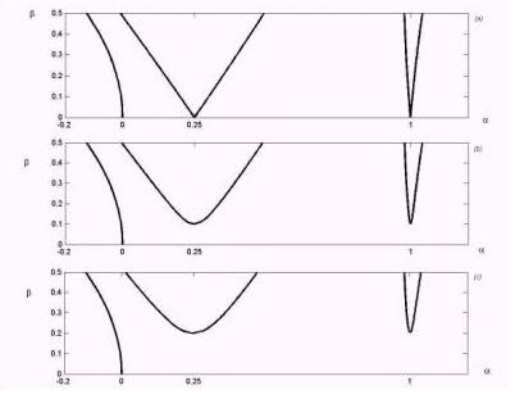

(b) Figure showing how damping makes the curves separating the the different unstable regions less pronounced.

Figure 3.3: Mathieu stability diagrams, shown with and without damping.

A system without damping, excitation and coupling between pitch and surge will give the stability digram showed in figure 3.3a. If these effects are included the diagram will change somewhat with less pronounced curves like in figure 3.3b.

The lowest period which can trigger the Mathieu effect is $T = \frac{1}{2}T_{n,5}$, which can occur if the natural period in heave is half the natural period in pitch or if there is significant wave energy at half the natural period of pitch. If this condition is fulfilled, the pitch motion would be Mathieu unstable. Spar buoys are therefore designed to have large natural periods in heave and pitch to avoid this. However, this does not mean that the Mathieu instability will not occur.

Envelope Effect

The heave motion may oscillate at two different periods, the heave natural period and the wave period. There can be several reasons for the oscillation at the natural frequency, but the important one in this case is when the second order response contains a frequency component at the natural frequency.

When the heave motion oscillates with the natural frequency and the wave frequency, this creates an envelope process due to the difference frequency between the two frequencies of oscillation.

$$\begin{aligned} \omega_{envelope} &= \Delta\omega \\ &\Downarrow \\ T_{envelope} &= \frac{1}{\frac{1}{T_{wave}} + \frac{1}{T_{N,3}}} \end{aligned} \tag{3.10}$$

If this envelope period coincides with the pitch natural period, instability can occur. The wave period for which this happens is denoted $T_{critical}$.

$$T_{envelope} = T_{n,5} \leftarrow T_{wave} = \frac{1}{\frac{1}{T_{n,5}} + \frac{1}{T_{n,3}}} \stackrel{def}{=} T_{critical} \tag{3.11}$$

In addition a non linear interaction effect between heave, pitch and surge may also occur. This effect is the vertical component of the horizontal first order total force when the platform has a pitch inclination.

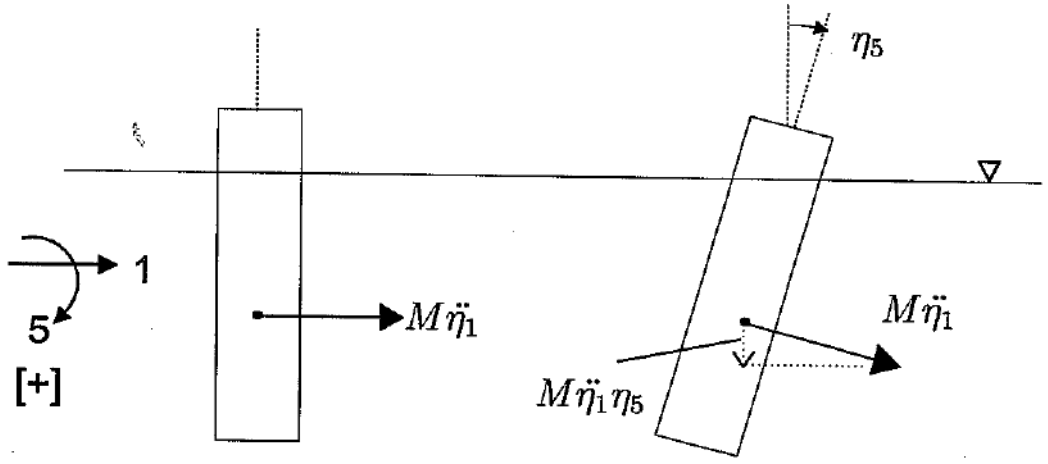

Figure 3.4: The second order heave force which occurs when pitch and surge interacts [9].

By assuming harmonic components the second order heave force may be expressed as

$$F_3^{(2)} = \omega_{wave}^2 M \eta_{1,a} \cos(\omega_{wave} t + \delta_{wave}) \eta_{5,a} \cos(\omega_{5,n} t + \delta_5) \tag{3.12}$$

This can be split into a difference frequency and a sum frequency term. It is the difference frequency which is of importance here

$$\begin{aligned} F_3^{(2)} = &\frac{1}{2}\omega_{wave}^2 \eta_{1,a} M \eta_{5,a} \cos[(\omega_{wave} - \omega_{5,n})t + \delta_{wave} - \delta_5)] \\ &+\frac{1}{2}\omega_{wave}^2 \eta_{1,a} M \eta_{5,a} \cos[(\omega_{wave} + \omega_{5,n})t + \delta_{wave} + \delta_5)] \end{aligned} \tag{3.13}$$

If the condition in equation 3.11 is fulfilled, the pitch equation will be Mathieu unstable

$$T_{wave} = T_{critical} = \frac{1}{\frac{1}{T_{5,N}} + \frac{1}{T_{3,N}}} \Leftrightarrow \omega_{wave} = 2\pi(\frac{1}{T_{5,N}} + \frac{1}{T_{3,N}}) \tag{3.14}$$

and the difference frequency in heave may be written

$$\Delta\omega = \omega_{wave} - \omega_{5,N} = 2\pi(\frac{1}{T_{5,N}} + \frac{1}{T_{3,N}}) - 2\pi(\frac{1}{T_{5,N}}) = \omega_{N,3} \tag{3.15}$$

It can thus be shown that the same wave which triggers the Mathieu instability in the pitch equation, makes the non linear heave force shown in equation 3.13 oscillate with the natural

frequency in heave. This means that there is a mutual amplification in the pitch and heave interaction.

As can be seen in the figure below, the pitch instability makes the pitch response large, which further amplifies the non linear heave term ($F_3^{(2)} = M\ddot{\eta}_1\eta_5$). This amplifies the heave motion at the natural period of heave and amplitudes increase which finally makes the pitch instability increase. This mutual amplification circle is illustrated in figure 3.5.

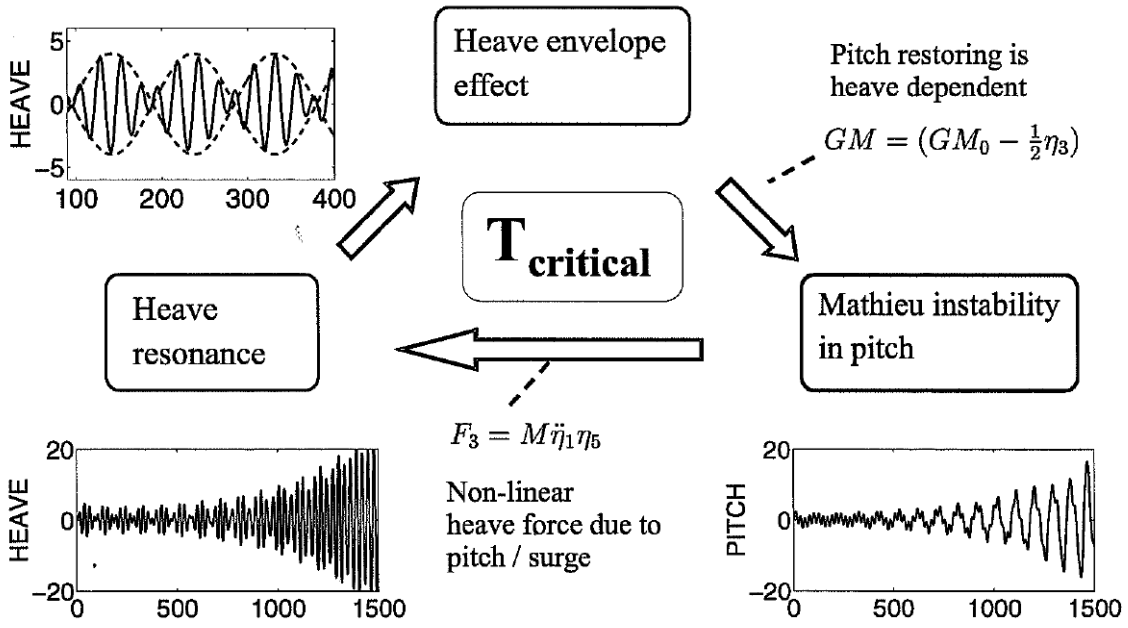

Figure 3.5: The mutual interaction between the heave, pitch and surge motion. The interaction amplifies the motion response in both degrees of freedom [9].

In order to illustrate the importance of the interaction effect between the non linear heave force and the pitch Haslum preformed simulations both with and without the non linear heave included. When the non linear heave force was neglected, the mutual interaction disappeared and both heave and pitch response were reduced considerably.

3.2.2 The Mathieu Effect and the Octabuoy

There are several ways to avoid the Mathieu effect

1. Reducing the parametric coupling
2. Avoid that the ratio between the response variables are in the critical region
3. Increase damping

Method three is complicated as it has proven difficult to provide damping that minimizes the effect sufficiently. This means for instance that even though a spar buoy platform has large

damping forces at the unstable frequencies the damping could still be too small. The Octabuoy is applying method 1, reducing the parametric coupling. This is done by shaping the platform legs such that the water plane area varies as the platform moves which leads to a GM that is almost free for variation over time.

The Octabuoy concept has a water plane area and second moment which changes together with the heave motion. This has the following consequence

$$S_{11,new} = S_{11} - S'_{11}\eta_3 \tag{3.16}$$

$$z_{B,new} = z_B + \frac{1}{2}\eta_3 - \frac{1}{3}\frac{S'_0}{S_0}\eta_3 \tag{3.17}$$

$$z_{G,new} = z_G + \eta_3 \tag{3.18}$$

$$\nabla_{s,new} = \nabla_s - S\eta_3 + \frac{1}{2}S'_0\eta_3^2 \tag{3.19}$$

Here

$$S' = \left.\frac{dS}{dz}\right|_{z=0}; \quad S_{11} = \left.\frac{dS_{11}}{dz}\right|_{z=0} \qquad \text{for the Octabuoy } S'_{11} < 0 \text{ so that } S_{11,new} > S_{11} \text{ for } \eta_3 > 0 \tag{3.20}$$

For small heave displacements the changes in the z_B and z_G are about the same as for a wall sided floater, this simplifies the expression of the restoring force to

$$\begin{aligned} C_{55,new} &= \rho g(S_{11} - S'_{11}\eta_3) + \rho g(\nabla_s - S\eta_3 + \frac{1}{2}S'\eta_3^2))(z_B - z_G - \frac{1}{2}\eta_3 + O(\eta_3^2)) \\ &= C_{55} - \underbrace{\frac{1}{2}\rho g[\nabla_s + 2S(z_B - z_G + S'_{11})]}_{\text{must be minimized as much as possible}}\ \eta_3 + O(\eta_3^2) \end{aligned} \tag{3.21}$$

The pitch motion has a minimal contribution to change in pitch restoring which is considered negligible.

As mentioned in the equation, in order to reduce the variation in the pitch stiffness the term proportional to η_3 in equation 3.21 must be minimized and if possible eliminated. What this means is that it is possible to optimize the geometry to avoid oscillatory pitch restoring. It can be done by requiring that the rate of change of the second moment of water plane area can be determined by

$$\frac{dS_{11}}{dz} = -[\nabla_s + 2S(z_B - z_G)] \tag{3.22}$$

S_{11} can be found analytically. Although the cross-sections of the columns are circular, the radius and distance to the centre varies with z in the free surface zone. For a single column the expression becomes

$$s_{11} = \iint_s [Y(z) + x']^2 \mathrm{d}S \tag{3.23}$$

$Y(z)$ is the position of the centre of the column and x' is the local x-coordinate measured from the centre. This results in

$$s_{11}(z) = [Y(z)^2 + \frac{1}{4}R(z)^2]s(z) \tag{3.24}$$

where

$$s(z) = \pi R(z)^2$$

is the cross-sectional area of one column. Adding all the columns gives

$$S_{11}(z) = \pi[4Y(z)^2 + R(z)^2]R(z)^2 \tag{3.25}$$

Assuming $|\frac{dY}{dz}| << |\frac{dR}{dz}|$, the rate of change of S_{11} can be approximated by

$$\frac{dS_{11}}{dz} = 4\pi R(R^2 + 2Y^2)\frac{dR}{dz} \tag{3.26}$$

The parametric effect can be minimized by fulfilling the following requirement

$$\frac{dS_{11}}{dz} = -[\nabla_s + 2S(z_B - z_G)] = 4\pi R(R^2 + 2Y^2)\frac{dR}{dz} \Rightarrow |\frac{dR}{dz}| = \frac{\nabla_s + 2S(z_B - z_G)}{4\pi R(R^2 + 2Y^2)} \tag{3.27}$$

For Octabuoy geometry the optimum deadrise angel is

$$\alpha = \cot^{-1}|\frac{\partial R}{\partial z}| = 49.2deg \tag{3.28}$$

The Octabuoy has a deadrise angle of 60 degrees which is close to the ideal angle. This means that oscillation of the pitch restoring is almost eliminated.

3.2.3 Slowly Varying Forces

Slow-drift motions are motions caused by slowly varying drift loads connected with second-order difference-frequency effects. Mean drift forces due to second order effects may vary over time and thus induce a slowly varying second order force. An illustration of the phenomena can be seen in figure 3.6. This force is of concern when it occurs close to the resonance period of a structure, which can typically be the case for floating platforms like spar buoys and Octabuoys. These platforms have small water plane areas which means that the restoring term on the vertical plane is small and the eigenperiods in heave, pitch and roll are large, in the order of O(30 s) or larger. For a moored structure where the horizontal eigenperiods are in an order of minutes, the slow drift motions can occur in the horizontal plane. For a structure with both small water plane area and mooring, the slow drift motion can occur both in horizontal and vertical directions as for instance with a moored spar buoy [10] [11].

Slowly varying forces means long periods and low frequencies which is consistent with small linear wave radiation and large amplifications if the motion is near resonance. This means that the wave making damping is low and the viscous damping is of importance.

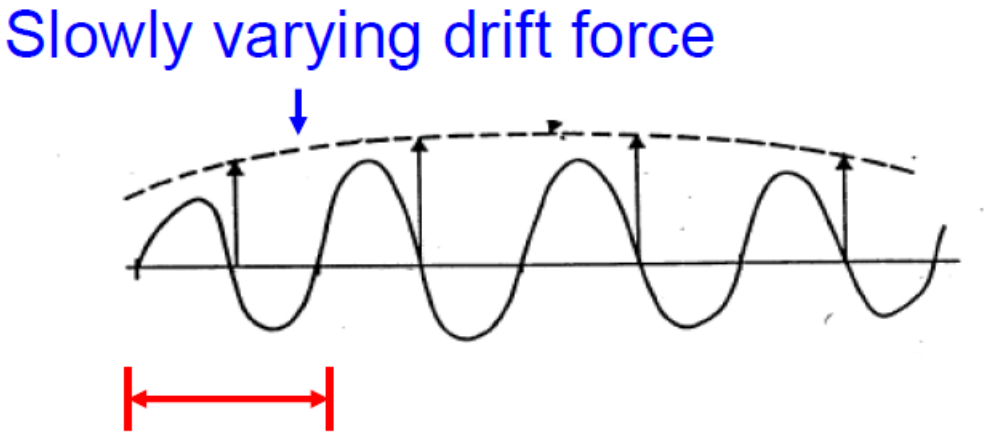

Figure 3.6: Illustration of the slowly varying drift force [10].

In some cases the slow drift motions may exceed the linear motions since the incident wave periods are far from the eigenfrequencies of the structure while the slow drift motions occur close to resonance periods. However because the motions are slowly varying the velocities and accelerations are small compared to the linear velocities and accelerations [10].

3.3 Damping

In hydrodynamic motion analysis, most of the forces may be calculated using potential theory. In potential theory solvers only radiation damping is usually included. However, the damping evaluation of floating offshore systems and ships is at times also quite dependent on the viscous

effects which are not considered in these numerical models using the potential theory. This means for instance that for a ship the roll motion amplitude at resonance will be overestimated using only potential theory. In these cases it is common to use different methods for estimating the damping [12]. The total damping can be separated into potential and viscous damping, the first one is often evaluated numerically and the second through for instance experiments at reduced scale model or other more complicated methods. Fourier transform (FT) spectral analysis and Hilbert Huang transform (HHT) can be used to evaluate a decay signal natural frequency and with HHT this can be done in the time domain. A linear method is not sufficient to predict the damping coefficient for all cases, because in many of them the viscous damping is better represented by a quadratic fit [12].

The spar buoy is a large volume structure which can be subject to large resonant heave motions. Motion damping for these kind of structures usually consists of wave radiation damping, hull skin friction damping, hull eddy damping, viscous damping from bilge keels and other appendices and viscous damping from risers and mooring. When there is resonance the response is controlled by these different damping effects. Viscous drag effects dominate the damping when large response amplitudes occur and consequently the damping can be viewed as quadratic [6]. The non linear damping problem may be solved by several approaches. When geometries are simple, like for instance with a simple spar, Computational Fluid Dynamics (CFD) can be used to asses the viscous damping [7].

In many cases the non linearities can be satisfactorily linearised. Linear superposition can be used if the non linear damping is linearized.

3.3.1 Viscous damping

As already mentioned, large wave periods mean low frequencies. This means that the wave radiation linear damping is small and large amplification of motions occurs close to resonance. When this is the case viscous damping becomes important [10].

Haslum discussed the importance of viscous damping in his thesis (see page 39), where it was concluded that viscous drag effects dominated the damping when large responses occurred. Similar results can be found in a report published by the Seventeenth International Offshore and Polar Engineering Conference in 2007 [13]. In the report, slender spar buoys were investigated ($\frac{Diameter}{draft} < 0.1$). The spar used in this thesis has a ratio of 0.18, but the results are still interesting for the general spar buoy case. It was found that for slender buoy systems the viscous friction is the dominant damping mechanism near resonance. The results showed that in the absence of viscous damping with small wave radiation damping terms, the maximum heave response predicted near the resonance frequency was overestimated by a factor of 10-20 in most cases as compared to laboratory measurements. However, when the drag coefficient C_d was properly calibrated the WAMIT-MATLAB model agreed very well with measurements, even near the resonance frequency.

For the Octabuoy platform concept, the viscous damping can possibly play a significant part in the motion characteristics. The square shaped octagonal pontoon is one of the key features of the design and they may contribute to a viscous damping of motion.

3.4 Main Sources

A couple of texts have been especially significant for the analysis of the spar buoy and the general understanding of the non linear effects discussed in the thesis. They both concern non linear response and are mentioned here due to their significance in the verification of analysis results.

3.4.1 Haslum's Phd

In 2000 Herbjørn Alf Haslum wrote his doctoral thesis under guidance from professor Odd Magnus Faltinsen concerning the non linear motions of a spar platform. The thesis has already been extensively referred to. In his doctoral thesis Haslum preformed model tests at Marin Teknisk Senter in Trondheim. In this master thesis a recreation of Haslums experimental results is attempted and his thesis results are also used as a key source and for verification.

Model tests of 1:300 scale were carried out to qualitatively verify the physical phenomenon and the numerical results. Two types of tests were done, the first to study the Mathieu instability phenomenon and to verify the developed numerical calculation method, and the second to systematically investigate the Mathieu instability and the effect of different damping devices. These model tests are important in the verification process of the analyses preformed in Wasim and Waqum.

The platform model consisted of a circular cylinder with diameter 0.125 m and length 0.755 m. The following full scale parameters were used

- Radius of roll/pitch gyration $R_{xx,yy} = 80m$
- Draft 202,5 m
- Airgap 24 m
- Natural pitch period 99s
- Natural heave period 29.4 s
- Critical damping heave, 1.5%
- Critical damping pitch, 2%

Haslum's model tests were preformed without moon pool.

With an eigenperiod in heave of 29.4s and a pitch period of 99s the following period was found to trigger the Mathieu effect

$$T_{envelope} = \frac{1}{2}T_{N,5} \Longleftrightarrow T_{wave} = \frac{1}{\frac{2}{T_{N,5}} + \frac{1}{T_{N,3}}} = 22.6s \tag{3.29}$$

Haslum's results showed that when the platform was exposed to regular waves of this period the pitch/heave instability was clear. He also found that the higher the incoming wave amplitude, the stronger the instability and larger excitations. The results from the non linear numerical

method he developed corresponded well with the results from the model tests. Results from a linear time domain analysis were also compared. The motion response in the non linear analyses was approximately 10 times larger than in an ordinary frequency domain analysis or a linear time domain analysis. Haslum concluded that this was due to the Mathieu effect.

3.4.2 Exxon mobile and MIT cooperation

An experiment preformed by Exxon mobile and following research preformed by MIT [14] also had non linear effects on a spar buoy as focus. This text is of relevance because it discusses the same phenomena as Haslum but has other conclusions and was published very recently.

In 1998 Exxon Mobile preformed a study of global motion of a deep draft caisson vessel (DDCV, ie. spar buoy) in their Offshore Technology Research Centre Wave Basin. The experiments showed that when a regular period approached to approximately 22 seconds, the DDCV underwent in addition to the wave-frequency motions, large amplitude natural frequency heave (with period 29s) and pitch period (99s) motions. The observed resonant heave and pitch motions of the DDCV were not predicted by the classical linear wave theory. Haslum and Faltinsen attributed such coupled resonant heave and pitch motions to the effect of the Mathieu instability due to hydrostatic coupling of heave and pitch motions. This is however not the conclusion of the MIT researchers looking into Exxon's model tests.

The text investigates the problem in the context of general non linear wave-wave and wave-body interactions. Linear instability analyses are preformed to understand fundamental mechanisms for the occurrence of unstable coupled heave-pitch motions of floating structures. A simplified analytical model was developed which included the dominant interactions for prediction of the onset and evolution of unstable motion. The analytical model results were then compared to the experimental data and was used for investigation of the dependencies of unstable motions on frequency detuning, wave amplitude, damping of the system and irregular sea states.

The model used in the experiment and numerical methods had a diameter of 37 m, a draft of 198 m and a radius of pitch gyration 75 m. The centre of gravity was located 95 m from the keel. Also in this research the effect of the moonpool was neglected for simplicity. This cylinder has eigenfrequency in heave of $\omega_{3n} = 0.217 rad/s$ (corresponding to a period of 29 s) and in pitch of $\omega_{5n} = 0.063 rad/s$ (corresponding to a period of 99 s). From the condition $\omega = \omega_{3n} + \omega_{5n}$ the wave under consideration has a frequency of $\omega = 0.28 rad/s$ (a period of 22 s). The platform had a very similar geometry specifications as Haslum's thesis.

Both the analytical prediction and experiment showed that in the initial stage of the wave-cylinder interaction ($t < 200s$), the wave frequency oscillation is dominant over the natural frequency motion. As the interaction continues the natural frequency motion increased rapidly while the wave frequency oscillation remained almost unchanged. Overall comparison indicated that the simulation resulted in heave and pitch motions properly reflected the instability effect and gave a satisfactory prediction of the unstable resonant heave and pitch motions.

It was concluded that coupled heave-pitch resonant motions of the DDCV in waves resulted from the second order difference frequency interactions between surface waves and body motions and not from the Mathieu instability. In general, larger wave amplitude and/or smaller damping lead

to larger resonant responses and wider (resonance) frequency bandwidth. The coupled heave-pitch resonance of the DDVC could also occur in irregular waves depending on the peak wave period, the significant wave height of the spectrum and the natural heave and pitch periods.

Chapter 4

Mooring

As mentioned in the introduction, to obtain more hydrocarbon sources it becomes a requirement to seek deeper waters. Depths of over 3000 meters is now a realistic situation when building a floating unit. The modelling of the mooring lines and riser for these floating units can be one of the most challenging tasks of the construction. The vessel, its mooring system and their interaction is important to predict with accuracy [24]. From model tests, numerical experiments and real life testing, one can see that current forces on a mooring system can become the dominant environmental load. The importance of modelling the mooring lines correctly increases with increasing depth. It is observed that it can contribute with as much as 75% of the mean drift forces on a floating production system [25].

The primary function of the mooring lines on a floating unit is to counteract the horizontal environmental forces so that the floater remains within specified position tolerance. Mooring was discussed quite extensively in the project thesis. Some of that discussion is repeated here, and some new information is added.

There are several interaction effects between the vessel motion and mooring lines.

- Stiffness forces
- Damping forces
- Inertia forces
- Mean forces
- Excitation forces

An unwanted effect from the mooring is the coupling between surge and pitch. As the mooring lines contribute with vertical forces, these introduce heeling and pitch movement. This coupling effect is especially significant for vessels with a small water plane area which includes semi submersibles and deep floaters. The damping contribution from the mooring lines are also significant in these situations, in particular as depth increases.

Current on the mooring lines will induce drag forces, and as depth increases, so does the exposed line and consequently the mean force. Current varies with depth which means that the drag

force will as well. Perfect correlation between these fluctuations can lead to significant excitation of the mooring lines in deep water.

Dependent on area of interest, waves contain 1^{st} order energy in a period range of approximately 5-25 s. This means that the natural period of the vessels is of large importance for the design. A typical characteristic for floating units is that they have large natural periods in the horizontal degrees of freedom, typically larger than 100s. This is due to small damping and stiffness in the horizontal plane. In order for the mooring line to allow for wave frequency motion, one combines geometrical and axial elasticity of the lines. These geometrical variations makes the mooring system susceptible to considerable dynamic effects. The dynamic effects are mainly due to the transverse drag forces. The vertical motions of a platform can be said to be almost independent of depth. This is in contrast to the horizontal motions, which are highly sensitive to the depth. A general rule for all moored structures is that the wave frequency motions are relatively unaffected/independent by depth (unless very shallow waters), while the low frequency forces and mean offset will tend to increase with depth. For catenary mooring systems, the dynamic mooring forces show the same tendency in deeper water. This is mostly due to the increase in the transverse drag force. Another effect of the increasing depth is that the damping induced by the mooring lines will increase. The other sources of damping will not grow in a similar way which will affect the motion response of the vessel [25].

An accurate analysis of the mooring damping is thus important to obtain a realistic simulation of the moored vessel. Configuration of mooring lines is an important parameter in the preliminary design of deep water mooring system which again has great influence on platform motion and the dynamics of the mooring system itself. Long distance low frequency drift motions can be induced by slowly varying frequency wave, wind and current forces. In addition, the wave frequency force and current can cause large geometric alterations and drag loads to the mooring system. All of these loads can cause strong dynamic responses in the mooring system and are therefore important to study in detail. However this is not straight forward and analysis of mooring systems can be very complicated. Especially when the structure motion, hydrodynamic load and seabed friction are all taken into consideration [24].

Both structures analysed in this thesis have motion characteristics which depend on their mooring configurations. For the spar buoy, mooring configurations may have large influence on the motion. In a report from 2004 it was for instance concluded that "*[...] mooring lines and riser buoyancy-can play an important role in the Mathieu instability analysis of a spar platform through increasing damping/shifting pitch natural period. Thus the possibility of Mathieu instability is expected to be overestimated without proper modelling of [...] mooring lines.*" [15].

An important topic in the project thesis was the effect of mooring configurations on the Octabuoy motions. Wasim was used for simulations and the program can model mooring lines in two ways, both working like linear springs.

1. Anchor Elements. The input is horizontal and vertical stiffness, as well as angle and pretension. The pretension represents the mass of the mooring line, which is needed in order to get a statically correct system. In other words, the mass is modelled as a force.
2. Restoring Matrix. The stiffness of the mooring line is added in an additional stiffness matrix. The mass of the lines are modelled as point masses at the positions of the mooring lines.

The main advantage of the first method is that it allows for structural analysis which takes into consideration the force from the mooring lines. These can then be analysed in the sectional loads. The second option is better when the aim of the analysis is the motion of the vessel. This is due to the fact that the weight is modelled as a force in the first alternative and as a mass in the second. Whether or not it is modelled as a mass will have an effect on the natural periods. Thus, for analyses where motion is the focal point, a method which models the mass correctly is preferable [1].

In the project thesis two fields with different depths were discussed. The Cheviot has a depth of 150 m while the Gulf of Mexico is 1500 m deep. A question was whether the large depth at the Gulf of Mexico would make the anchor lines a much more significant contributor to the total load on the platform. The mooring lines were modelled as an additional stiffness matrix where the coefficients were determined from pull out tests preformed on Orcaflex. The results from the pull out tests can be seen in figure 4.1. These results showed the same trends as the pull out tests preformed in model tests by MARINTEK (figure 4.2). However MARINTEKs values were higher for the Cheviot field and lower for the Gulf of Mexico. Further description on the model tests can be found in the project thesis. From the figures it is clear that the Cheviot showed non-linear behaviour, while the restoring in Gulf of Mexico was close to linear. The polyester part which makes up most of the mooring line at the Gulf of Mexico is taught and stretches according to linear elastic theory. However, for the Cheviot fields, the mooring lines are not acting linearly. The restoring of the chain is largely due to the weight of the chain, and the restoring forces are not linear [3].

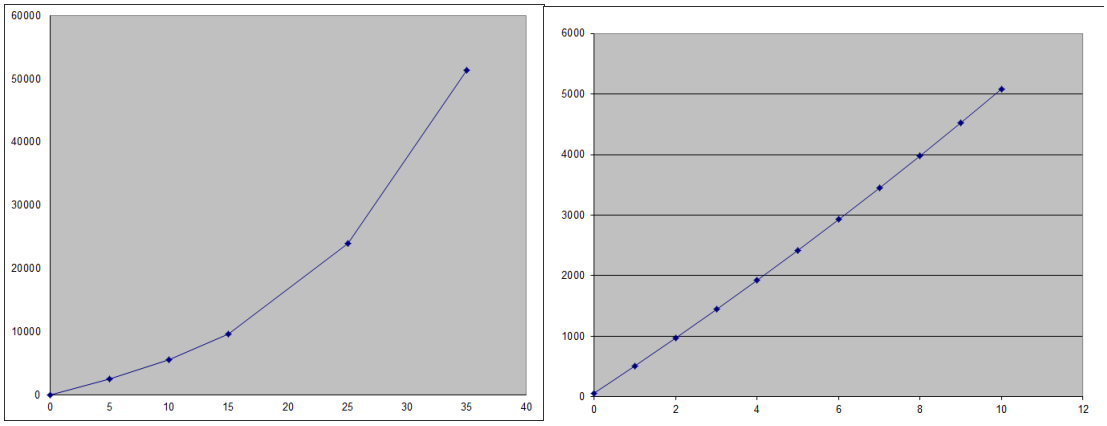

(a) (b)

Figure 4.1: Horizontal Restoring Cheviot and Gulf of Mexico fields found in pull out tests preformed by Moss Maritime AS.

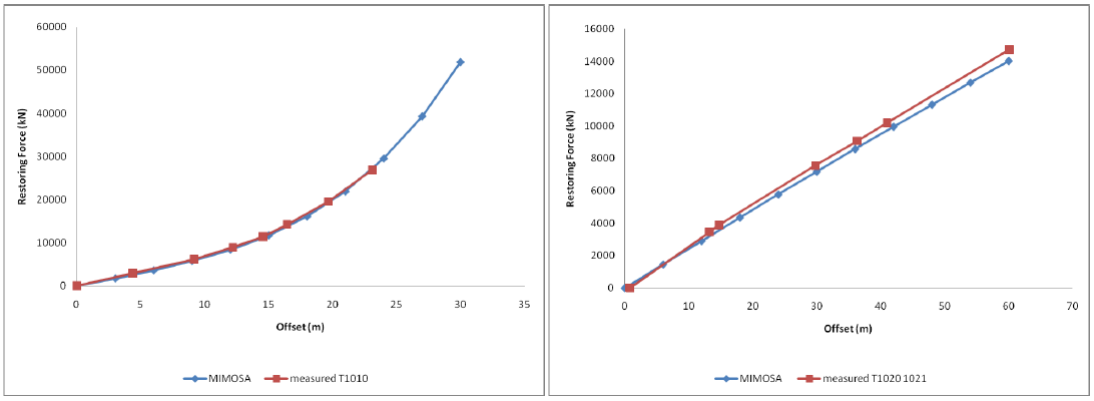

(a) (b)

Figure 4.2: Horizontal Restoring Cheviot and Gulf of Mexico fields found in model pull out test preformed by MARINTEK [28].

The modelling of mooring lines as linear springs was therefore wrong in the case of the Cheviot field. The project hypothesis was that Wasim would be superior in the relatively shallow waters of the Cheviot field, while OrcaFlex would be superior at the large depth of the Gulf of Mexico. However, at 1500 m depth, the mooring stiffness increased linearly, which means that the stiffness was more correctly modelled in this condition. The importance of the mooring lines on the Octabuoy motion characteristics was discussed with researchers at MARINTEK during the project work. They expressed that in their view the mooring lines had small effect on the motion of the platform. It was viewed as unproblematic that the truncated model used in the model tests did not include the dynamic effects of the mooring lines[3].

With Waqum the modelling is different. Like in Wasim linear springs can be added but as described in section 5.2 forces may be added to the equation of motion. This means that the restoring can be added as a force in the equation of motion. For the Octabuoy there are the pull out tests from both Orcaflex and model tests. Equations were established to fit these pull out test curves and the equations were inserted into Waqum. This makes it possible to investigate how large effect different mooring line configurations will have on the motion. The equations for the mooring forces are found from the pull out tests and best fit equations are made for the measured points. They all apply to horizontal restoring.

$$GoM, Orcaflex = -0.0029x^6 + 0.4995x^5 - 33.281x^4 + 1084.1x^3 - 17752x^2 + 138714x \quad (4.1)$$

$$Cheviot, Orcaflex = -6.2129x^4 + 535.75x^3 - 13195x^2 + 149942x \quad (4.2)$$

$$GoM, modeltest = 0.03x^3 - 199.29x^2 + 245470x \quad (4.3)$$

$$Cheviot, modeltest = 1254.1x^3 - 5782.1x^2 + 551920x \tag{4.4}$$

If no anchor lines are added, the structure will drift during the analysis. This is undesired and when mooring lines were not applied, motion control springs were added in the horizontal degrees of freedom, surge, sway and yaw to counter this effect. When adding springs a crucial aspect is to ensure that the springs do not affect the analysis result. To do this the eigenperiod of the springs must not coincide to any of the natural periods (or a multiple of these) of the degrees of freedom. In addition, the damping level must be fairly low, so as to only prevent drifting and not affect the analysis results further. Several spring modifications were tested to ensure that the springs did not have any effect on the analysis outcome. Variation in both eigenperiod of springs and their percentage of critical damping was tested.

Chapter 5

Software

Several softwares are used in the analyses in this master thesis. In the project thesis, Wasim was the main software, and it has also been used in this thesis. In addition Waqum has been used. Here follows a short description of these softwares. Theory of the softwares is included here and not in the earlier theory description as this is important for the understanding of the software features. The Wasim introduction is similar to the one given in the project thesis.

5.1 Wasim

Wasim is a hydrodynamic program developed by DNV. Wasim can run non linear hydrodynamic analysis in time domain on both fixed and floating vessels. This includes the calculation of global motions and local pressure loads. Wasim is part of the HydroD package, and was originally designed for ships with forward speed [16].

Wasim solves the fully 3-dimensional diffraction/radiation problem by use of the Rankine panel method. The problem is solved on the mean surface and mean wetted surface. This requires panels on both the structure model and the free surface[26]. The Rankine panel model is an effective and robust method to predict wave induced response of general three dimensional floating structures. The method is able to handle various free-surface conditions. This means it can take into account the coupling between steady and unsteady flow fields around a floating vessel. To take care of the radiation conditions waves are absorbed by a numerical beach. The theoretic basis of Wasim is based on a method developed by Kring et al. [27].

The following explanation of the modelling of the velocity potential and damping is from an article by Zhi Shu and Torgeir Moan [26].

$$\Phi = \Phi_B + \Phi_I + \Phi_m + \Phi_l \tag{5.1}$$

Here

- Φ_B is the base flow, it accounts for the presence of the hull even though it does not satisfy the actual boundary conditions for the ship, but only depends on the submerged hull.

- Φ_I is the incident wave potential, it represents the incoming flow. In most cases a set of sinusoidal waves.
- Φ_m is the memory flow, it represents the reflection of the waves on the hull. Purpose is to cancel the effect of the incoming wave at the hull, and make sure the free surface conditions are satisfied.
- Φ_l is the local flow. The local flow basically represents the response of the ship. On the free surface local flow is zero , which means that the local flow is only dependent on the motion of the body, not on the wave frequency.

These velocity potentials have to satisfy the following flowing conditions in the fluid domain:

$$\nabla^2\Phi = 0 \qquad \text{in fluid domain} \quad (5.2)$$

$$\Phi_l = 0 \qquad \text{on } z = 0 \quad (5.3)$$

$$\frac{\partial\zeta}{\partial t} - (U - \nabla\Phi_B)\nabla\zeta = \frac{\partial^2\Phi_B}{\partial z^2}\zeta + \frac{\partial\Phi_l}{\partial z} + \frac{\partial\Phi_m}{\partial z} \qquad \text{on } z = 0 \quad (5.4)$$

$$\frac{\partial\Phi_l}{\partial t} - (U - \nabla\Phi_B)\nabla\Phi_l = -g\zeta + U\nabla\Phi_B - \frac{1}{2}\nabla\Phi_B\nabla\Phi_B \qquad \text{on } z = 0 \quad (5.5)$$

$$\frac{\partial\Phi_I}{\partial n} = \nu_n \qquad \text{on the body surface} \quad (5.6)$$

$$\frac{\partial\Phi_m}{\partial n} = -\frac{\partial\Phi_I}{\partial n} \qquad \text{on the body surface} \quad (5.7)$$

Hydrodynamic pressure on the body is defined by Bernoulli's equation:

$$p - p_a = \rho(gz + \frac{\partial\Phi}{\partial t} + \frac{1}{2}\nabla\Phi\nabla\Phi) \quad (5.8)$$

Wasim accounts for some, but not all non linear effects. In addition to the previously discussed mooring lines from section 4, the program for instance models waves either as Airy waves or Stokes 5^{th} order waves. This means that the program does not model non-linear irregular sea. When input to an irregular sea state is given it is transformed into a regular wave set. The free surface is thus modelled linearly. An irregular sea modelled non linearly will increase the CPU time considerably.

The non-linear effects included are:

1. Varying wetness
2. Non-linear hydrostatics
3. Non-linear Froude-Kriloff forces
4. Inertia and gravity terms

These non-linearities can contribute considerably to motions and global loads in large waves. However the radiation forces and diffraction wave force is still given by linear theory [2].

Wasim is usually run through another program, HydroD. If HydroD is not used, Wasim must be run through scripting the input and running the program through for instance Python. HydroD is a GUI program from which one can run both Wadam and Wasim. HydroD was initially designed for Wadam, while Wasim was run through scripting. Wasim was eventually integrated into the HydroD package to facilitate the usage. However since HydroD initially was designed for Wadam, which is programmed different than Wasim, this has led to some problems when running Wasim. Examples of this can be found in the project thesis. At the time this thesis is written HydroD is being remade and all software update on the old version is frozen.

A new version of Wasim has been developed by DNV called Wasim Harmonic. The program is basically Wasim split in two where the radiation and diffraction problems are calculated separately. This makes the program more robust.

Wadam is a linear frequency domain program which is also part of the HydroD package. In this thesis its usage is simple analysis to obtain input for the Waqum analysis.

5.2 Waqum

Waqum is an impulse response function based simulator performing hydrodynamic analysis in the time domain. It uses convolution integrals to describe motion of floating bodies and can handle non-linear loads. Where no other source is given the source of information is the unfinished Waqum manual [17]. Waqum imports hydrodynamic coefficients from a frequency domain analysis preformed in for instance Wadam or Wasim Harmonic. Wadam is much faster than Wasim Harmonic and is therefore the better program to use when many different model configurations are to be tested. This was not the case in this thesis, but due to time limitations, it was decided that Wadam was adequate. Through the impulse response functions this input is then translated into the time domain.

The motion of a floating structure, $x(t)$, can be described by the equation of motion. The equation is based on the assumption that no parts of the equations depend on the absolute time except from the excitation force and response.

$$[M + A(\omega)]\ddot{x} + B(\omega)\dot{x} + Cx = Fx \tag{5.9}$$

Here the different coefficients are as follows:

- M, structural mass and inertia
- A, added mass, dependent on frequency
- B, damping, dependent on frequency
- C, restoring force
- F, Excitation force proportional to x (harmonic)

The response, $x(t)$, to an arbitrary force, $f(t)$, in a linear system can by use of the response $r(t)$ to a unit impulse be written as follows:

$$\int_{-\infty}^{+\infty} f(\tau)r(t-\tau)\,\mathrm{d}\tau \overset{casuality}{=} \int_{-\infty}^{t} f(\tau)r(t-\tau)\,\mathrm{d}\tau = f \otimes r \tag{5.10}$$

Because one can assume that no response can come from an impulse before it happened, the convolution integral can be limited to an upper limit t. Here $\otimes$ is the convolution operator which will be explained further below.

In Waqum forces can be inserted on the right hand side of the equation of motion. This means that non linear effects can be included which are not represented by the frequency domain found coefficients. Like for instance in this thesis, non linear restoring is added on the right hand side. This opens for many possibilities when it comes to the choice of effects that can be included in the analysis.

5.2.1 Non Harmonic Loading and Transient Response

Cummins [19] discussed the fact that the existence of a free surface in hydrodynamics causes the physical system to have a "memory". This means that what happens at one instance affects the system for all time afterwards. If for instance a ship is given an impulse load it will have response lasting much longer than the duration of the impulse. With a succession of impulses, it can be assumed that the response at any time is a sum of responses to individual impulses. Impulses can be assumed to occur closer and closer together until they are integrated instead of added. Through this approach one finds that the existence of the free surface causes the physical system to have a "memory". What happens at one time instance affects the system for all time after. The impulse response method exhibits very clearly the basic contribution of the free surface to the hydrodynamic problem.

When a dynamic system is excited by a non periodic load, $F(t)$, the result will be a transient response. For the general time dependent force the problem can be solved by numerical integration. Fourier theory may also be used by representing the general non-periodic excitation as a sum of harmonic components or by the impulse-response method. Waqum uses the impulse-response method [18].

Impulse is the time integration of the force

$$I = \int F(t)\,\mathrm{d}t \tag{5.11}$$

A unit response or delta function, $\delta(t)$ is defined from the following requirements:

$$\delta(t-a) = 0 \qquad \text{for } t \neq a \tag{5.12}$$

$$\int_{-\infty}^{\infty} \delta(t-a)\,\mathrm{d}t = 1 \tag{5.13}$$

The response of the dynamic system caused by this unit impulse is

$$m\ddot{x} + b\dot{x} + cx = F(t) = \delta(t) \tag{5.14}$$

The response of the system due to the unit pulse id denoted $h(t)$ and called the *impulse response function*

$$x(t) = h(t) \tag{5.15}$$

For a random impulse I, at time T, with a force $F(t) = I\delta(t - \tau)$ the response will be

$$x(t) = Ih(t - \tau) \tag{5.16}$$

This impulse response relationship is illustrated below.

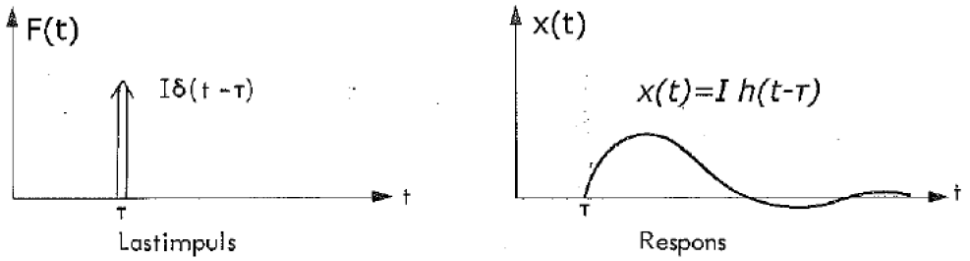

Figure 5.1: Illustration of unit impulse and response [18]

This method can be applied to find the total response to an arbitrary excitation, $F(t)$. The load is split into a series of impulses which occur at different time steps, Δt_i. Below is shown an illustration of this. The impulse acts at $t = \tau$ which gives an impulse equal to $F(\tau)\Delta\tau$

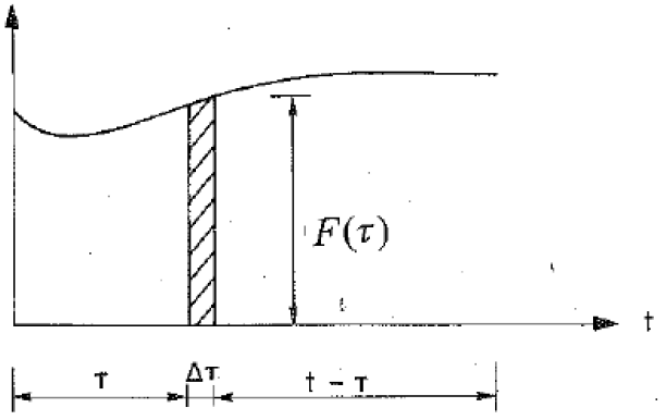

Figure 5.2: An arbitrary force modelled as a series of impulses [18].

Using equation 5.11 this single impulse gives the following response

$$x(t,\tau) = F(\tau)\Delta\tau\, h(t-\tau) \tag{5.17}$$

By integration over all the impulses gives the *convolution integral*

$$x(t) = \int_0^t h(t-\tau)F(\tau)\,\mathrm{d}\tau \tag{5.18}$$

Fundamental assumptions in the convolution method approach are:

- It is assumed that the structural dynamic system is linear. This implies that there is a linear relationship between force and response
- A non-linear force model is allowed. The relationship between incident wave and force may be non-linear

Frequency dependence of added mass and damping

Both the added mass and the hydrodynamic damping are (in general) dependent on the frequency of oscillation. This means that the values changes with frequency and mode of oscillation. When load case is time dependent, the frequency dependency of the added mass and damping introduces a memory effect on the system. This effect should be included in the response calculation and one way of doing it is through the retardation function [20].

Orgilvie gives the following expressions for the retardation function:

$$h(t) = \frac{2}{\pi}\int_0^\infty b(\omega)\cos(\omega t)\,\mathrm{d}\omega \tag{5.19}$$

$$h(t) = -\frac{2}{\pi}\int_0^\infty \omega a(\omega)\sin(\omega t)\,\mathrm{d}\omega \tag{5.20}$$

An analytical model must be created and one way of validating the model is to find the retardation function and use it in the following equations found from Orgilvie.

$$A(\omega) = A^\infty - \frac{1}{\omega}\int_0^\infty h(t)\sin(\omega t)\,\mathrm{d}t \tag{5.21}$$

$$B(\omega) = B^\infty + \int_0^\infty h(t)\cos(\omega t)\,\mathrm{d}t \tag{5.22}$$

For high frequencies the added mass and damping coefficients reach asymptotic values. One may therefore split these coefficients as follows:

$$A(\omega_e) = A^\infty + a^0(\omega_e) \tag{5.23}$$

$$B(\omega_e) = B^\infty + b^0(\omega_e) \tag{5.24}$$

Here ∞ indicated the high frequency asymptote, while 0 is the deviation from this value.

As shown the retardation function can be calculated from either the added mass or the damping. If the function is found through the damping, a continuous representation of the damping, $b(\omega)$ is required. The asymptotic behaviour of two quantities connected by the Kramers-Kroning relationship is such that the added mass and damping coefficients can be approximated by short inverse power series. In Waqum the continuous representation of the damping is as follows:

$$B(\omega) = \begin{cases} \hat{B}(\omega) & \text{for } \omega \leq \omega_u \\ B^{\infty} + \frac{k_1}{\omega^2} & \text{for } \omega > \omega_u \end{cases} \tag{5.25}$$

5.2.2 Runge-Kutta method

In Waqum there are several numerical methods to solve the differential equation. In this project the Runge-Kutta 4^{th} order method (RK4) is used. This is a method of numerically integrating ordinary differential equations by using a trial step at the midpoint with an explicit/implicit iterative method. The method is reasonably simple and robust and is a good general candidate for numerical solution of differential equations when combined with an intelligent adaptive size. Most authorities proclaim that it is not necessary to go to a higher order method because the increased accuracy is offset by additional computational effort[21]. The fourth order formula is as follows

$$\begin{aligned} k_1 &= h\, f(x_n, y_n) \\ k_2 &= h\, f(x_n + \frac{1}{2}, y_n + \frac{1}{2}k_1) \\ k_3 &= h\, f(x_n + \frac{1}{2}, y_n + \frac{1}{2}k_2) \\ k_4 &= h\, f(x_n + h, y_n + k_3) \\ y_{n+1} &= y_n + \frac{1}{6}k_1 + \frac{1}{3}k_2 + \frac{1}{6}k_4 + O(h^5) \end{aligned} \tag{5.26}$$

5.3 Star-CCM+

CFD stands for computational fluid dynamics, and it is known as the science of producing numerical solutions to a system of partial differential equations which describes the fluid flow. In this thesis it is used to find the viscous damping of the spar platform as it moves in heave. For CFD analysis Star-CCM+ is used. The program is developed by CD-Adapco and can be used for fully non linear calculation of excitation forces. Star-CCM+ is built on the COMET code and is a state of the art CFD code. The COMET code is by many regarded as the best viscous CFD code for marine applications. The "CCM" stands for Computational Continuum Mechanics. STAR-CCm+ has the strengths of the COMED code and in addition more ease of use and a wide range of applications[22].

Star-CCM+ is programmed as a Reynold averaged Navier-Stokes(RANS) code. The RANS equations are time averaged equations of motions for fluid flow built on the regular Navier-Stokes equations. For a stationary, incompressible Newtonian fluid, they can be written as:

$$\rho\overline{u}_j\frac{\partial\overline{u}_j}{\partial x_j} = \rho\overline{f}_i + \frac{\partial}{\partial x_j}[-\overline{p}\delta_{ij} + \mu(\frac{\partial\overline{u}_j}{\partial x_j} + \frac{\partial\overline{u}_j}{\partial x_i}) - \rho\overline{u_i'u_j'}][23] \tag{5.27}$$

The code uses the volume of flow method for computing and modelling breaking waves and near free surface flows. This means the grid cells are filled partially with air and water to simulate the real near surface behaviours based on the following criteria

$$\frac{\partial C}{\partial t} + v\nabla C = 0 \tag{5.28}$$

Star-CCM+ has been applied to many marine applications by a variety of companies in the marine industry. Coupled simulations of flows and flow induced motions of floating bodies are wanted for different sea keeping problems. As these simulations should be implicit, there are no restrictions on the time-step size for stability reasons. These simulations can in principle handle all complexity required in naval architectural applications.

5.4 Python

All the programming in the master thesis is preformed in Python. This a general-purpose programming language whose design has put emphasis on the readability.

Waqum is programmed in Python, and can only be run through it. Some of the code is added in the appendix, but most is not, as this would mean including the whole Waqum code. Some scripts are included in the appendix. These are scripts which have been altered significantly or constructed only for this thesis. The scripts found in the appendix (and the ones not considered important enough to be included) are all written with the extensive help of Håvard Nordtveit Austefjord and Tormod Landet.

Chapter 6

Analysis

The focus of all analyses of the spar buoy and the Octabuoy in both softwares will primarily concern the vertical degrees of freedom heave and roll/pitch. Since both platforms are symmetrical, roll and pitch are assumed to be the same, and only pitch will be discussed from here on.

6.1 Spar Buoy in Wasim

In Haslum's thesis there are two frequently used platform configurations. He used only one of these two for the model test verifications. The particularities of the platform used in the model tests was therefore used in this thesis. A section model of the spar was programmed in Python. The model is simply a circular cylinder with a disk at the bottom with geometries specified as follows

draft (d)	202.5 m
diameter (D)	37.5 m
radius of gyration (xx,yy)	80 m
vertical centre of gravity	-97.25 m
metacentric height (GM)	4.0 m
airgap	24 m
natural pitch period	99 s
natural heave period	29.4 s
damping in pitch	2% of critical damping
damping in heave	1.5% of critical damping

Table 6.1: Geometrical details on the two platforms used in Haslum's thesis.

No mass was given by Haslum so a mass model was determined from the displacement. The radius of gyration $R_{xx,yy}$ and the vertical centre of gravity was used to construct the final mass model. Decay tests were preformed to verify that the modelled spar had the correct eigenperiods. Haslum gave two values for the metacentric height (GM) for the spar, 4.0m and 4.4 m. With the given vertical centre of gravity (97.25 m from WL) the GM value was incorrect and approximately

-4 m. An attempt was therefore made to put the centre of gravity 97.25 m from the keel. This gave the same GM values as given in Haslum's thesis.

Motion control springs were added to keep the platform from drifting. The decay test in heave was preformed with 1 m initial displacement. The pitch decay test was preformed with 2 degrees initial displacement.

In accordance to the model tests, the platform was exposed to regular waves with a period of 22.6 s. From equation 3.11 this was calculated to trigger the Mathieu instability. All amplitudes between 3 and 9 meters were tested. Haslum's analyses only had a duration of 1500s. The analyses in this thesis were run for 5000 s. In addition to the critical Mathieu period, periods 21s, 22s, 23.6 s and 25 s were also tested.

The program ForceInspector was used to monitor the force signals of all the time series.

6.2 Octabuoy in Wasim

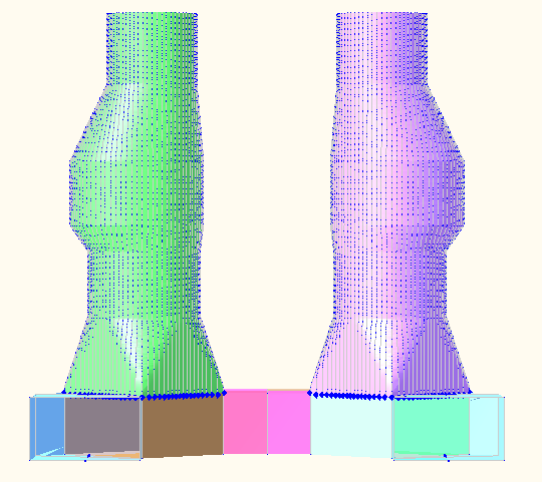

Figure 6.1: Section model Octabuoy

To analyse in Wasim a special type of model, a section model, is needed. In figure 6.1 the section model of the Octabuoy is shown. The explanation of the set up of the Octabouy hydro model in Wasim can be found in the project thesis. This includes how the section model and the mass model were made, the environmental set up etc. It was not considered relevant enough to be included in this thesis. The configuration of the mooring lines in Wasim is considered relevant and the discussion for this can be found in chapter 4.

The restoring coefficients were found from pull out tests in Orcaflex with 5 meters offset in the horizontal plane and 1 m in the vertical plane

Restoring Coefficients	Cheviot	Gulf of Mexico
C_{11} and C_{22}	515.545 kN/m	374.808 kN/m
C_{33}	392 kN/m	448.849 kN/m
C_{44} and C_{55}	22500 kNm/deg	33015 kNm/deg
C_{66}	913548.3 kNm/deg	913548.3 kNm/de

Table 6.2: Additional stiffness due to mooring.

Moss Maritim ran analyses in OrcaFlex with an added damping of 5% of the critical damping. The Wasim analyses were run with the same critical damping.

Damping	Cheviot and Gulf of Mexico
$B_{11} = B_{22} = B_{33} = B_{44} = B_{55} = B_{66}$	5% of critical damping

Table 6.3: Additional damping

As discussed in chapter 2 it was desired to complete the analysis from the project thesis in order to finish the work started there. The analyses are also an important part of this master thesis. Comparison is to be made between linear and non linear effects and their impact on the Octabuoy. In in such comparisons Wasim is highly suitable as it may analyse both linearly and non linearly on the same model. The project work analyses were completed with long crested waves replacing the spreading function. All the analyses were also run linearly. Only the Gulf of Mexico sea states were analysed due to complications with the Cheviot field analyses which are further explained in the project thesis. All analyses were run with a 3 hour (10800 s) duration.

The following analyses were preformed on the Octabuoy in Wasim

Wave spectrum	H_s [m]	T_p [s]	T_z	Analysis Type
1 year Winter Storm - Telemark	4.2	9.0		Linear
1 year Winter Storm - Telemark	4.2	9.0		Non linear, Longcrested
1 year Hurricane - Telemark	3.9	9.8		Linear
1 year Hurricane - Telemark	3.9	9.8		Non Linear, Longcrested
10 year Winter Storm - Telemark	5.6	10.4		Linear
10 year Winter Storm - Telemark	5.6	10.4		Non Linear, Longcrested
10 year Hurricane - API	10.0	13.0		Linear
10 year Hurricane - API	10.0	13.0		Non Linear, Longcrested
100 year Winter Storm - Telemark	6.7	11.4		Linear
100 year Winter Storm - Telemark	6.7	11.4		Non Linear, Longcrested
100 year Hurricane - API	15.8	15.4		Linear
100 year Hurricane - API	15.8	15.4		Non Linear, Longcrested
100 Hurricane - Telemark	15.2	14.9		Linear
100 Hurricane - Telemark	15.2	14.9		Non Linear, Longcrested
100 year Extreme H_s	17.0	15.8		Linear
100 year Extreme H_s	17.0	15.8		Non Linear, Longcrested
1000 year Hurricane - API	19.8	17.2		Linear
1000 year Hurricane - API	19.8	17.2		Non Linear, Longcrested

Table 6.4: Analyses preformed on the Octabuoy in Wasim. All H_s-T_p combinations are for the Gulf of Mexico field.

For JONSWAP spectra the zero upcrossing wave period, T_z is needed. This was found by the following formula from the recommended practice for environmental calculations made by DNV [7]

$$T_z = T_p(0.6673 + 0.05037\gamma - 0.006230\gamma^2 + 0.0003341\gamma^3) \tag{6.1}$$

$$\tag{6.2}$$

The gamma value used was $\gamma = 2.2$. The value was given by Arne Braathen at Moss Maritime, and is the same one they used for their analyses of these sea states.

New runs with correct irregular spectrum were preformed. All these analyses generated a large amount of data which had to be post processed. The time series were gathered and maximum, minimum and standard deviations were found. This has some values as the linear and non linear values are realisations of the same sea state. However for the data to yield some proper statistical values most probable largest (MPL) value was found. Before this could be done, tests to confirm that the data set was Gaussian distributed were be made. Histograms were made from the sea states and the heave and pitch motion to verify the distribution. QQ tests were also preformed, comparing linear to non linear time series. A QQ plot is a graphical method for comparing two probability distributions by plotting their quantiles against each other. The plotted points create a pattern which is used to interpret the distributions. To make the Q-Q plot the two sets were ordered in increasing order and plotted against the normal distribution

quantiles. The Python script for this operation can be found in the appendix. Most probable largest value was found with the following formula

$$H_{MPL} = \sqrt{2m_0 \ln n} = \sqrt{2\sigma^2 \ln n} \tag{6.3}$$
$$n = \frac{Duration}{Period} = \frac{10800}{T_z}$$

6.3 Spar Buoy in Waqum

A frequency domain analysis was preformed in Wadam which covered periods from 2 s to 110 s in head sea. The result file from this frequency domain analysis was the foundation for the Waqum analysis.

The non linear restoring which is important in triggering the Mathieu effect was added to the Waqum analysis as a force on the right hand side of the equation of motion. How the equation is established can be found in section 3.2.1. The term added to the right hand side was without the origianl C_{55} term, which makes the inserted expression

$$= -(-\frac{1}{2}\rho g[\nabla_s + 2S(z_B - z_G)]\eta_3 + \frac{1}{2}\rho g S\eta_3) \tag{6.4}$$

In addition to the restoring term the coupling non linear heave force term was added. This is crucial to include in order to capture the interaction effect between the heave and pitch motion.

$$F_3^{(2)} = \ddot{\eta}_1\eta_5 \tag{6.5}$$

As discussed in chapter 3.3.1 the viscous damping is of importance when excitation is triggered close to the eigenperiods far from the periods when the wave radiation is significant. A simple CFD analysis in Star-CCM+ was used to approximate the non linear damping coefficient. Forced oscillations at a constant period were applied to a model of the spar. As the damping varies with the amplitude of heave motion the amplitude was varied to find the variation in the damping. The CFD analysis were preformed with the help of Cosmin Ciortan of the Maritime Advisory department at DNV. Three amplitudes were tested, 4m, 6m and 8m. All had the same oscillation period of 22.6 s.

The force signals from the analyses were post processed in a python script which can be found in the appendix. The script preformed the least square method on the force signal to separate it. The least square method is a mathematical procedure for finding the best fitting curve to a given set of points. This is done by minimizing the sum of squared residuals, a residual being the difference between an observed value and the fitted value provided by a model. Because squares of residuals are used, outlying points can have a disproportionate effect on the fit, an effect which may or may not be desirable depending on the problem at hand.

The signal was split one component in phase with the sine component and one in phase with the cosine component. In the CFD analysis the speed was defined as

$$v = \zeta_a \omega sin(\omega t) \tag{6.6}$$

Since damping is proportional to the speed the damping part of the signal was assumed to be the force in phase with the sine. The drawback of using the least square method is that the damping is partly linearized by it. The dependence on the amplitude still makes it partly non-linear, but using only the part in phase with the sine wave, the damping is somewhat linearized. How large this effect is not clear.

A regular wave with period 22.6 s and amplitude 6 m was applied to the platform and motion control springs were added to keep the platform from drifting.

6.4 Octabuoy in Waqum

Testing Waqum on the spar buoy had two purposes; Looking into non linear effects and verifying that Waqum can handle analyses with non linearities. The next step was to apply the program to the Octabuoy. A Wadam run was preformed on the platform to obtain the basic hydrodynamic coefficients and these were used as input.

Waqum would also be used for testing of different mooring configurations. The applied mooring configurations can be seen in chapter 4.

Chapter 7

Software Issues

An error in HydroD was discovered a couple of weeks before the deadline of the master thesis. Analyses of the Octabuoy had been preformed in Wasim through HydroD and statistical operations were attempted on the resulting time series. For the linear sea states it was expected that the free surface elevation would follow a normal Gaussian distribution. However, when the time series was plotted in a histogram the distribution looked like the distribution of a sinusoidal wave. Most of the energy was concentrated around ± 1. When looking closer at the time series they too seemed to behave almost like sinusoidal waves. FFTs were therefore preformed on the input wave signals to check that the wave spectra actually had the JONSWAP energy distribution.

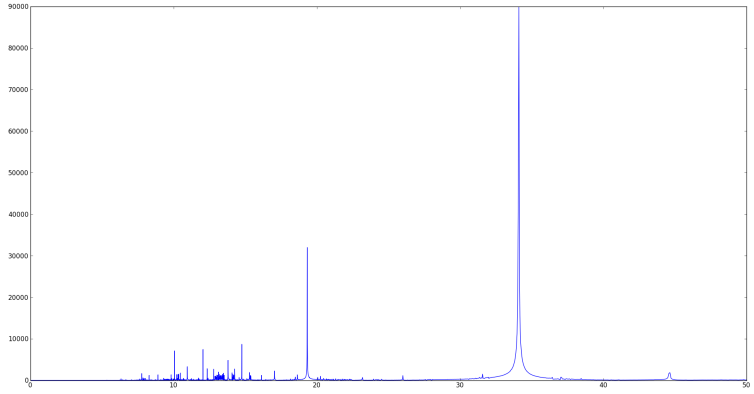

Figure 7.1: The result from the FFT preformed on the the input wave signal for the first 1 year sea state, $H_s = 4.2m, T_p = 9s$. Clearly this does not have a JONSWAP energy distribution.

As can be seen from figure 7.1, the spectrum created in HydroD is in reality a few periods with much energy. The rest of the periods are given a very little amount of energy and almost appear to be noise. Probably HydroD creates a spectrum after certain guidelines which are fulfilled even though the spectrum created is far from correct.

The discovery of the error meant that the previous analyses run with the irregular spectra were all wrong. Any statistical operation or comparison between linear and non linear runs would give unreliable information. The analysis were therefore rerun. This time the wave spectra was generated in a program called WaveGenerator which generates the JONSWAP spectrum from the given H_s, T_z and γ values. To avoid any more unknown errors in HydroD, Wasim was run directly by programming a script in Python which imported the generated spectra directly. The script can be found in the appendix.

The regular wave tests in Wasim run through HydroD on the spar buoy are still considered to be perfectly fine.

Chapter 8

Results and Discussion

8.1 Spar Buoy in Wasim

Decay test in heave was preformed with 1 m initial vertical displacement. This gave an eigenperiod of 29.3 s.

The pitch decay test was preformed with 2 degrees initial displacement. In chapter 6.1 the vertical centre of gravity was moved from 97.25 m to 105.25 m below mean water line. This was done to obtain the correct GM value. However, this setting gave an incorrect eigenperiod in pitch. Calculations were made to "force" the eigenperiod in pitch to 99 s. This gave a vertical centre of gravity at 104.4 m below the mean water line. The shift of the vertical centre of gravity gave new GM values, 3.249 in roll and 3.251 in pitch.

In accordance with the model tests, the platform was exposed to regular waves with a period of 22.6 s. From equation 3.11 this was calculated to trigger the Mathieu instability. All amplitudes between 3 and 9 meters were tested. Haslum's analyses only had a duration of 1500s. The analyses in this thesis were run for 5000 s. More results can be found in the appendix. Below the result from analysis with 6m amplitude wave is shown.

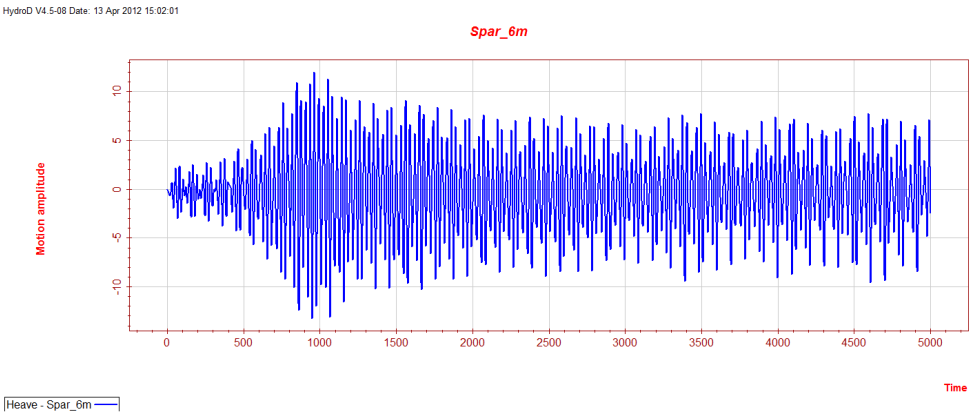

Figure 8.1: Heave at regular wave with 6m amplitude and period of 22.6 s.

The triggering of non linear excitation is recognizable in the figure above. At first there is only small excitation, then a larger response builds up before it decreases slightly and stays stable but large. The motion does not diminish as the regular wave continues. These are symptoms of the Mathieu effect. Results from the last 100s of this analysis were animated in GLview and images from the animation can be seen below. As can be seen in the images and the figures 8.2 and 8.3 the platform experiences large motions.

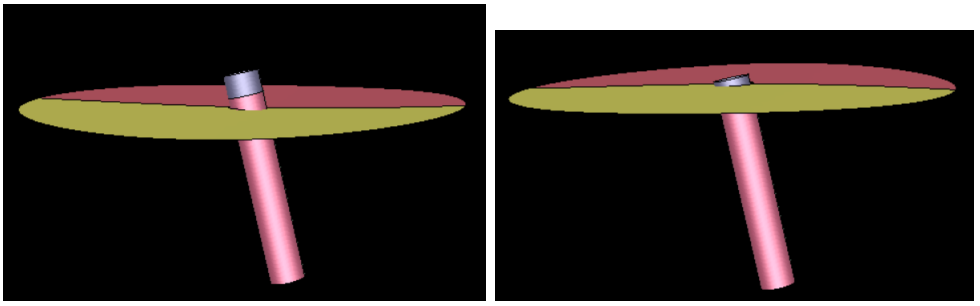

(a) (b)

Figure 8.2: Screen shots of the spar motion from animation in GLview.

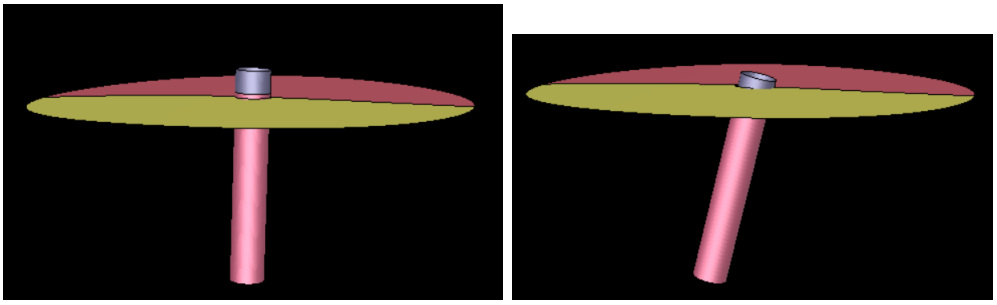

(a) (b)

Figure 8.3: Screen shots of the spar motion from animation in GLview.

Due to the short duration of Haslum's model trials and numerical simulations they only capture the build up of the large excitations. They cannot confirm nor negate the results in Wasim after the build up/the first 1500s. However it seems that at least in the first 1500 seconds the analyses from Wasim are more similar to the model test results than the numerical model Haslum made. This is assumed to indicate that Wasim is closer to the model tests than Haslum's numerical model. The results from a run with 8 m amplitude is shown together with Haslum's results for the same regular wave both from the numerical model and the model test results.

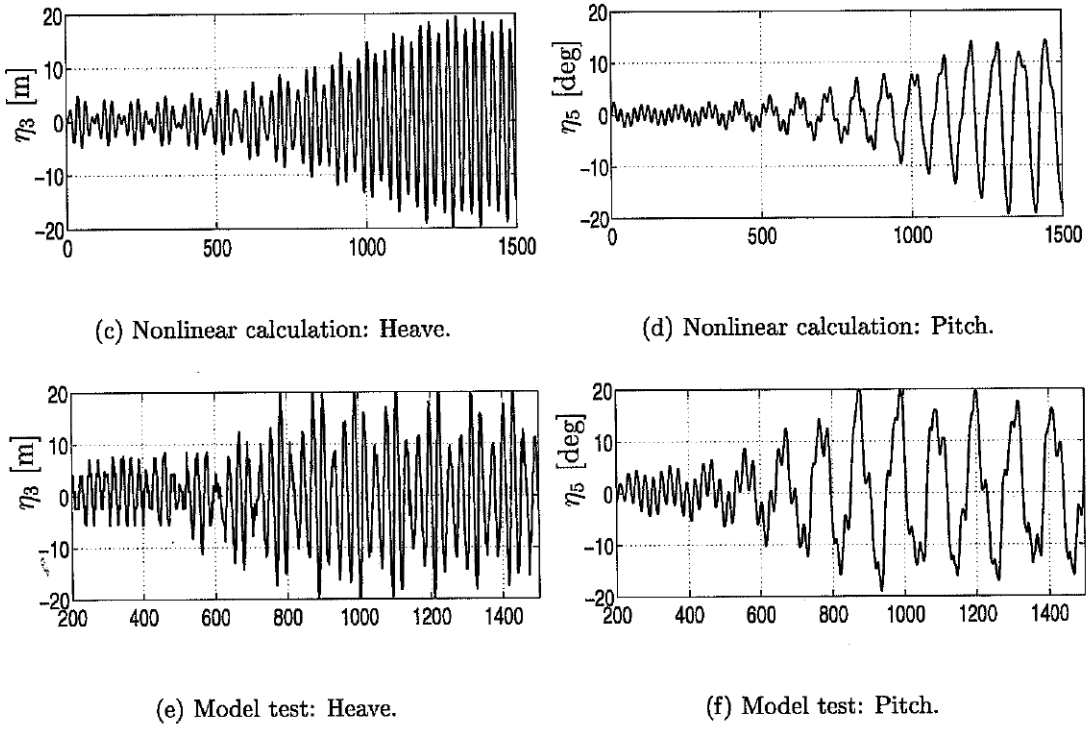

(c) Nonlinear calculation: Heave.

(d) Nonlinear calculation: Pitch.

(e) Model test: Heave.

(f) Model test: Pitch.

Figure 8.4: Haslum's results in heave and pitch for numerical trials and model tests [9].

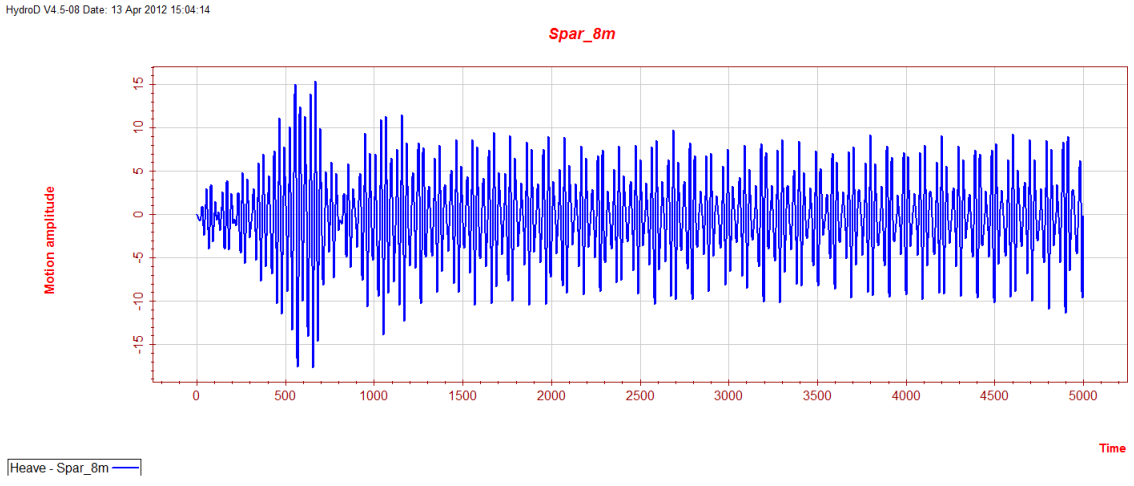

Figure 8.5: Heave motion for regular wave with amplitude 8 m, i.e. the same input as for the results in figure 8.4.

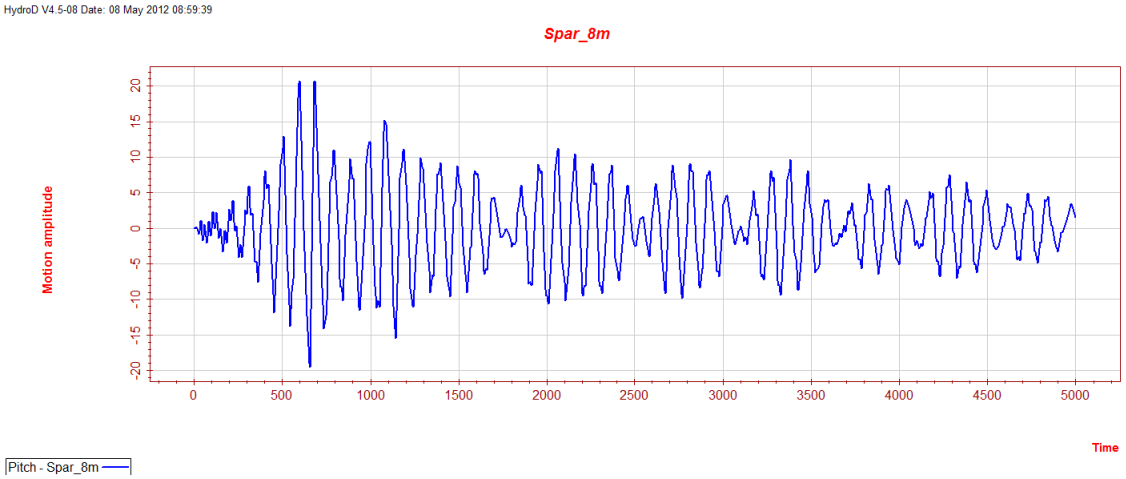

Figure 8.6: Pitch motion for regular wave with amplitude 8 m, i.e. the same input as for the results in figure 8.4.

The analyses show that the instability occurs more rapid with increasing incoming wave amplitude. As the amplitude increases, the instability is triggered faster. For instance with the 8 and 9 m amplitude waves instability was triggered almost immediately. For the lowest amplitudes 5000 s was not enough to trigger significant instability, only the beginning of the build up could be observed. Further expansion of the simulation time is in utile as the probability for a regular wave such as this to have a duration longer than 5000 s is minimal.

All the analyses were rerun and the different force contributions where monitored and then analysed in ForceInspector, a simple Wasim application which allows for closer inspection into the forces. The forces in ForceInspector are defined such that

$$F_{gravity,5} + F_{hydrostatics,5} = C_{55}\eta_5 \tag{8.1}$$

From the inspector the force signals of the hydrostatics and gravity in pitch where found and the results from the run with 6m amplitude can be seen below.

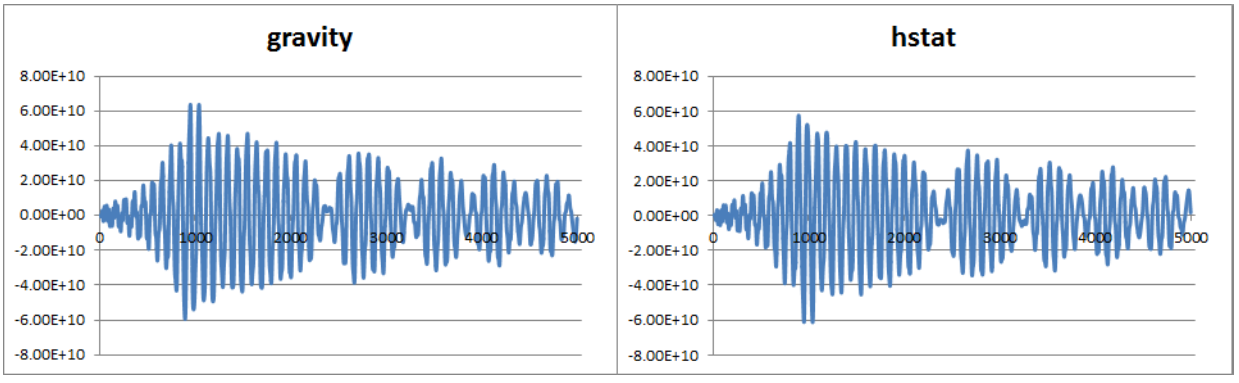

Figure 8.7: The force signals for gravity and hydrostatics in pitch for 6 m amplitude run.

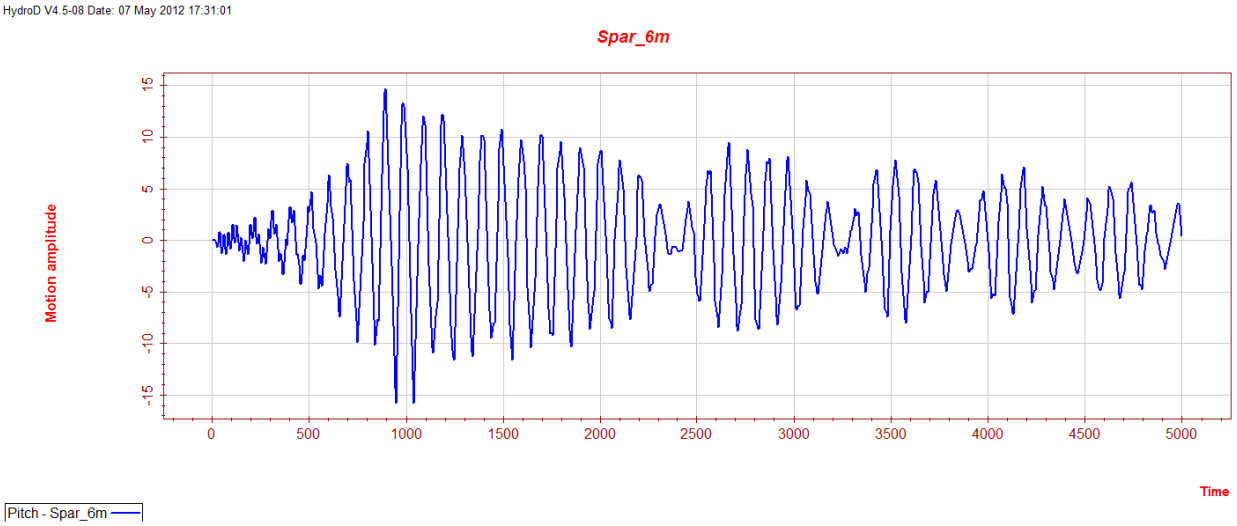

Figure 8.8: Pitch motion 6 m amplitude run.

Compared with the pitch time series a definite connection between the forces which makes up the restoring force and the pitch motion can be observed. This is another observation which supports the assumption that the observed excitation is a result of the Mathieu effect.

To discern further whether the observed motions actually are due to the Mathieu effect, new analyses were run with long periods, but not the period calculated to trigger the Mathieu effect. The periods chosen were 21s, 22s, 23.6 s and 25 s. These periods lead to long waves, from approximately 700 to 1000 meters. The only period which showed the non linear excitation was the analysis with a 22 s period. This is very close to the period which was calculated to trigger the Mathieu effect and it may still be only this effect. From the stability diagram in figure 3.3a it can be read that for certain cases when there for instance is low damping and large perturbation of the stiffness, the instability may be triggered in a relatively wide range of frequencies. Another factor is how the critical pitch period is dependent on the metacentric height GM, and GM is dependent on the heave motion. This means that the eigenperiod of pitch may vary during the heave motion cycle which again may widen the range of the period triggering the Mathieu [9].

As covered in chapter 3.4.2 Lui et al. [14] discussed the effect of non linear excitation on the spar. They believed the excitation on the platform was not caused by the Mathieu effect, but rather by slowly varying forces. To compare with the results from Wasim, the test results from Lui et. al are shown below.

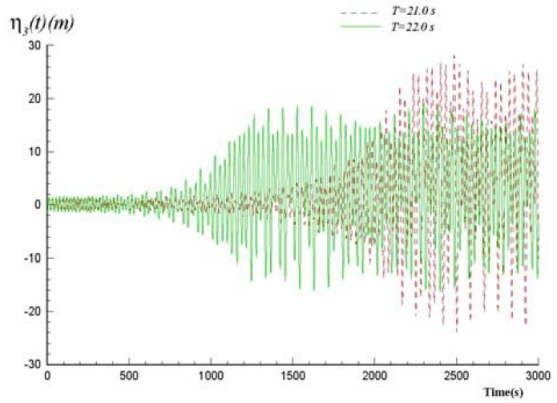

(a) Heave motion, Lui at al.

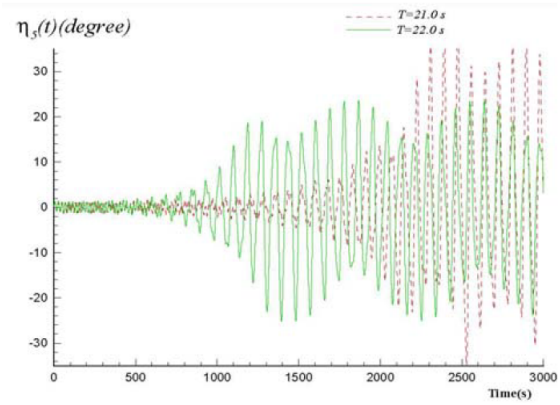

(b) Pitch motion, Lui at al.

Figure 8.9: Time history of heave and pitch motions with the incident wave period T = 21.0 s and 22.0 s. In the simulation $B_{33} = 4\%$ and $B_{55} = 5\%$ of critical damping, quadratic damping with CD = 1.0 for surge motion, and the incident wave amplitude A = 6.1 m were used [14].

From the figure 8.9 one can see that the results are quite similar to the results from Wasim and Haslum's model tests seen in figures 8.4, 8.5 and 8.6. With the eigenperiods given for the spar platform used by Lui et. als the incoming wave periods are close to the period which triggers Mathieu instability. With Haslum's formula the critical period for the spar used by Exxon and MIT is

$$T_{crit} = \frac{1}{\frac{1}{99} + \frac{1}{29}} = 22.43s \tag{8.2}$$

Unfortunately Wasim is not able to capture slowly varying motions. The free surface is modelled linearly and it was not possible to use this program to check whether Lui et. als results could be recreated. However it is observed that Lui et als work is in the very region which Haslum writes will trigger Mathieu, yet they claim that the effects are not Mathieu instability but rather an effect of slowly varying forces. It would be desirable with a better explanation of why the slow drift motions are considered the triggering effect. Also it would be interesting to see Lui et als analyses run over a wider range of periods.

Neither in the Wasim analyses nor in the Waqum analyses is the effect of moonpool included. The neglecting of the viscous damping of the moonpool makes the simulations appear too large. It can therefore be assumed that the results obtained in the analyses will be exaggerated although how much is not known.

8.2 Octabuoy in Wasim

From the resulting time series of the Wasim runs several statistical operations were preformed. Mean, min, max, standard deviation and most probable largest value form each time series was

found. Many of the time series and the table showing max and min can be found in the appendix. The time series which are not in the appendix are in the digital appendix. Below is shown the histogram plottings of both linear and non linear runs in heave and pitch. The sea states shown is the first 1 year sea state and the final 1000 year sea state.

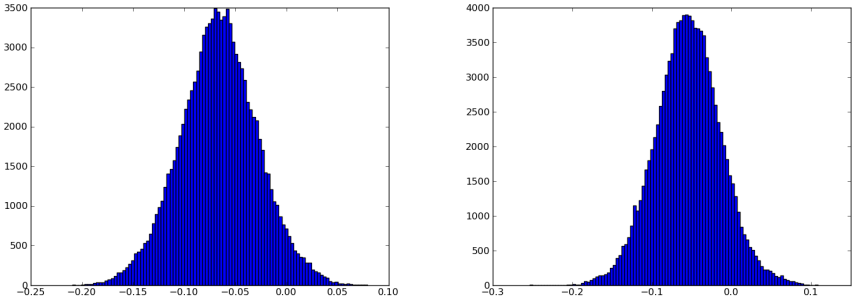

(a) Heave 1y1 linear (b) Heave 1y1 nonlinear

Figure 8.10: Histogram linear vs non linear heave 1 year 1.

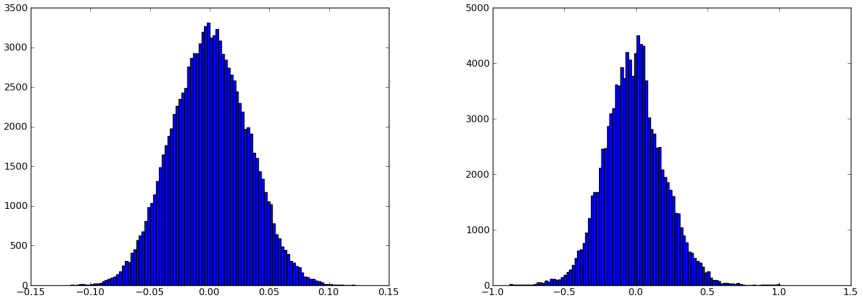

(a) Pitch 1y1 linear (b) Pitch 1y1 nonlinear

Figure 8.11: Histogram linear vs non linear Pitch 1 year 1.

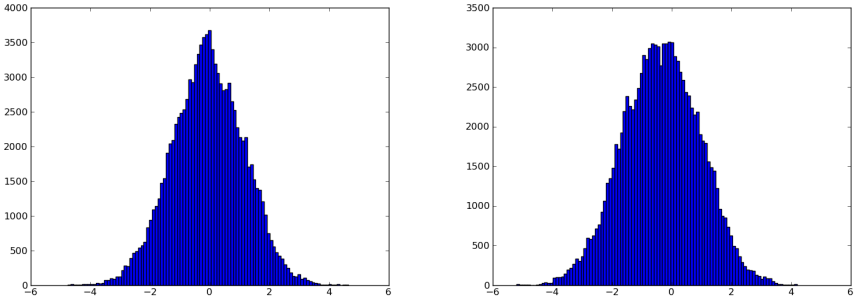

(a) Heave 1000y1 linear (b) Heave 1000y1 nonlinear

Figure 8.12: Histogram linear vs non linear heave 1000 years sea state.

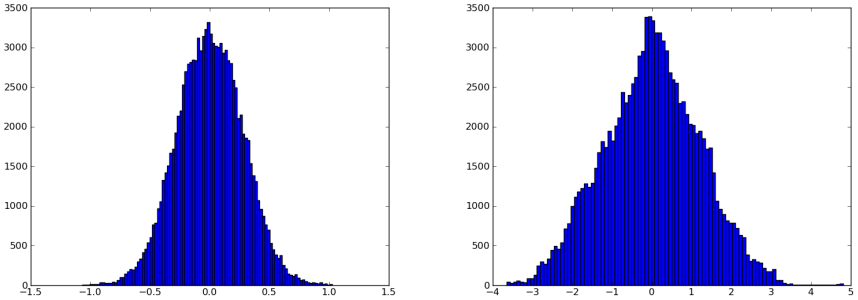

(a) Pitch 1000y1 linear (b) Pitch 1000y1 nonlinear

Figure 8.13: Histogram linear vs non linear Pitch 1000 years sea state.

From the histograms one can observe that the heave and pitch motion tends towards a normal distribution, although some are further from the normal distribution shape than others. The formula for MPL value is still used to find the largest statistical values. This may lead to errors because the formula is based on a Gaussian distribution. The MPL values can be found in the tables below. With the results are also shown the results from the Waqum analysis. These will be discussed later.

Heave Motion				
Analysis	MPL Linear [m]	Lin. Standard Deviation	MPL Non Linear [m]	Non Lin. Standard Deviation
1y1	0.2929	0.038138	0.3192	0.04156
1y2	0.3948	0.0516	0.4102	0.0537
10y1	0.7146	0.09839	0.7523	0.0989
10y2	2.8816	03047	2.3872	0.3188
100y1	1.1416	0.1510	1.1860	0.1569
100y2	4.62315	0.6250	5.1924	0.7020
100y3	4.1714	0.5626	4.5741	0.6169
100y4	5.2910	0.7166	6.0177	0.8151
1000y1	8.8106	1.2009	9.4940	1.2997

Table 8.1: Most probable largest (MPL) value and standard deviation in heave from linear and non linear analysis.

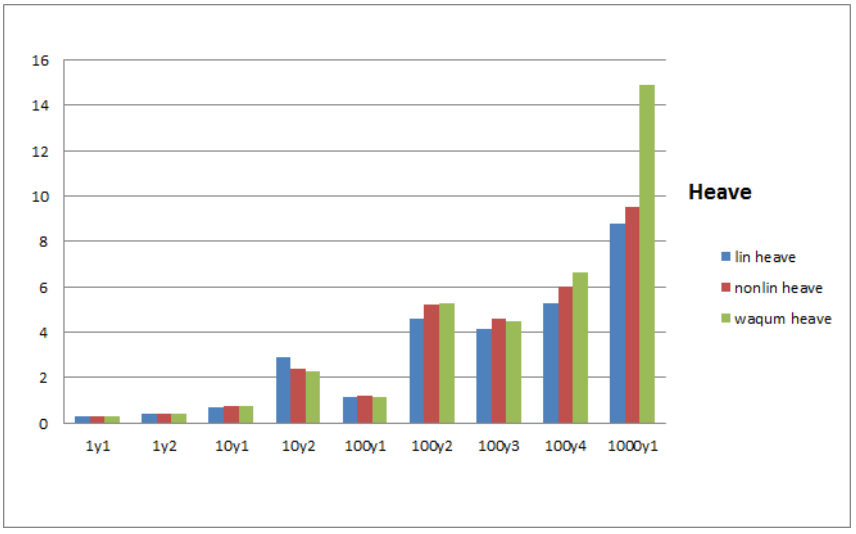

Figure 8.14: Histogram showing the heave motion from linear, non linear and Waqum runs.

Pitch Motion				
Analysis	MPL Linear [deg]	Lin. Standard Deviation	MPL Non Linear [deg]	Non Lin. Standard Deviation
1y1	0.2431	0.0316	1.5912	0.2072
1y2	0.2459	0.0322	1.2217	0.15997
10y1	0.3768	0.0495	2.0909	0.2749
10y2	0.8294	0.1107	3.6203	0.4835
100y1	0.49	0.0652	1.97	0.2616
100y2	1.487	0.2010	5.948	0.7971
100y3	1.3979	0.1885	5.9487	0.8023
100y4	1.6318	0.2210	6.8476	0.9275
1000y1	2.0397	0.2780	8.9052	1.2138

Table 8.2: Most probable largest (MPL) value and standard deviation in pitch from linear and non linear analysis.

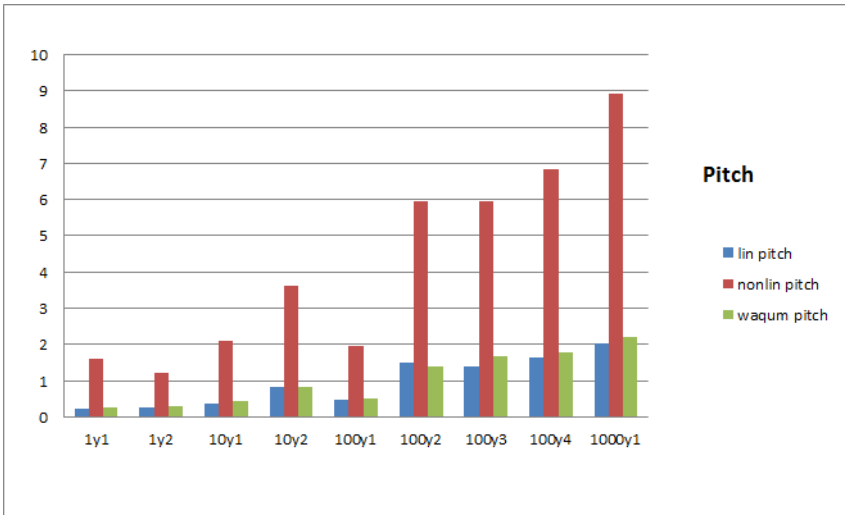

Figure 8.15: Histogram showing the pitch motion from linear, non linear and Waqum runs.

Percentage difference between MPL			
Analysis	Linear	Non Linear	Waqum
1y1	100 %	109 %	108 %
1y2	100 %	104 %	103 %
10y1	100 %	105 %	105 %
10y2	100 %	83 %	79 %
100y1	100 %	104 %	100 %
100y2	100 %	112 %	115 %
100y3	100 %	110 %	107 %
100y4	100 %	114 %	126 %
1000y1	100 %	108 %	169 %

Table 8.3: MPL of heave compared with percentage. The linear value is the benchmark value.

Below one can see the QQ plots of the time series plotted against a normal distribution. The QQ plots for heave and pitch are shown for the 1st 1 year sea state and for the 1000 years sea state. More results can be found in the appendix and/or in the digital appendix. Since there is a difference between the linear and non linear pitch time series, these are also shown separately.

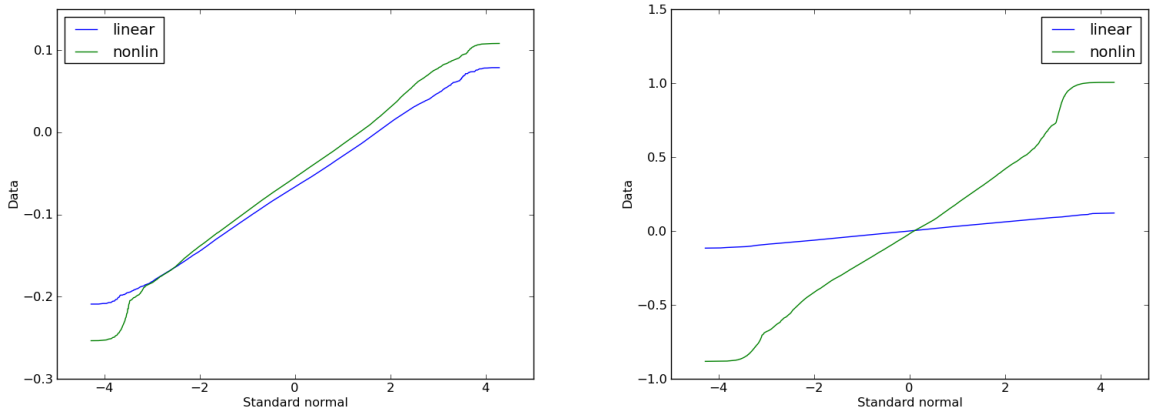

(a) QQ Heave 1y1

(b) QQ Pitch 1y1

Figure 8.16: QQ plots Heave and Pitch 1y1 linear and non linear vs Normal distribution.

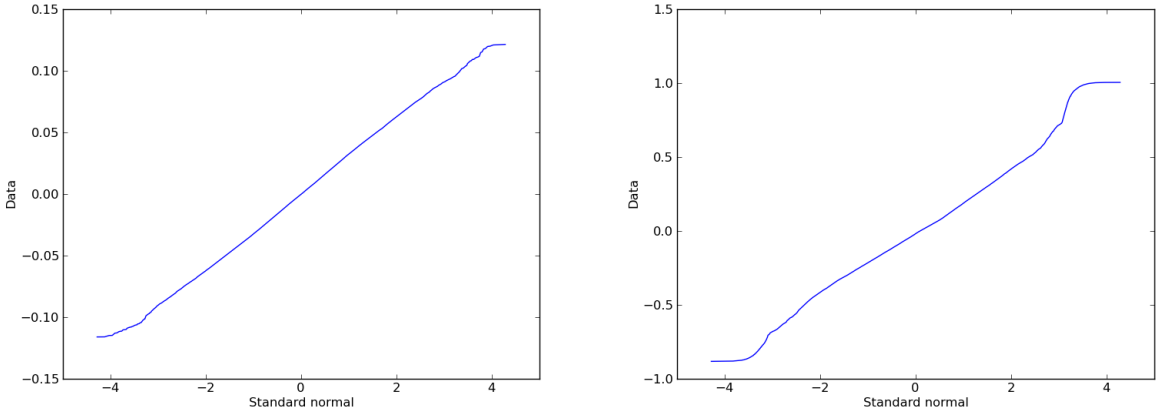

(a) QQ Pitch Linear 1y1

(b) QQ Pitch Non Linear 1y1

Figure 8.17: QQ plots Pitch 1y1 linear and non linear vs Normal distribution.

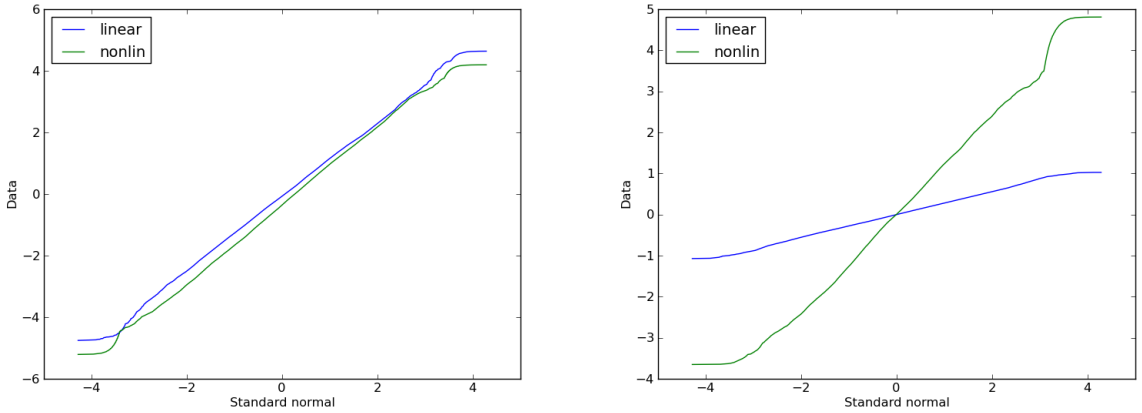

(a) QQ Heave 1000y1

(b) QQ Pitch 1000y1

Figure 8.18: QQ plots Heave and Pitch 1000y1 linear and non linear vs Normal distribution.

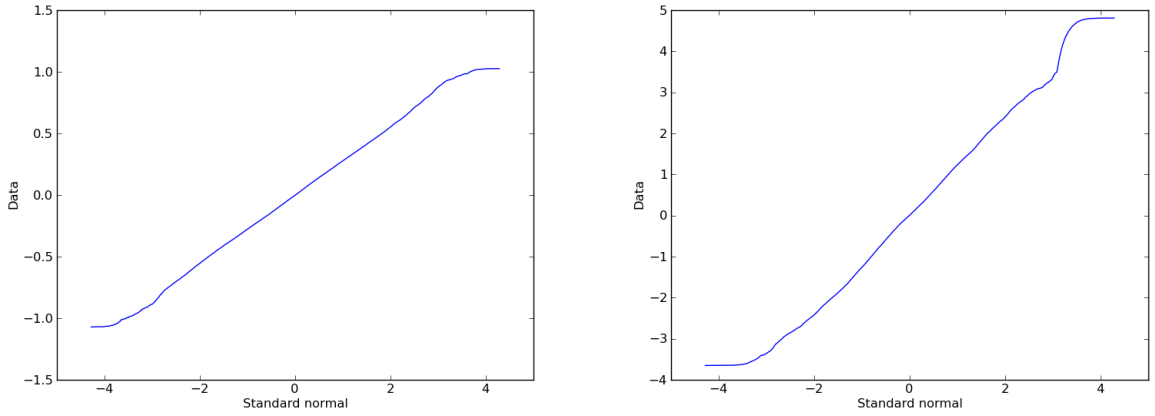

(a) QQ Pitch Linear 1000y1

(b) QQ Pitch Non Linear 1000y1

Figure 8.19: QQ plots Pitch 1000y1 linear and non linear vs Normal distribution.

Both time series are reasonably well represented as normal distributions. The trend is the same for all the sea state. The QQ plots tend to bend a little at the ends. This might be due to fewer points plotted at the extreme values of each run. It might also mean that the sample deviates from the normal distribution in the smallest and largest values. When looking at the MPL values it should be taken into account that this is calculated with the assumption of normal distribution. This does not mean that the samples do not vary from the distribution and there is room for error in the statistical results.

Table values and QQ plots show that for the heave motion there is little variance between linear and non linear analyses. This is not the case for the pitch motion, which clearly is larger when the analysis is run non linearly and the difference between linear and non linear simulation is

significant. In the QQ plots the non linear time series show a much larger variation than the linear ones. When plotted alone both linear and non linear pitch motion time series seem to fit fairly well with the normal distribution. The histograms of the pitch motion also confirm this, in figure 8.13 it can be observed that the distribution of the non linear run is further from the normal distribution shape than the linear run. Since the roll and pitch motions are considered equal for this symmetrical platform it can be assumed that these results also apply to the roll motion. To sum up, this means that in the vertical motion aspect, the translational motion is almost unaffected by non linear effects, while rotational degrees of freedom are quite largely affected.

Since Wasim models the free surface linearly, non linear excitation force/moment in the wave zone can be eliminated as the reason for the non linear effect on the roll and pitch. Other reasons can be non linear radiation/diffraction effects or non linear hydrostatic effects. Non linear Wasim includes non linear Froude Krylov and hydrostatics and one of these must be the reason for the non linear pitch excitation.

Octabuoy is designed to avoid non linear hydrostatic effects in pitch and roll. The ideal dead rise angle was in chapter 3.2.2 found to be 49.2 degrees while the Octabuoy columns have a dead rise angle of 60 degrees. Whether this small difference is the reason for the non linear effect on the rotational degrees of freedom is not known. Perhaps the 10.8 degrees difference is the reason for the non linear pitch excitation. This could be tested by attempting to provoke the coupling effect but there was not enough time to preform this analysis in this thesis.

In chapter 2 it was discussed how the short crested simulations gave bad results especially with respect to the motion perpendicular to the main wave heading. After the error in the HydroD spectrum generator was discovered (discussed in chapter 7), this was shed new light on. The theory was that the analyses went wrong because there were too few wave components (only 200). This is probably part of the problem, as generally speaking a short crested sea state is known to need more wave components than a long crested sea state to be accurate. However the error in the spectrum generated by HydroD means that very few waves get much energy while the rest of the waves are simply noise. It can therefore be assumed that the large perpendicular motions may be due to large waves with angles $\neq 180^\circ$ which contained unrealistic amounts of energy.

8.3 Spar Buoy in Waqum

The results from the frequency dependent Wadam analysis were imported into the Waqum Explorer post processor where RAOs were inspected together with mass matrices etc. to make sure the model behaved according to specifications. They appeared correct and the .SIF file was imported in Waqum.

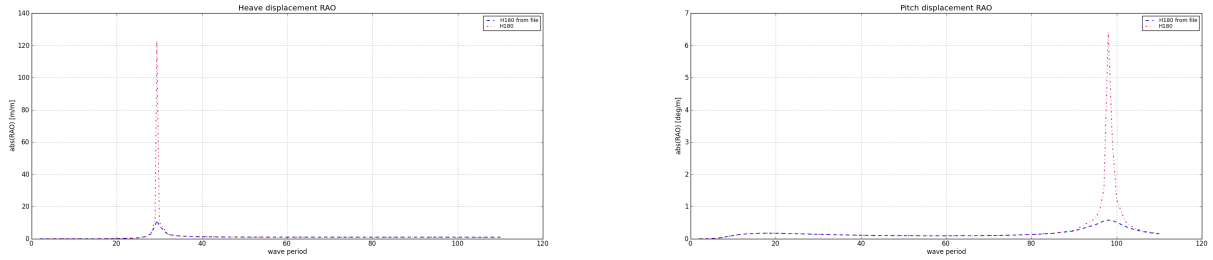

(a) Heave RAO

(b) Pitch RAO

Figure 8.20: RAOs from Waqum Explorer based on the result file from Wadam.

Spring configurations were tested to check the effect on the motion characteristics, some results can be seen in the appendix. The largest variation in results can be found in the surge displacement at the pitch decay test. Compared to the magnitude of displacement in pitch, this was considered to be a minor variance. The period of 320 s and a critical damping of 5% was used in the analyses. With these settings eigenfrequencies were controlled for heave, roll and pitch by Fast Fourier Transform (FFT).

The eigenfrequencies are shown below.

Degree of freedom	Period [s]
Heave	29.44
Roll	98.42
Pitch	98.40

Table 8.4: Eigenfrequencies/periods found through FFT.

The result from the regular wave of 22.6s and amplitude 6m can be seen below together with a linear run from Wasim with the same conditions. The plots are very similar. Both start of with response which deceases and steadies after a while. Then the response is completely regular.

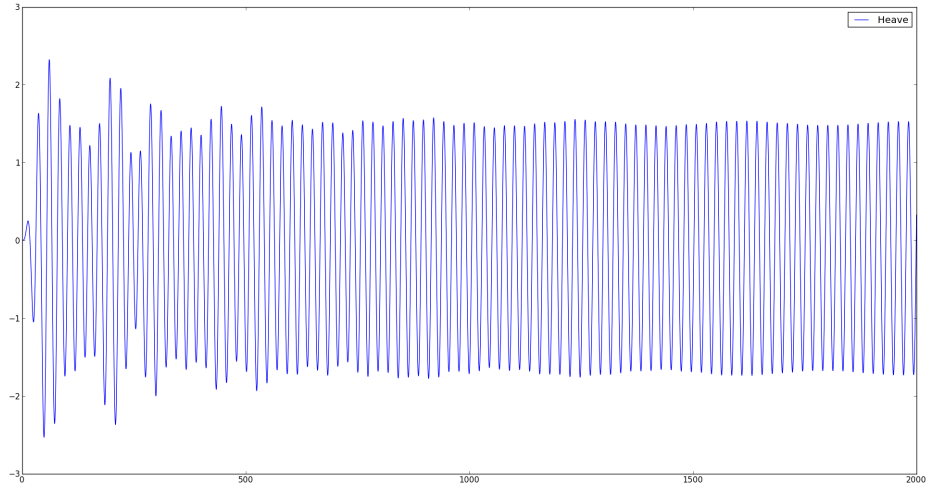

Figure 8.21: Heave motion from Waqum analysis with T=22.6s and amplitude 6 m.

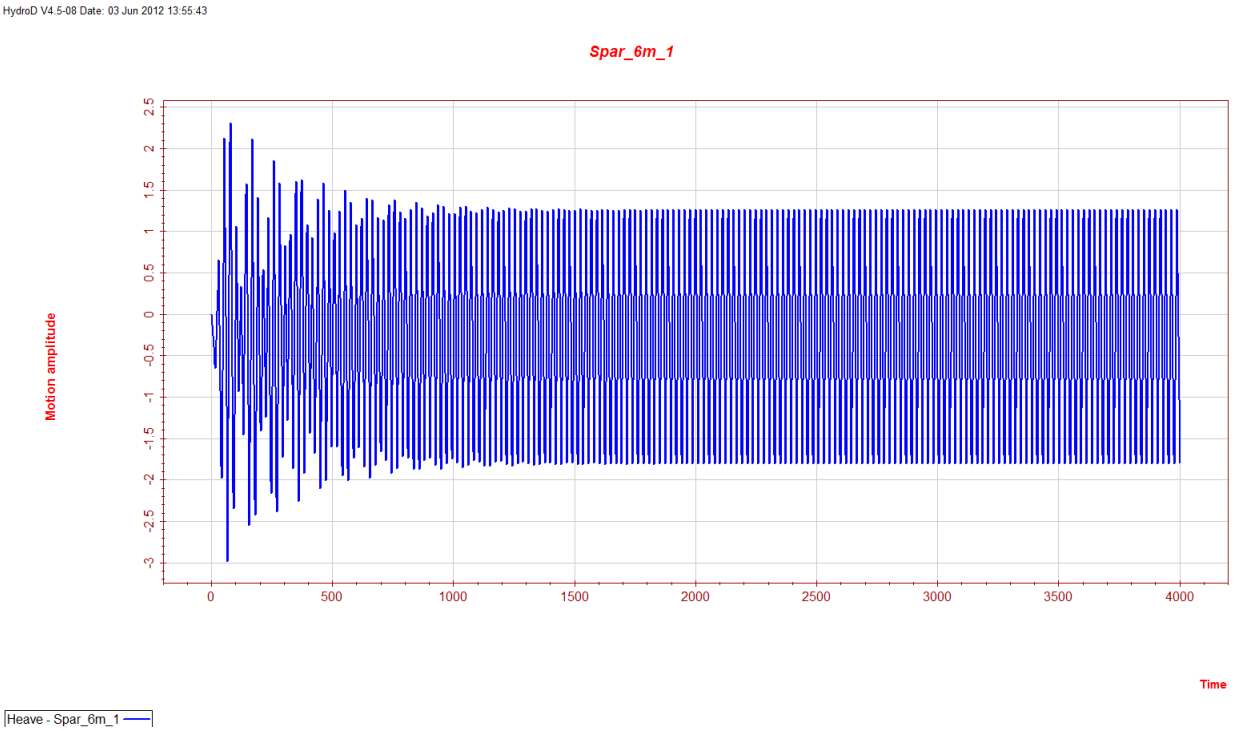

Figure 8.22: Heave motion from linear Wasim analysis with T=22.6s and amplitude 6 m.

Although many attempts were made to trigger the Mathieu effect, it was not accomplished through analysis in Waqum. Attempts were made to lower the damping as much as possible, analysis with and without convolution integrals was tested, amplification of forces to provoke

reaction, smaller time step and other similar things were tried without success.

With more time an FFT would be preformed on the spar buoy time series from Wasim to compare with the Waqum time series.

The spar buoy was studied intensively in this thesis for two reasons; learning more about non linear effects (which are known to appear with the concept), and to verify that Wasim and Waqum can be used for the Octabuoy analysis. Wasim analysis turned out good and are assumed to be trust worthy. The same verification has not been made with Waqum. Still all analyses of the Octabuoy in Waqum were carried out and the results are assessed in the chapter 8.4.

8.4 Octabuoy in Waqum

WAQUM RESULTS, HEAVE AND PITCH				
Analysis	Heave MPL [m]	Heave Standard Deviation	Pitch MPL [deg]	Pitch Standard Deviation
1y1	0.3162	0.411	0.2676	0.0348
1y2	0.4057	0.0531	0.3029	0.0396
10y1	0.7507	0.0987	0.4314	0.0567
10y2	2.2768	0.3040	0.8099	0.1081
100y1	1.1407	0.1509	0.5186	.0.686
100y2	5.2941	0.7158	1.3957	0.1887
100y3	4.4597	0.6015	1.6717	0.2254
100y4	6.6430	0.8998	1.7975	0.2434
1000y1	14.8874	2.0290	2.2123	0.3015

Table 8.5: Results from the Waqum analysis in both heave and pitch.

A linear run of all the sea states from the Wasim analysis was preformed in Waqum. The heave results from all analyses are showed in table 8.1. From this and the histograms it can be seen that the Waqum results are in quite good agreement with the Wasim results for most sea states. However in the largest sea states, especially the final two, the heave motion becomes very large, 69% larger than the linear results at the most. In pitch however, Waqum is in good agreement with Wasim in all the sea states.

What is the reason for the large heave values in the final runs? This could perhaps been identified by checking whether the change is frequency dependent or amplitude dependent. If the large part of the energy of the spectra is still contained in an area similar to the lesser sea states the problems are probably not frequency dependent. This again can indicate that it is not connected with acceleration and the frequency dependent added mass. If the reason is the large amplitude of the sea state then this can indicate that some non linearity is occurring despite Waqums linear build up. More verification is needed and a monitoring of the different forces could be used to observe where the change occurs.

Waqum offers the possibility to insert forces, and this was used for testing of mooring line configurations. 4 different mooring line configurations were tested, two from MARINTEK's model test pull outs and two from pull out tests in Orcaflex.

WAQUM RESULTS HEAVE AND PITCH CHEVIOT ANCHOR LINE ORCAFLEX				
Analysis	Heave MPL [m]	Heave Standard Deviation	Pitch MPL [deg]	Pitch Standard Deviation
1y1	0.3162	0.411	0.2766	0.0360
1y2	0.4057	0.0531	0.7430	0.0973
10y1	0.7507	0.0987	0.7121	0.0936
10y2	2.2768	0.3040	1.2330	0.1646
100y1	1.1407	0.1509	1.0431	0.1380
100y2	5.2941	0.7158	2.9461	0.3307
100y3	4.4597	0.6015	4.5346	0.6116
100y4	6.6430	0.8998	5.8604	0.7938
1000y1	14.8874	2.0290	3.3674	0.4589

Table 8.6: Results from the Waqum analysis in both heave and pitch with Cheviot field mooring lines found in Orcaflex.

WAQUM RESULTS HEAVE AND PITCH CHEVIOT ANCHOR LINE MODEL TEST				
Analysis	Heave MPL [m]	Heave Standard Deviation	Pitch MPL [deg]	Pitch Standard Deviation
1y1	0.3162	0.4116	0.3028	0.0394
1y2	0.4057	0.0531	0.8546	0.1119
10y1	0.7507	0.0987	1.3045	0.1715
10y2	2.2768	0.3040	1.2330	0.1837
100y1	1.1407	0.1509	0.7482	0.0990
100y2	5.2941	0.7158	1.7527	0.2369
100y3	4.4597	0.6015	8.2614	1.1142
100y4	6.6430	0.8998	4.7020	0.6369
1000y1	14.8874	2.0290	10.4118	1.4200

Table 8.7: Results from the Waqum analysis in both heave and pitch with Cheviot field mooring lines found from model test.

The analyses are fast and the results are promising. From the tables 8.6 and 8.7 it can be seen that the pitch motion seems to increase when the mooring lines are applied. For the Cheviot field the run with mooring lines with model test values in most cases have larger pitch values than the one with Orcaflex mooring lines. This is consistent with the fact that MARINTEKS pull out test gave larger values for the Cheviot field restoring. The heave motion seems completely unaffected. As discussed in chapters 2 and 4 there is coupling between surge and pitch and the mooring lines can introduce heeling and pitch movement. This might lead to an increase in the pitch. The unaffected heave motion is be questioned, but at this stage accepted because the forces are only applied to the horizontal degrees of freedom. No coupling between heave and surge/sway has been added in Waqum. This thesis has main focus on the vertical degrees of freedom and the horizontal are not studied. To discern whether the results obtained here are correct, a more thorough analysis including the horizontal degrees of freedom is needed. The Gulf of Mexico results can be found in the appendix.

In the simulations, the water is assumed to be very deep. Because of this the dynamic effect of

mooring lines will in reality probably become quite large. Viscous effect, inertia mass and current force on mooring system should ideally have been taken into considerations in the analysis of the motion response. The floater and the mooring system should be calculated together as a coupled dynamic system. This would mean solving equations containing the dynamic characteristics of mooring system and the six degrees of freedom of the rigid body motion at the same time. This type of equation could in the future be inserted into Waqum for a complete analysis.

8.5 CFD

There were many difficulties with the CFD analysis. The idea was that this could be run quite easily and then a sensitivity analysis could be preformed to see how much the viscous damping affected the spar motion. To compare, a run with linearized damping was also planned.

To verify that the CFD analysis were correct, LSQ was preformed on the complete force signal (not only the viscous part). The acceleration term of the LSQ would then be compared to the added mass from Wadam to make sure that they were of the same order of magnitude. If this was confirmed then the viscous part of the force signal would be inserted into the LSQ and the velocity term would be added to the Waqum run to check the effect of the viscous damping. Before the LSQ could be preformed, the restoring force signal was subtracted from the total signal. The script from the LSQ operation can be found in the appendix. Unfortunately the LSQ did not give the right results. This could be due to an error in the signal, but more probably due to an error in the post processing. It may be that the added mass is affected by for instance the Keulegan Carpeter number and therefore is not the same as the added mass found in linear frequency domain analysis. However, there was no more time to figure out why the CFD signal was not acting according to expectations.

If one can assume a linear system, Faltinsen[**?**] shows how one can decompose the force components of the signal. To find the added mass one can multiply the equation of motion by the acceleration and integrate over one period/multiple of one period. This will give zero contribution from the damping part of the signal, since it is 90 degrees out of phase with the acceleration.

$$F_z = -A_{33}\ddot{x} - B_{33}\dot{x} - C_{33}x(1) \tag{8.3}$$

$$A_{33} = \frac{\int_{-\frac{T}{2}}^{+\frac{2T}{3}} (Fz(t)\ddot{x})\,\mathrm{d}t - \int_{-\frac{T}{2}}^{+\frac{2T}{3}} C_{33}x\ddot{x}\,\mathrm{d}t}{\int_{-\frac{T}{2}}^{+\frac{2T}{3}} \ddot{x}\ddot{x}\,\mathrm{d}t} \tag{8.4}$$

The same operation can be preformed to obtain the damping. Then the equation must be multiplied with the velocity and integrated in which case the added mass and restoring will give zero contribution.

$$B_{33} = \frac{\int_{-\frac{T}{2}}^{+\frac{2T}{3}} (Fz(t)\dot{x}\,\mathrm{d}t}{\int_{-\frac{T}{2}}^{+\frac{2T}{3}} \dot{x}\dot{x}\,\mathrm{d}t} \tag{8.5}$$

With more time attempts this would have been used to try to find the added mass and damping through this method.

A simple CFD analysis was also envisioned for the Octabuoy. This was considered especially interesting with regards to the octagonal pontoon. Since the CFD on the much simpler spar geometry did not work and time ran out this could not be completed.

8.6 Wasim and Waqum

Wasim and Waqum are quite different programs both in terms of how the they calculate, what is demanded of the user, and not in the least the CPU time. If nothing is added to Waqum, it will only do a linear analysis and its main advantage over Wasim is that it is a very fast solver. A large analysis of 3 hours duration is solved in a matter of minutes. This makes testing different input, like different sea states or waves much easier. Additional linear and non linear forces may be added and taken into account equally fast. However this is also the feature that demands most from the user, who needs a certain amount of knowledge for the program to be useful. Since all non linear effects have to be added as a force, the user needs to know exactly what input is needed to capture such an effect. If the object of analysis is unknown to the user, this is difficult.

Wasim is a good program when the non linear effects are important and particularly if the mooring line effects are not as important. Wasim has large CPU time and analysis are time consuming as well as computer space demanding.

Chapter 9

Conclusion

Non linear effects are important in the motion characteristics of a spar buoy, and the platform concept was used as a benchmark for analyses and as a starting point for learning and discussing non linear effects and mooring lines. The non linear effects are to a large extent captured by analysis in the time domain analysis software Wasim. Analyses run in the impulse response function program Waqum were not able to capture the same effects. This may be due to the inexperienced user. All effects outside of the linear frequency domain must be added by the user. Many attempts were made to trigger the Mathieu effect, but in the end the efforts were unsuccessful.

The Octabuoy platform developed by Moss Maritime was analysed in both Wasim and Waqum. Wasim analyses gave good results and the difference between linear and non linear analysis could be addressed. From the results it seems that the heave motion of the Octabuoy is relatively unaffected by non linear analysis. The pitch motion sees a large increase when the analysis is non linear. When the analyses were repeated in Waqum the results were promising. Up to the largest sea states, Waqum was in very good agreement with the linear Wasim results. This is expected when no additional effects are added to the program. Four different mooring line configurations were then tested on the Octabuoy in Waqum. The analysis showed that mooring lines led to a slight increase in the pitch results. The pitch motion is coupled with the surge motion which may be an explanation to the increase. Only the vertical degrees of freedom have been considered in the thesis. A more thorough analysis which also looks at the horizontal degrees of freedom is needed to discern whether the results are physically correct. The analyses did not include any viscous forces or transverse drag effects on the mooring lines. This should ideally be included, and through Waqum this can probably be done.

Working with Wasim through HydroD has been a challenging experience, and learning how to run the analysis through Python was a great relief. Wasim analyses takes a long time but the analyses are very comprehensive. Waqum allows for fast changes in the analysis and is ideal for screening. However, in this program the user must be very clear on what is being researched. Any non linear effect has to be added manually which requires much understanding from the user. Prospects are good for many types of non linear analyses in Waqum.

Chapter 10

Recommendations for Future Work

The master thesis has introduced new questions and possible analyses. Much remains unanswered at the end of the thesis. First of all is the issue with the failed spar analysis in Waqum. Being unable to recreate Haslum's experiments in Waqum is the primary lack of this thesis. As can be read in section 8.3, many things were attempted to solve the problem, but of course there is much which has not been tried. Perhaps the result is connected to the ramp time used or the length of the transient? These are things that could be looked into at a later stage.

Waqum introduces the possibility of adding many effects which are not included in Wasim. One aspect which has been mentioned is including transverse drag and other mooring line forces to the analysis. Further exploration of the possibilities into damping models in Waqum could reveal further useful areas for this software.

A recreation of the results found by Lui et al with a model where the free surface is modelled correctly could confirm or negate the claims made in their thesis. A wider range of periods would then be desirable to test. Are slowly varying forces triggering other non linear effects on a spar then the Mathieu? And if such is the case, are spar buoys these days built to withstand this load?

The results of the Octabuoy with regards to linear vs. non linear analysis are based on the results of 9 different sea states, each run only one time linearly and one time non linearly. For more thorough and reliable statistical data several analyses should be run at each sea state. From these more elaborate and more accurate statistics can be found. Had there been time for it in this master thesis a Monte Carlo simulation would be performed for each sea state to check the spreading of the time series sample. Also, with the difference found between linear and non linear analysis in the vertical rotational degrees of freedom it would be interesting to model the Octabuoy with the ideal deadrise angle to see whether this eliminates the non linear effect.

Finally, the viscous damping which was approached through STAR CCM+ should be finished and the damping added to the Waqum analysis. If the Mathieu effect is triggered in Waqum, the effect of the viscous damping would be especially interesting to observe.

In the digital appendix, many of the sources given in the bibliography are included, along with results, CFD time series etc. If any of the suggested work is carried out this could be a good starting point.

Bibliography

[1] Conversation with T. Vada
By mail, feb/march 2012 and visit 24/02-2012

[2] DNV
Luva - Octabuoy motion analysis
July 2011

[3] Henning Braaten of MARINTEK
Meeting Tuesday 29/11-2011

[4] Q.W. Ma, M.H. Patel
On the non linear forces acting on a floating spar platform in ocean waves
Applied Ocean Research nr 23, 2001

[5] Z. Jingrui, T. Yougang, S. Wenjun
A study on the Combination Resonance Response of a Classical Spar Platform
Journal of Vibration and Control, 2010.

[6] H. A. Haslum, O. M. Faltinsen
Alternative Shape of Spar Platforms for Use in Hostile Areas
Offshore Technology Conference 1999.

[7] Recommended Practice, DNV-RP-C205
Environmental conditions and environmental loads
April 2007

[8] W.C. Xie
Dynamic Stability of Structures
Cambridge University Press, 2006

[9] H. A. Haslum
Simplified Methods Applied to Nonlinear Motion of Spar Platforms
Department of Marine Hydrodynamics
Faculty of Marine Technology
Norwegian University of Science and Technology, 2000

[10] M.Greco
Lecture Notes TMR4215 Sea Loads
Fall 2010

[11] O.M. Faltinsen.
Sea Loads on Ships and Offshore Structures
Cambridge University Press 1990.

[12] ITTC- Recommended procedures
Numerical estimation of roll damping
Revision 00, 2011

[13] A.R. Grilli, J. Merrill, S.T. Grilli, M.L. Spaulding and J.T. Cheung
Experimental and Numerical Study of Spar Buoy-magnet/spring Oscillators Used as Wave Energy Absorbers
Proceedings of the Seventeenth International Offshore and Polar Engineering Conference
Lisbon, Portugal, July 1-6, 2007

[14] Y. Lui, H. Yan and TW Yung
Nonlinear Resonant Response of Deep Draft Platforms in Surface Waves
Proceedings of the ASME 2012 29th International Conference on Ocean, Offshore and Arctic Engineering

[15] B. J. Koo, M. H. Kim and R. E. Randall
Mathieu instability of a spar platform with mooring and risers
Ocean engineering 2004, vol. 31.

[16] DNV
Wasim-User's Manual

[17] DNV
Waqum-User's Manual

[18] J.V. Aarsnes
Lecture Notes "HYDROELASTICITY"
August 2011

[19] W.E. Cummins
The Impulse Response Function and Ship Motions
1962

[20] T.F. Orgilvie
Recent Progress Towards The Understanding And Prediction of Ship Motions
1962

[21] J.H. Mathews and K.K. Fink
Numerical Methods Using Matlab 4^{th} *edition*
Prentice-Hall Inc. New Jersey, 2004

[22] M. Peric and V. Bertram
Trends in Industry Applications of CFD for Maritime Flows
10^{th} International Conference on Computer and IT Applications in the Maritime Industries
Berlin May 2011

[23] S. Ransau
Lecture notes for the course:
Numerical Methods in Marine Hydrodynamics

[24] J.W. Sun, X.T. Fan, X.Z. Wan, S.X. Liu
Numerical Study on Hydrodynamic Behaviour of Deepwater Spar Platforms with Different Mooring Configurations
Applied Mechanics and Materials Vol. 137, 2012

[25] Specialist Committee on Deep Water Mooring
Final Report and Recommendations of the 22nd ITTC

[26] Z. Shu, T. Moan
Wave pressure Distribution Along the Midship Transverse Section of a VLCC
Proc. ASME 27th International Conference of Offshore Mechanics and Arctic Engineering Portugal 2008

[27] C.G Kring, Y.F. Huang, P. Sclavounos, T. Vada, A. Braathen
Nonlinear Ship Motions and Wave-induced Loads by a Rankine Method
Proc. 21st Symposium on Naval Hydrodynamics, Trondheim, Norway 1996

[28] MARINTEK
H. Braaten
Moss Maritime OCTABUOY - MODEL TESTS Cheviot and GOM Main Report
Bluewater Industries March 2011

Appendix A

A.1 Spar Buoy Analyses in Wasim

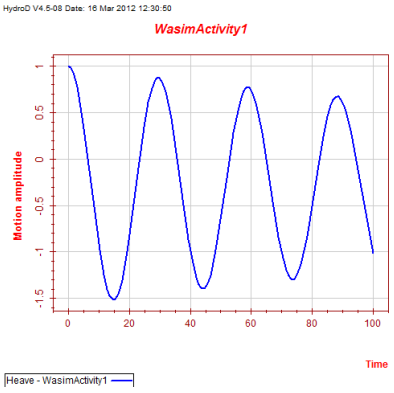

Figure A.1: Decay test heave.

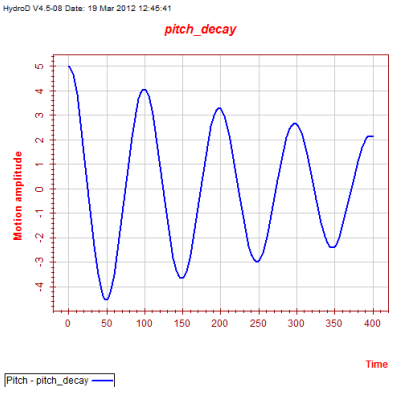

Figure A.2: Decay test pitch results in an eigenperiod 29.24 s.

A.1.1 Heave motion

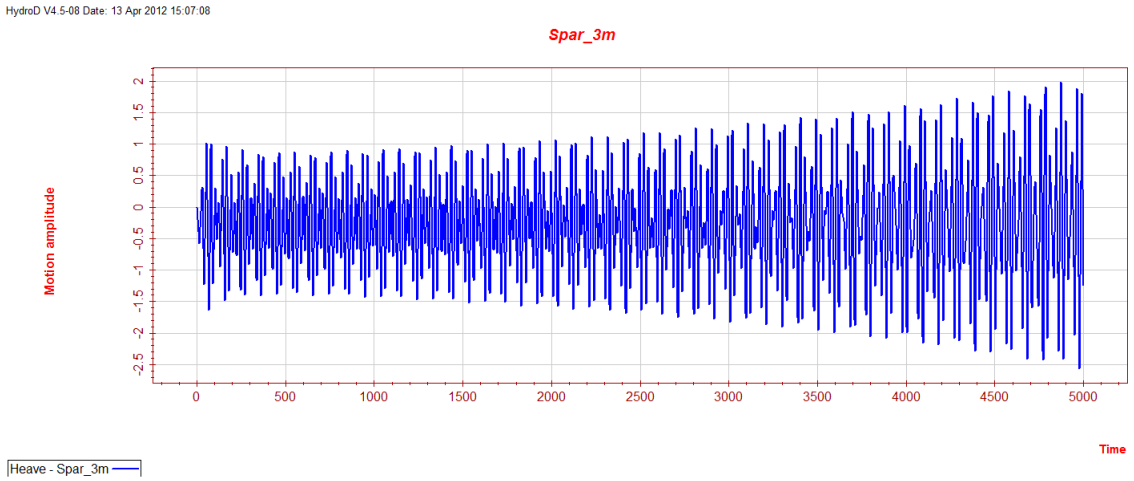

Figure A.3: Heave at regular wave with 3m amplitude and period of 22.6 s.

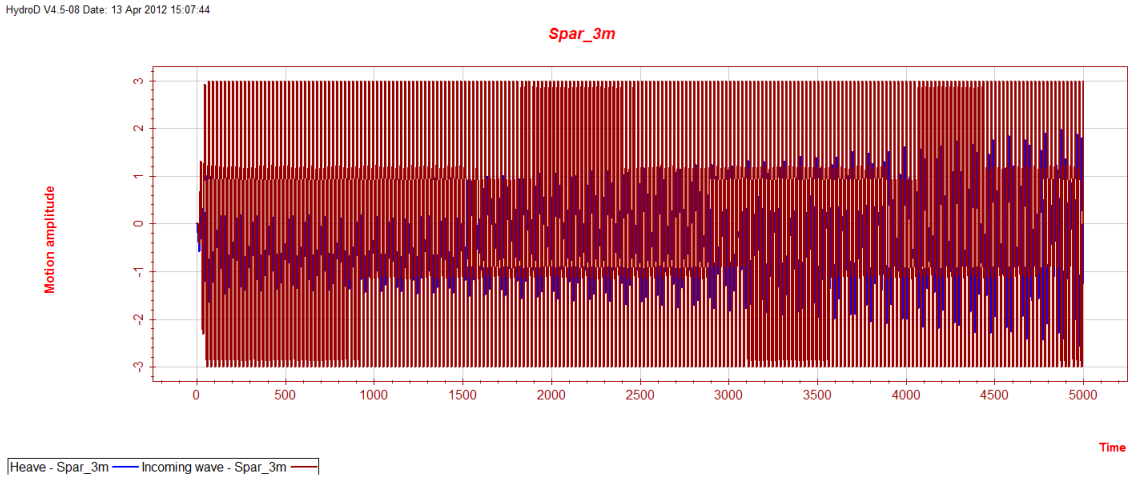

Figure A.4: Heave at regular wave with 3m amplitude and period of 22.6 s plotted together with the incoming wave.

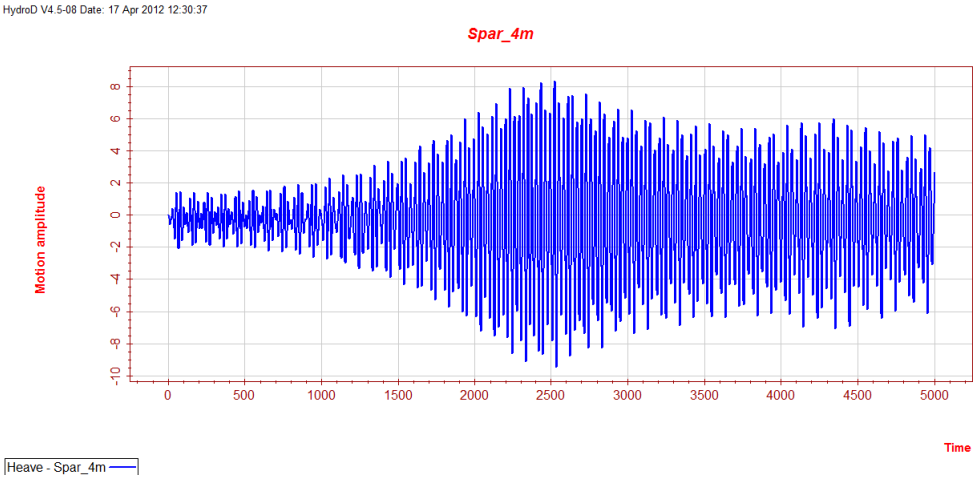

Figure A.5: Heave at regular wave with 4m amplitude and period of 22.6 s.

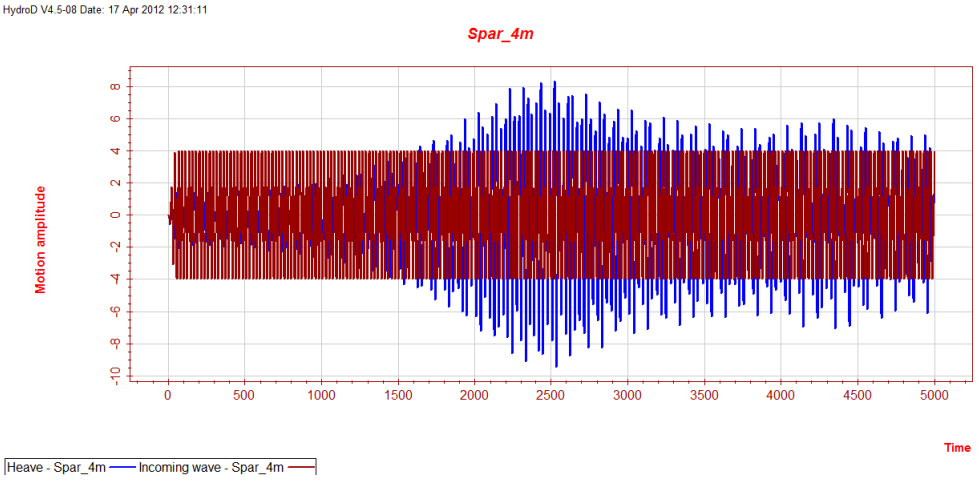

Figure A.6: Heave at regular wave with 4m amplitude and period of 22.6 s plotted together with the incoming wave.

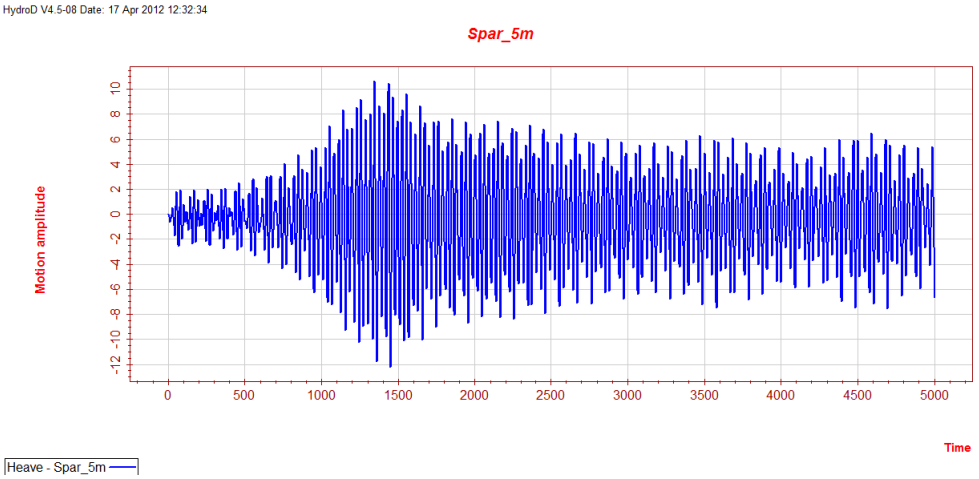

Figure A.7: Heave at regular wave with 5m amplitude and period of 22.6 s.

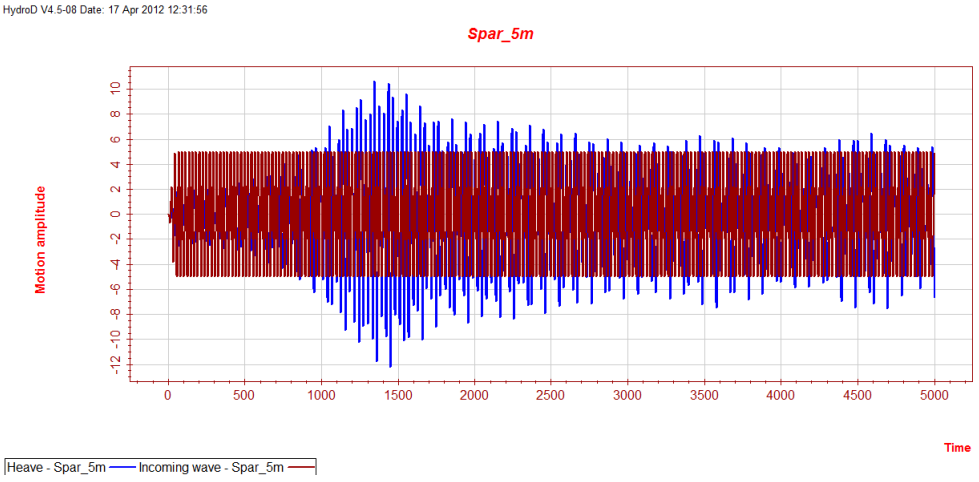

Figure A.8: Heave at regular wave with 5m amplitude and period of 22.6 s plotted together with the incoming wave.

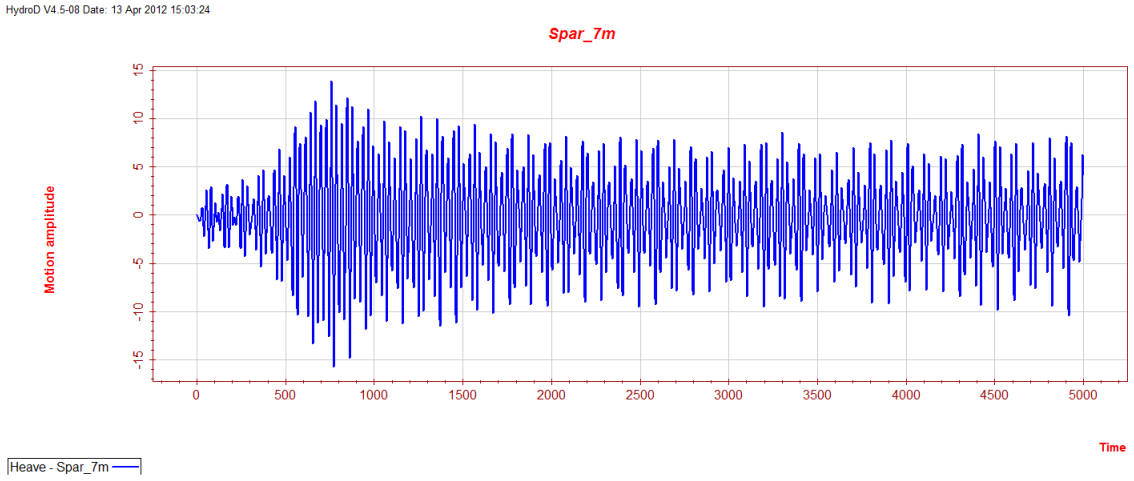

Figure A.9: Heave at regular wave with 7m amplitude and period of 22.6 s.

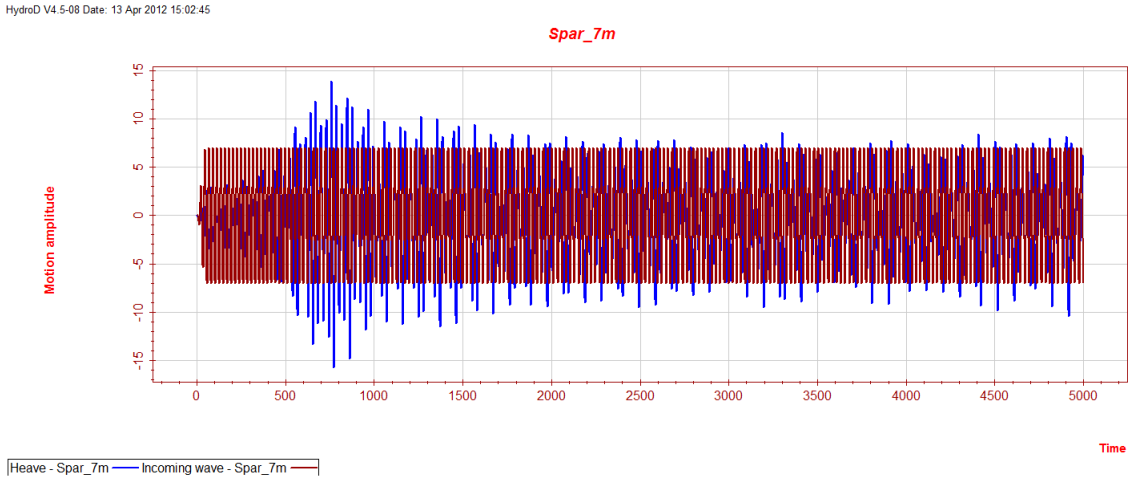

Figure A.10: Heave at regular wave with 7m amplitude and period of 22.6 s plotted together with the incoming wave.

A.1.2 Pitch Motion and ForceInspector

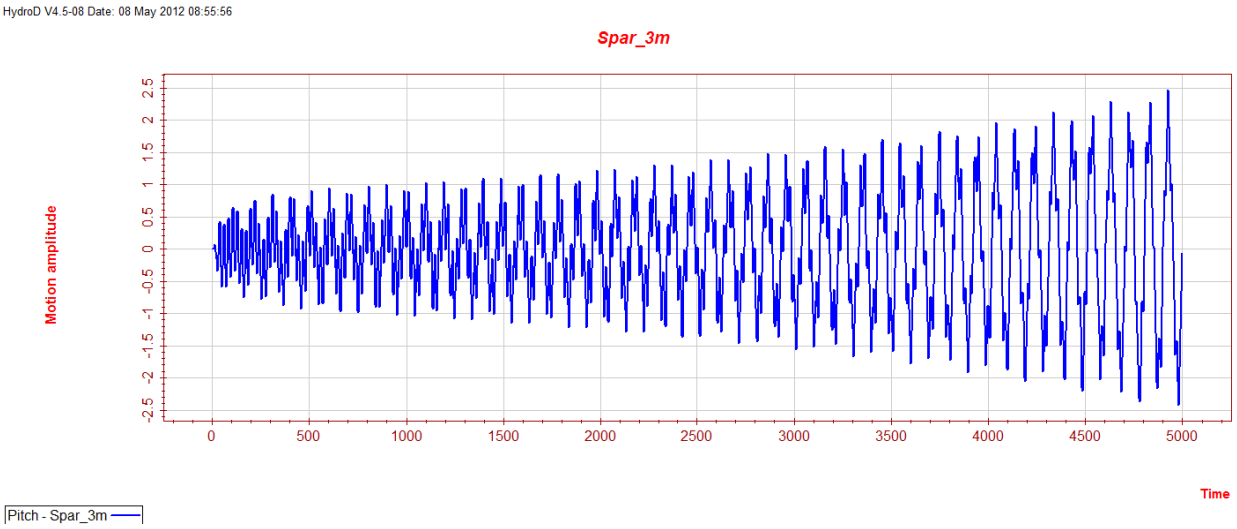

Figure A.11: Pitch, 3 m amp.

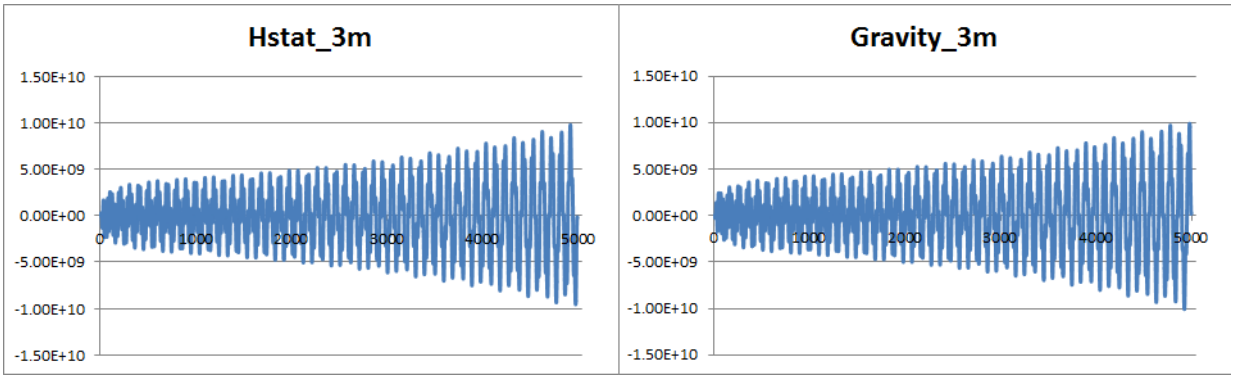

Figure A.12: Force signals gravity and hydrostatics in pitch, 3 m amp.

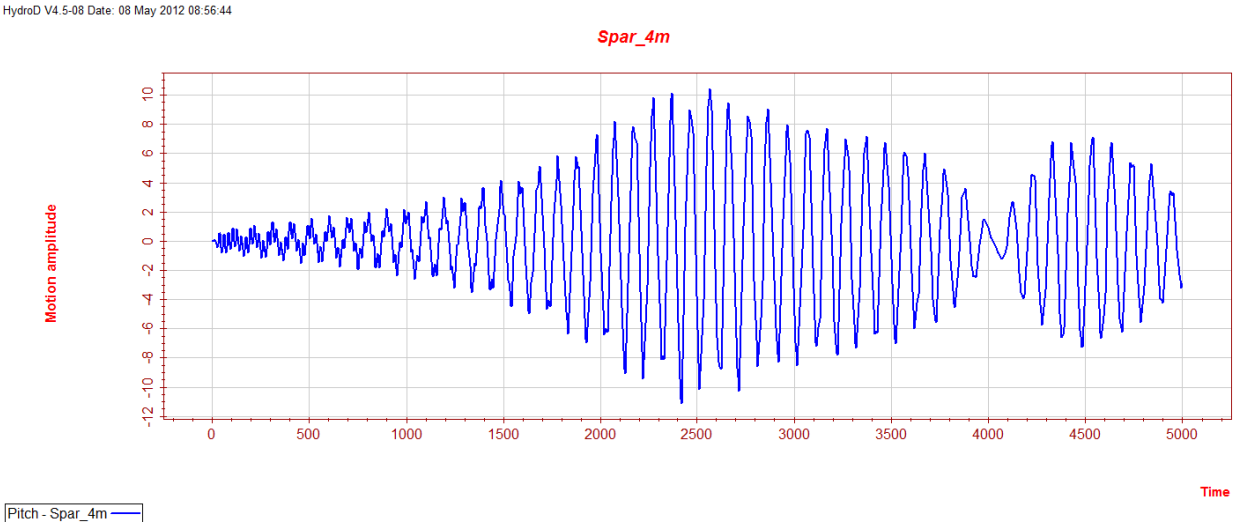

Figure A.13: Pitch, 4 m amp.

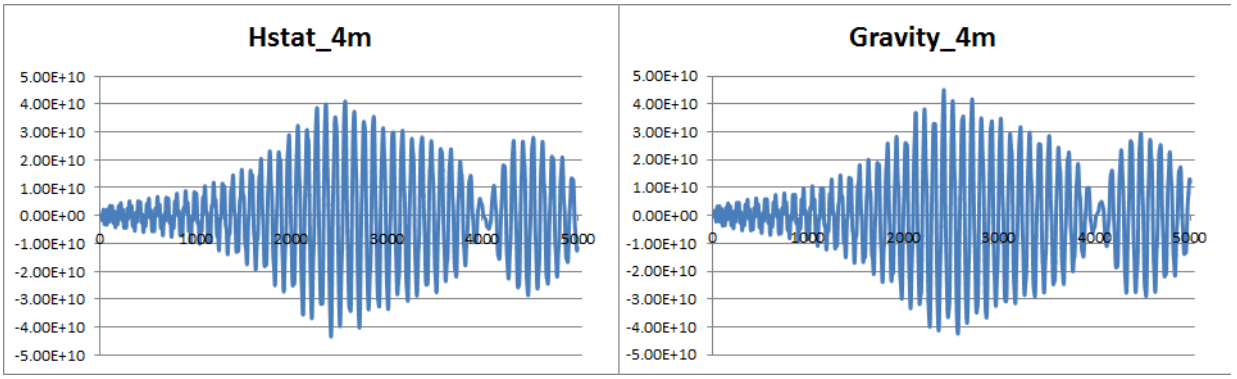

Figure A.14: Force signals gravity and hydrostatics in pitch, 4 m amp.

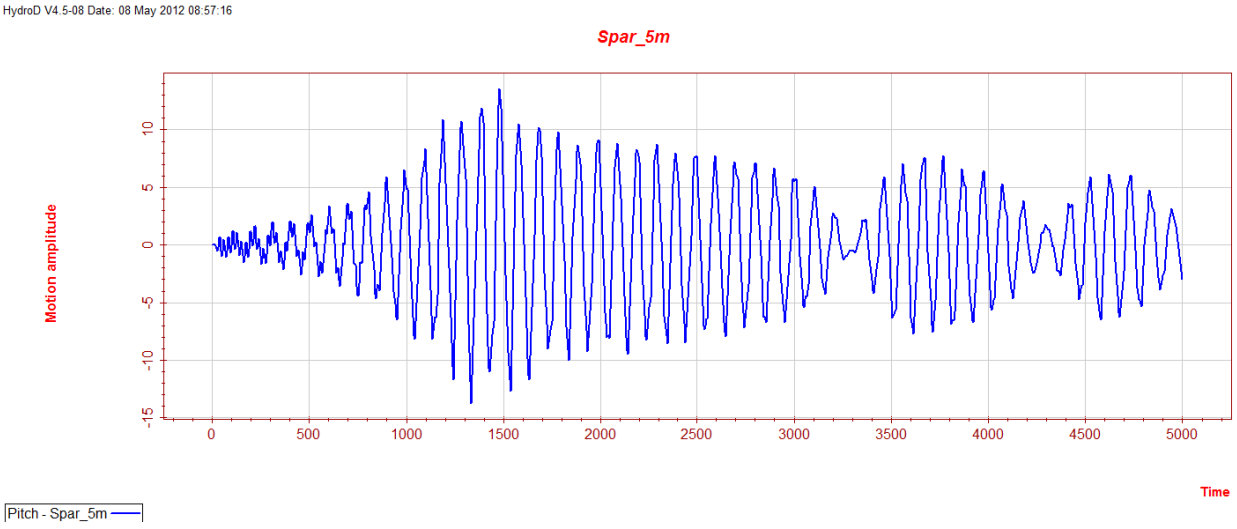

Figure A.15: Pitch, 5 m amp.

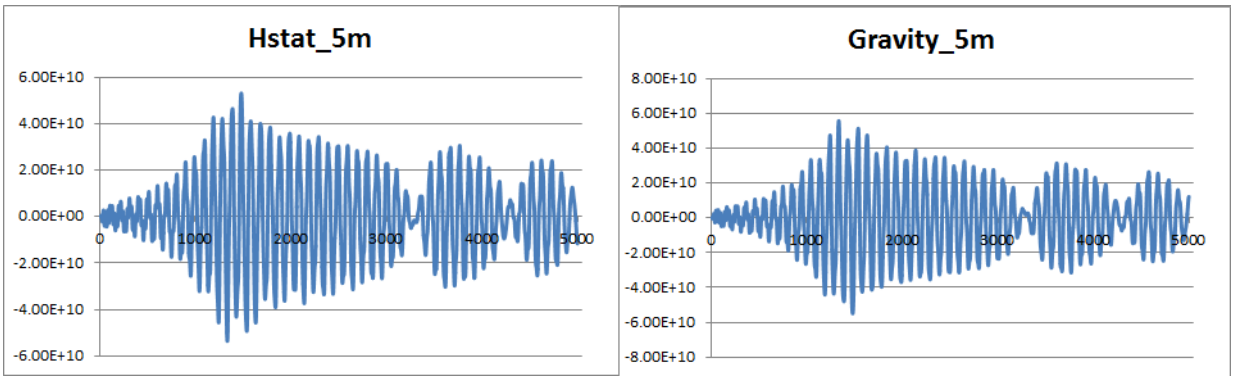

Figure A.16: Force signals gravity and hydrostatics in pitch, 5 m amp.

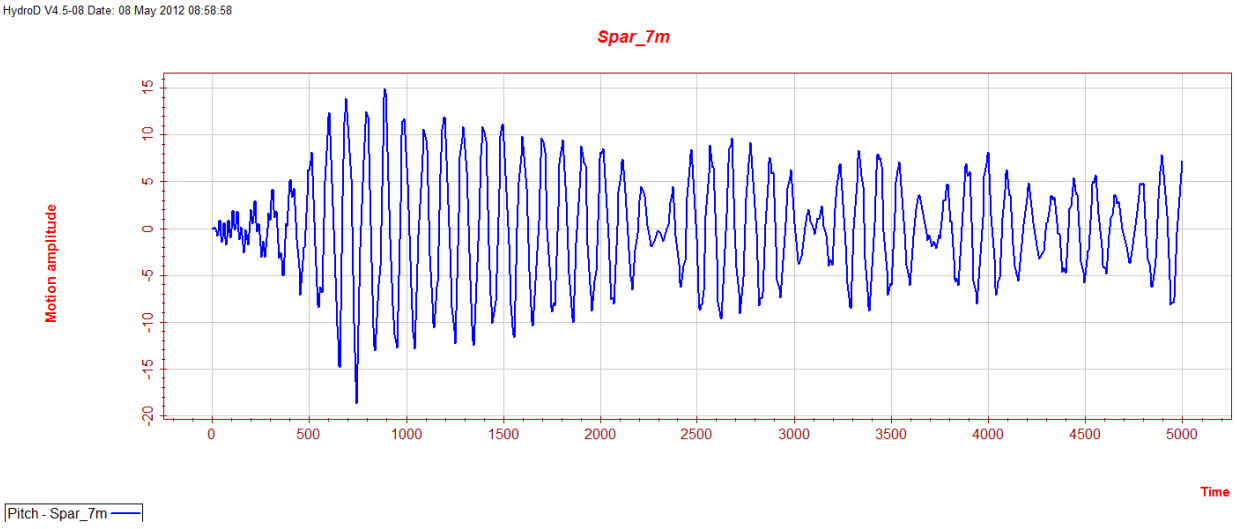

Figure A.17: Pitch, 7 m amp.

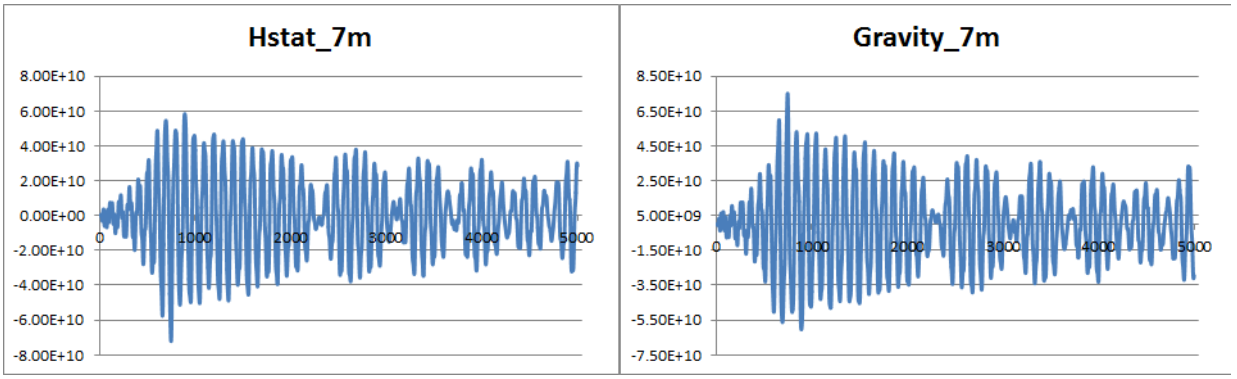

Figure A.18: Force signals gravity and hydrostatics in pitch, 7 m amp.

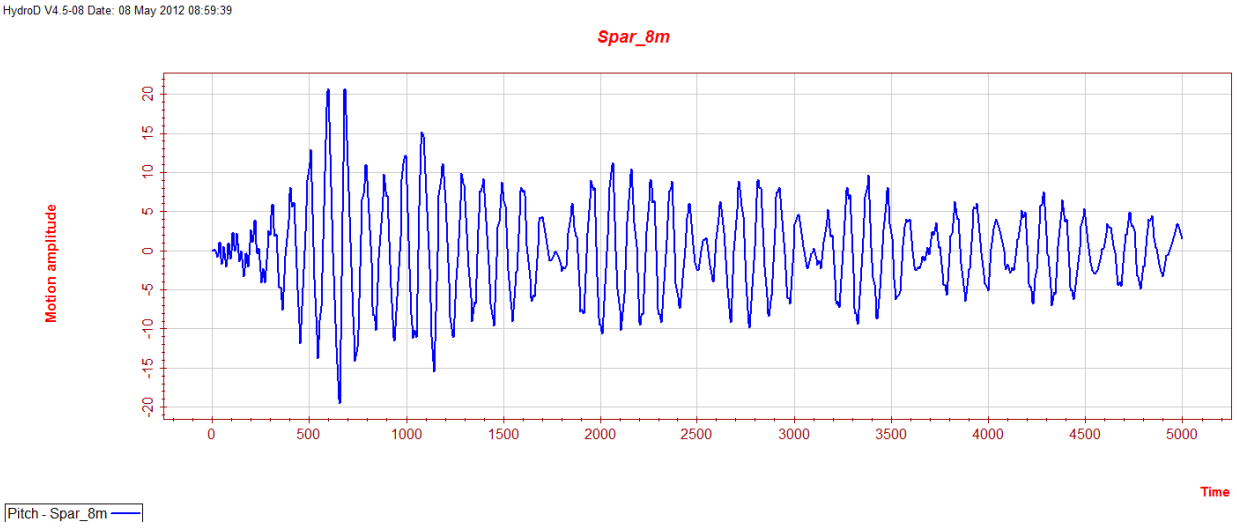

Figure A.19: Pitch, 8 m amp.

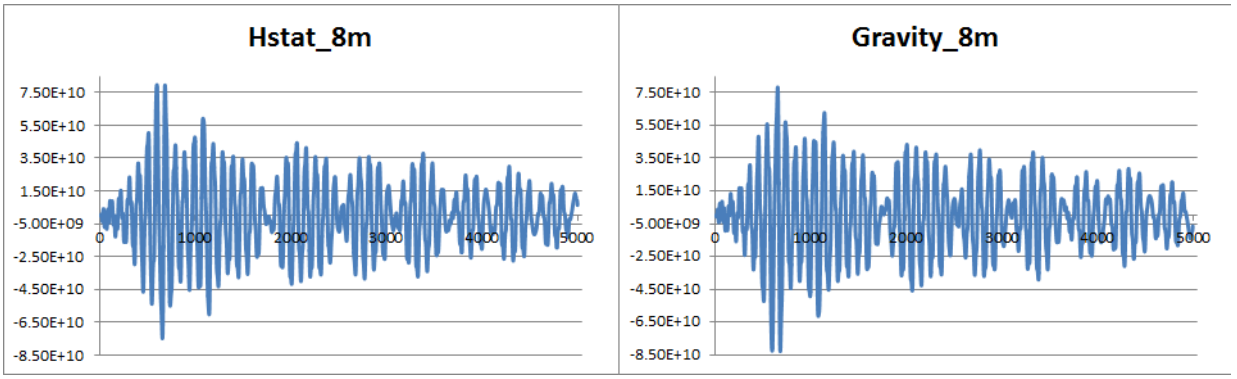

Figure A.20: Force signals gravity and hydrostatics in pitch, 8 m amp.

A.2 Octabuoy Analyses in Wasim

Results from the analysis of the Octabuoy in Wasim

	LINEAR				NON LINEAR			
1y1	average	min	max	std	average	min	max	std
HEAVE	-0.07	-0.21	0.08	0.04	-0.05	-0.25	0.11	0.04
PITCH	0.00	-0.12	0.12	0.03	-0.01	-0.88	1.01	0.21
1y2								
HEAVE	-0.07	-0.27	0.12	0.05	-0.06	-0.27	0.14	0.05
PITCH	0.00	-0.12	0.12	0.03	-0.01	-0.56	0.60	0.16
10y1								
HEAVE	-0.07	-0.40	0.26	0.09	-0.06	-0.46	0.31	0.10
PITCH	0.00	-0.18	0.20	0.05	-0.02	-1.42	1.43	0.27
10y2								
HEAVE	-0.07	-1.18	1.06	0.30	-0.10	-1.51	1.32	0.32
PITCH	0.00	-0.37	0.41	0.11	-0.02	-1.68	1.96	0.48
100y1								
HEAVE	-0.07	-0.61	0.48	0.15	-0.07	-0.80	0.42	0.16
PITCH	0.00	-0.23	0.24	0.07	-0.02	-0.94	1.24	0.26
100y2								
HEAVE	-0.07	-2.62	2.41	0.63	-0.20	-2.83	2.40	0.70
PITCH	0.00	-0.74	0.70	0.20	-0.03	-2.82	2.71	0.80
100y3								
HEAVE	-0.07	-2.48	2.44	0.56	-0.18	-3.29	1.90	0.62
PITCH	0.00	-0.88	0.72	0.19	-0.03	-2.99	2.95	0.80
100y4								
HEAVE	-0.07	-3.15	3.28	0.72	-0.24	-3.99	2.58	0.82
PITCH	0.00	-0.96	0.90	0.22	-0.01	-3.54	3.44	0.93
1000y1								
HEAVE	-0.07	-4.75	4.64	1.20	-0.35	-5.21	4.19	1.29
PITCH	0.00	-1.07	1.03	0.28	0.00	-3.65	4.81	1.21

Figure A.21: Statistical data from the Wasim analyses of Octabuoy.

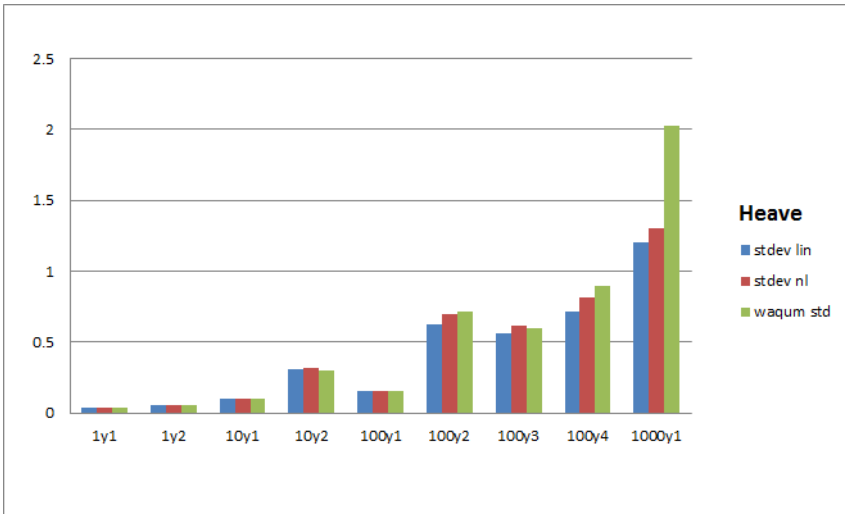

Figure A.22: Linear Heave motion sea state 1 year number 1.

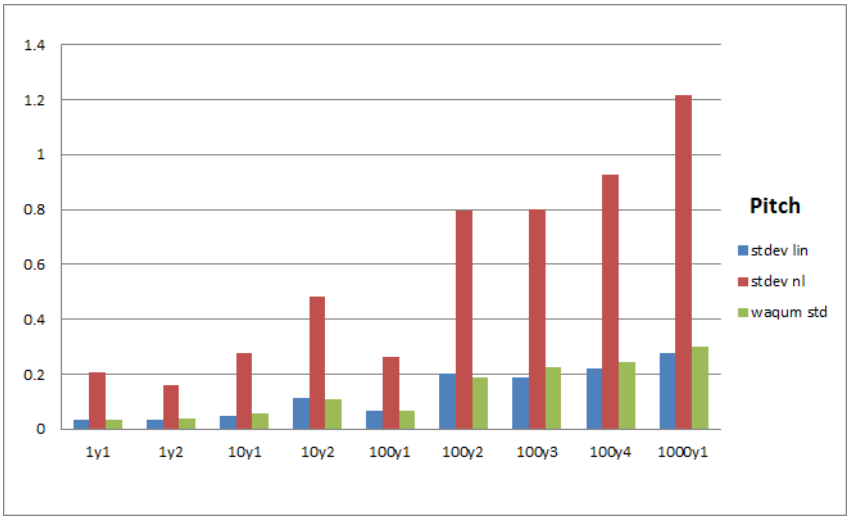

Figure A.23: Linear Heave motion sea state 1 year number 1.

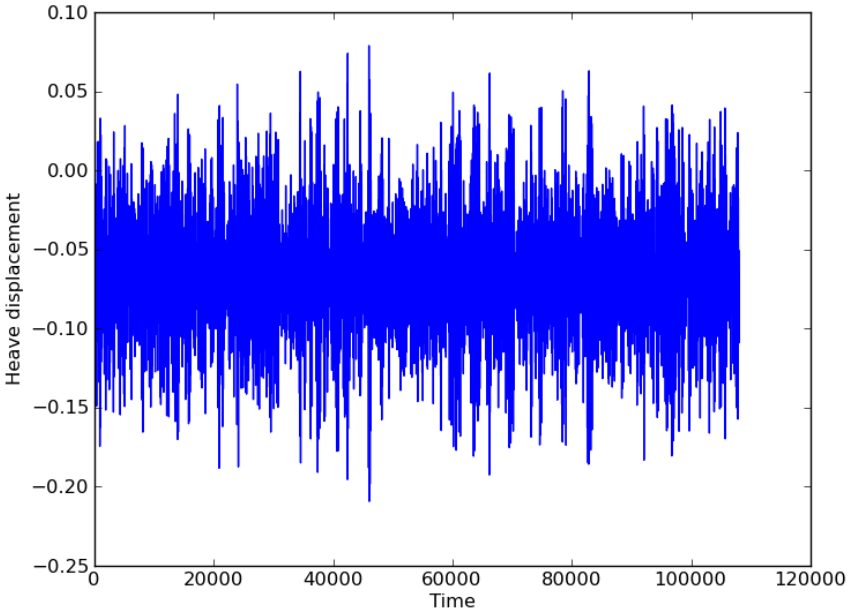

Figure A.24: Linear Heave motion sea state 1 year number 1.

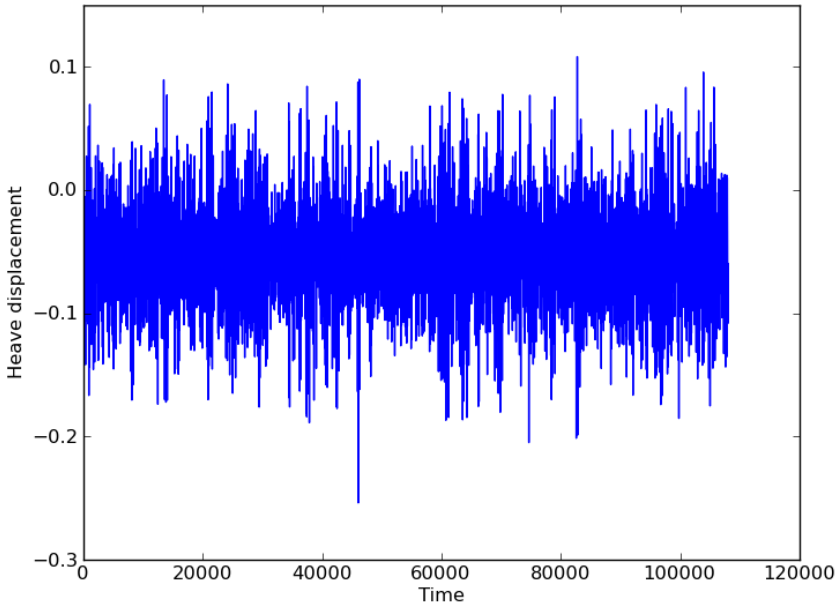

Figure A.25: Non Linear Heave motion sea state 1 year number 1.

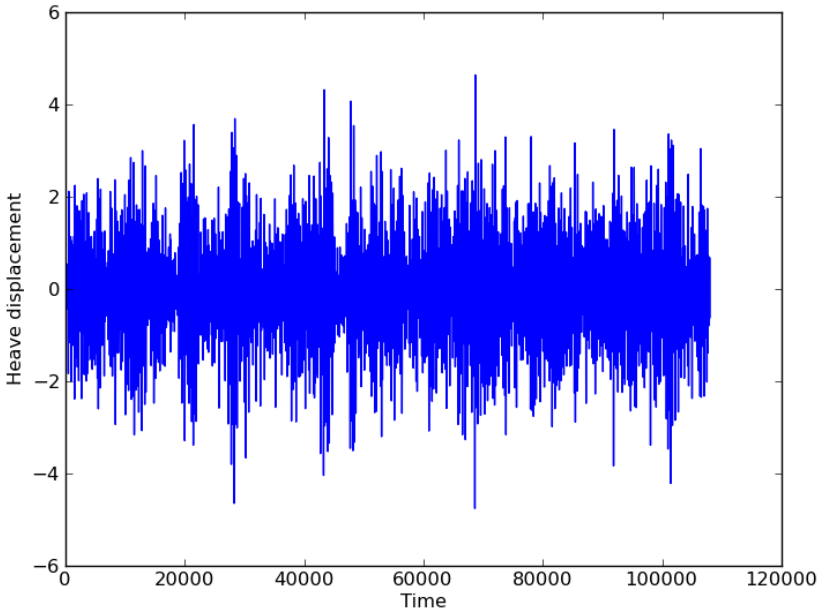

Figure A.26: Linear Heave motion sea state 1000 year number 1.

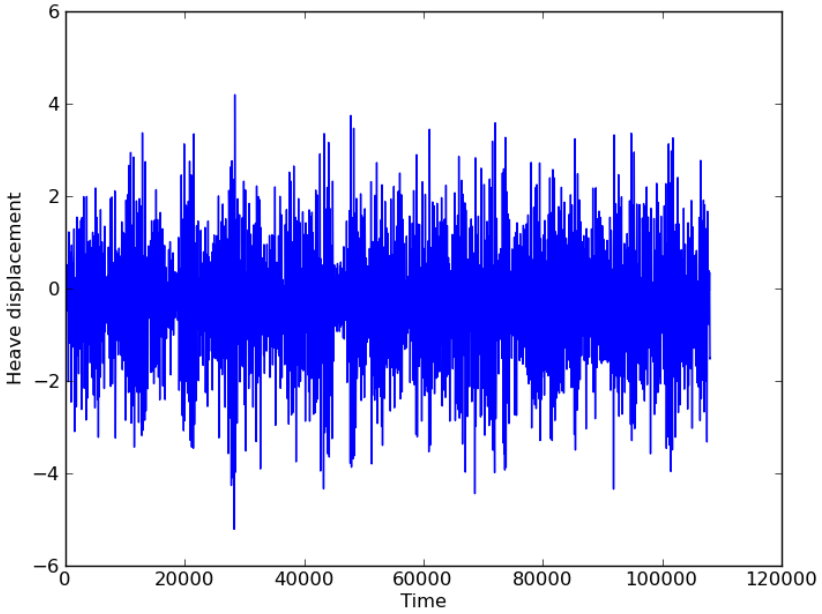

Figure A.27: Non Linear Heave motion sea state 1000 year number 1.

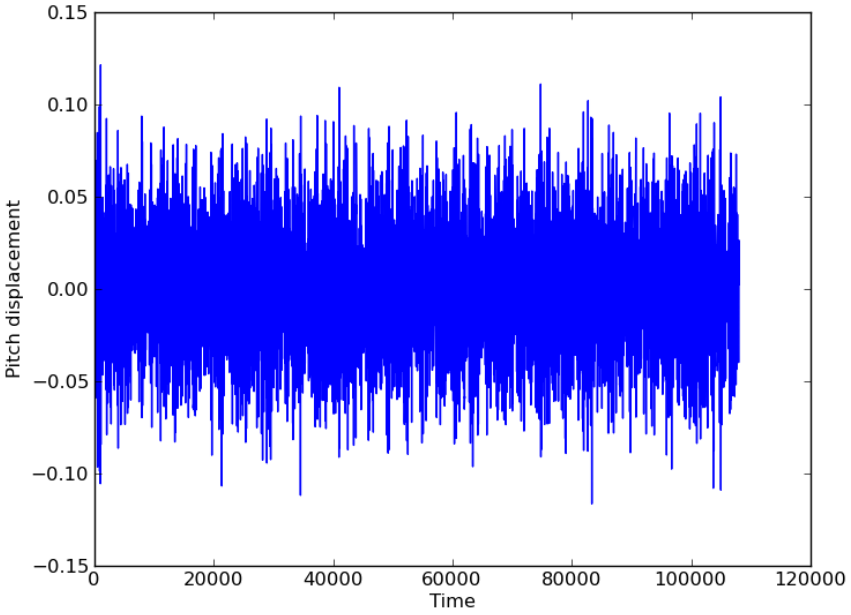

Figure A.28: Linear pitch motion sea state 1 year number 1.

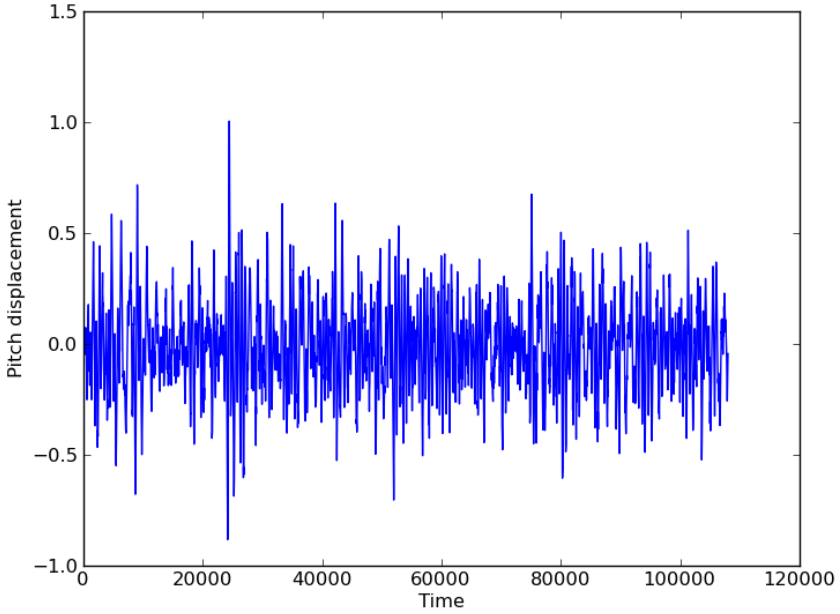

Figure A.29: Non Linear pitch motion sea state 1 year number 1.

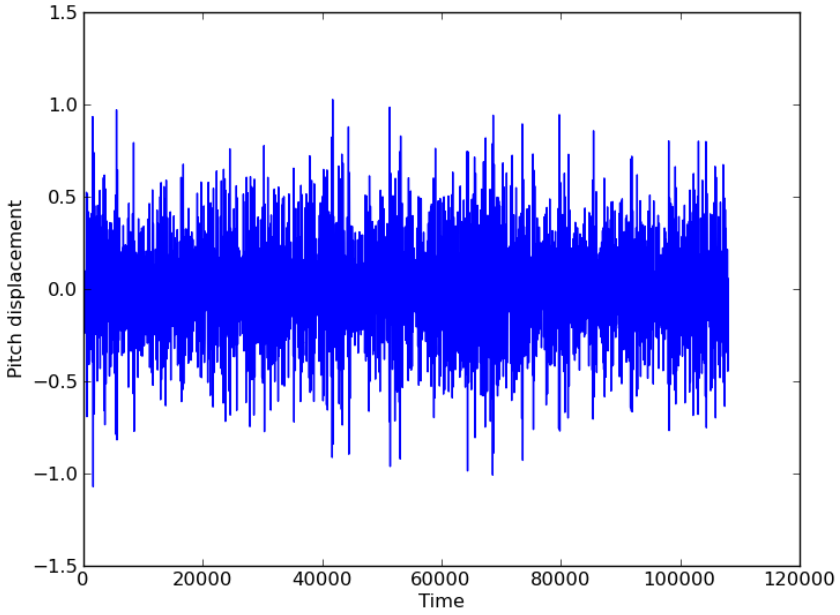

Figure A.30: Linear pitch motion sea state 1000 year number 1.

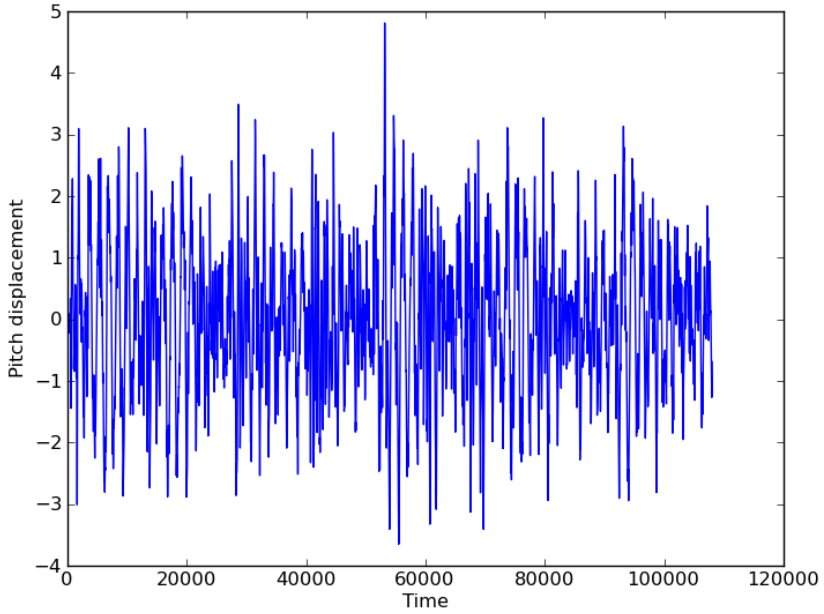

Figure A.31: Non Linear pitch motion sea state 1000 year number 1.

A.3 Spar Buoy in Waqum

Heave_decay		310_0.05	310_0.07	320_0.05	320_0.07	340_0.05	340_0.07	Mean	Standard Dev
Surge	max	1.45E-07	1.43E-07	1.45E-07	1.46E-07	1.43E-07	1.44E-07	1.44E-07	1.15379E-09
	min	0	0	0	0	0	0	0	0
Heave	max	1	1	1	1	1	1	1	0
	min	-0.94748	-0.94748	-0.94748	-0.94748	-0.94748	-0.94748	-9.47E-01	1.11022E-16
Pitch	max	1.48E-09	1.47E-09	1.49E-09	1.49E-09	1.47E-09	1.48E-09	1.48E-09	7.87102E-12
	min	-1.37E-09	-1.36E-09	-1.36E-09	-1.35E-09	-1.35E-09	-1.34E-09	-1.35E-09	9.86504E-12

Figure A.32: Results from decay with 1m vertical offset. The degrees of freedom where no displacement is mentioned all have a displacement of zero. 310 means a spring eigenfrequency of 310s and 0.05 means 5% critical damping. 320 means a spring with 310s eigenfrequency and 0.07 means a 7% critical damping etc.

Pitch_decay		310_0.05	310_0.07	320_0.05	320_0.07	340_0.05	340_0.07	Mean	Standard Dev
Surge	max	116.442	107.122	118.06	108.8	120.253	111.197	113.6457	4.881894327
	min	-132.886	-129.087	-135.105	-131.316	-139.185	-135.429	-133.835	3.229182077
Heave	max	0.000543	0.000543	0.000543	0.000543	0.000543	0.000543	0.000543	0
	min	-0.0005	-0.0005	-0.0005	-0.0005	-0.0005	-0.0005	-0.0005	9.06305E-09
Pitch	max	1	1	1	1	1	1	1	0
	min	-0.57094	-0.51971	-0.56768	-0.52815	-0.57562	-0.55667	-0.55313	0.021557974

Figure A.33: Results from decay with 1 rad offset. The degrees of freedom where no displacement is mentioned all have a displacement of zero. 310 means a spring eigenfrequency of 310s and 0.05 means 5% critical damping. 320 means a spring with 310s eigenfrequency and 0.07 means a 7% critical damping etc.

A.4 Results from CFD

	Total force	Total pressure force	Pressure force - Average force	Viscous force
Min	$2.07 * 10^9$	$2.07 * 10^9$	$-7.7 * 10^7$	$-1.72 * 10^5$
Max	$2.27 * 10^9$	$2.27 * 10^9$	$1.22 * 10^8$	$1.77 * 10^5$

Table A.1: Minimum and maximum values of the force and the force components.

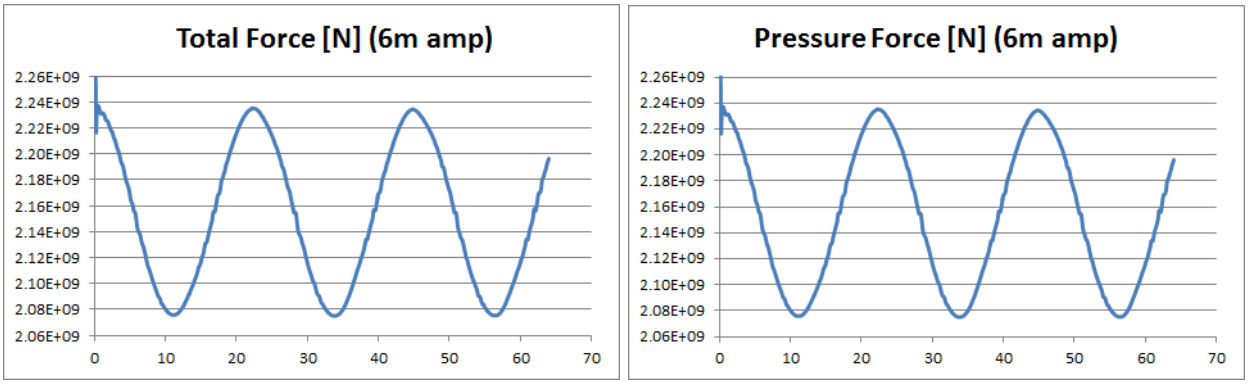

(a) Total force 6m amplitude

(b) Total pressure force 6m amplitude

Figure A.34: Total force and total pressure from CFD test at 6 m amplitude.

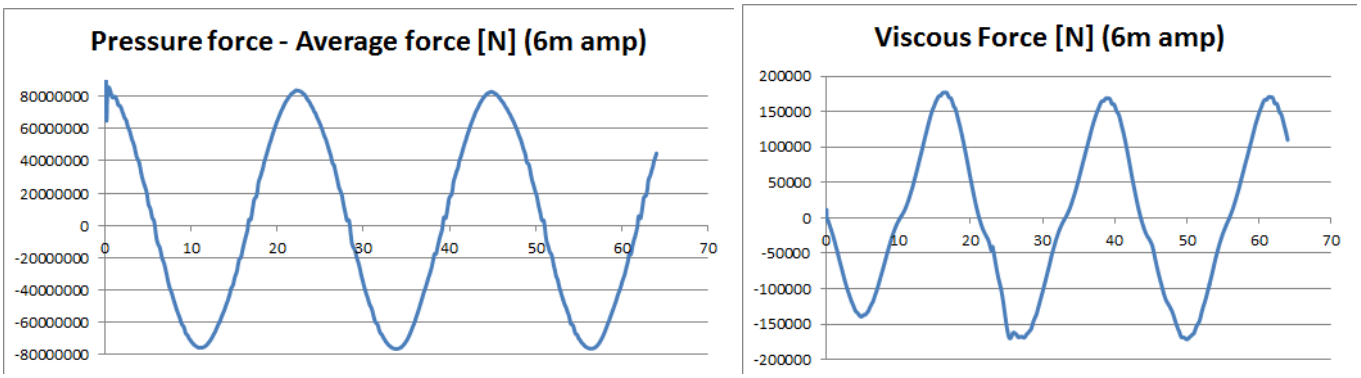

(a) Pressure force with average force subtracted (6m amplitude)

(b) Viscous force 6m amplitude

Figure A.35: Pressure force without the average value and total viscous force.

A.5 Octabuoy in Waqum

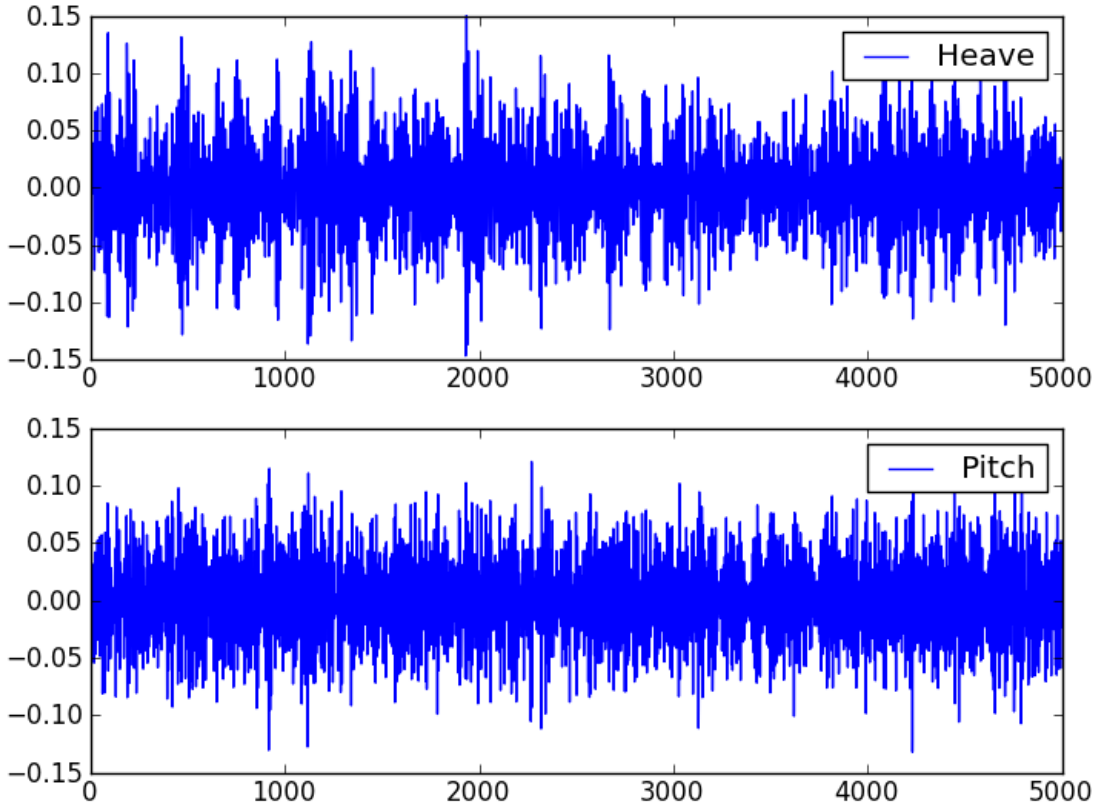

Figure A.36: Waqum analysis of Octabuoy, 1 year sea state number 1, no mooring line restoring added.

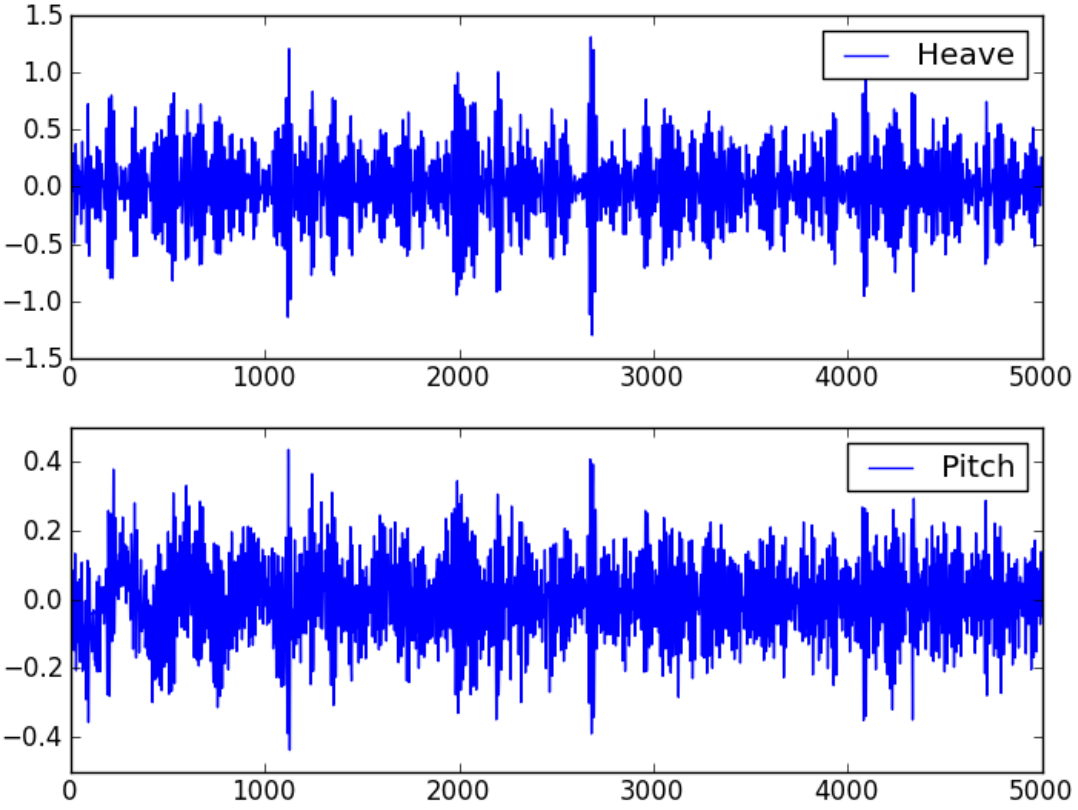

Figure A.37: Waqum analysis of Octabuoy, 10 year sea state number 2, no mooring line restoring added.

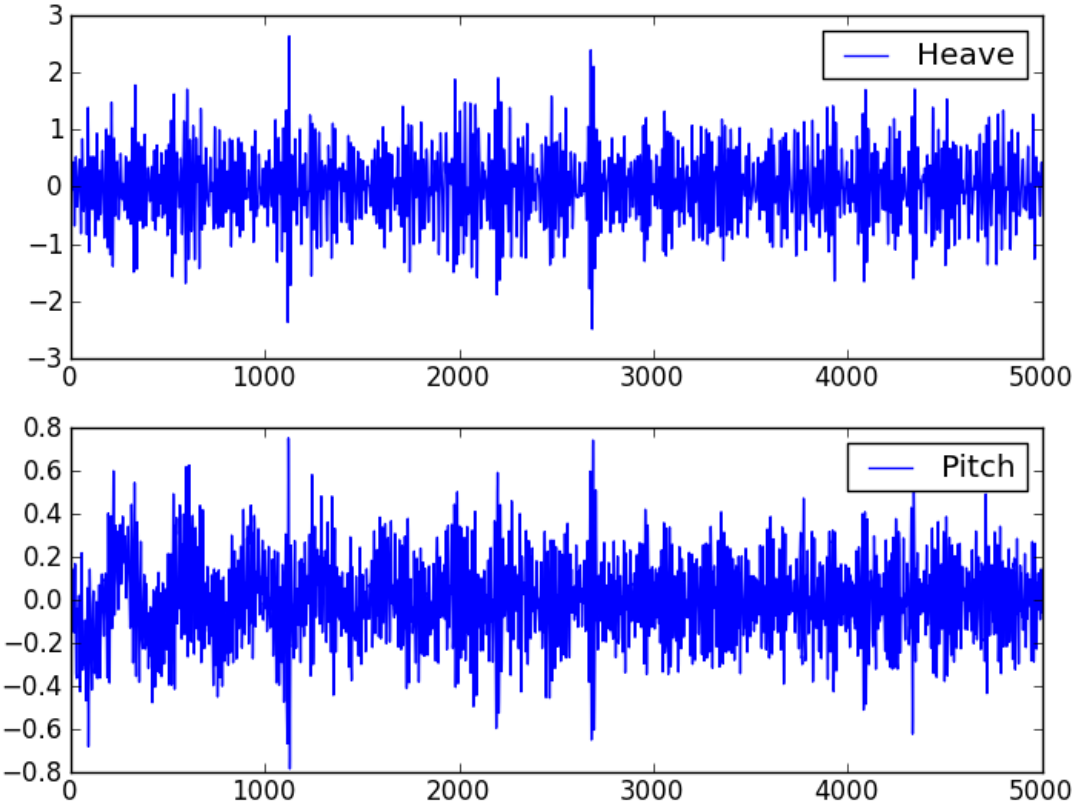

Figure A.38: Waqum analysis of Octabuoy, 100 year sea state number 3, no mooring line restoring added.

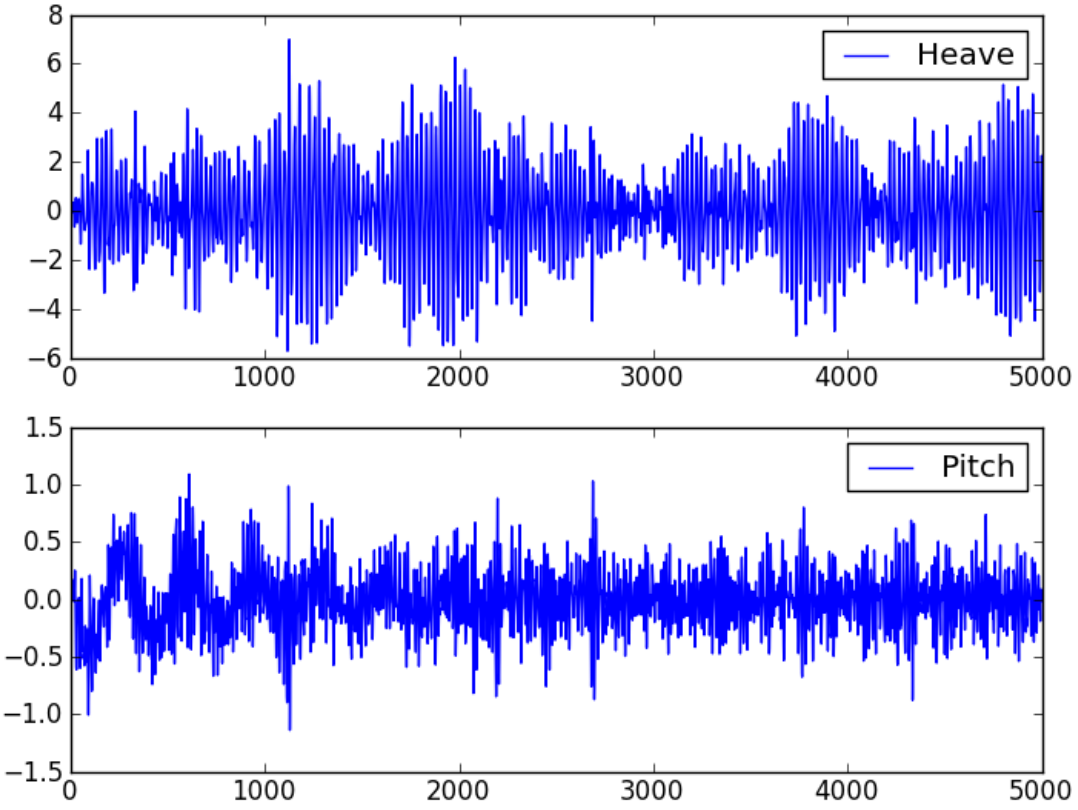

Figure A.39: Waqum analysis of Octabuoy, 1000 year sea state number 1, no mooring line restoring added.

WAQUM RESULTS HEAVE AND PITCH GoM ANCHOR LINE ORCAFLEX				
Analysis	Heave MPL [m]	Heave Standard Deviation	Pitch MPL [deg]	Pitch Standard Deviation
1y1	0.3162	0.4116	0.2860	0.0372
1y2	0.4057	0.0531	0.8149	0.1067
10y1	0.7507	0.0987	0.6213	0.0816
10y2	2.2768	0.3040	1.0999	0.1469
100y1	1.1407	0.1509	1.0353	0.1369
100y2	5.2941	0.7158	1.7572	0.2375
100y3	4.4597	0.6015	8.5507	1.1540
100y4	6.6430	0.8998	5.1206	0.6935
1000y1	14.8874	2.0290	8.6864	1.1839

Table A.2: Results from the Waqum analysis in both heave and pitch.

WAQUM RESULTS HEAVE AND PITCH GoM ANCHOR LINE MODEL TEST				
Analysis	Heave MPL [m]	Heave Standard Deviation	Pitch MPL [deg]	Pitch Standard Deviation
1y1	0.3162	0.4116	0.2742	0.0357
1y2	0.4057	0.0531	0.6276	0.0821
10y1	0.7507	0.0987	0.6473	0.0851
10y2	2.2768	0.3040	0.8793	0.1174
100y1	1.1407	0.1509	0.8441	0.1116
100y2	5.2941	0.7158	2.5063	0.3388
100y3	4.4597	0.6015	4.8667	0.6564
100y4	6.6430	0.8998	nan	nan
1000y1	14.8874	2.0290	nan	nan

Table A.3: Results from the Waqum analysis in both heave and pitch.

A.6 Python Scripts

A.6.1 Python Script Octabuoy in Wasim

```
"""Script to run Octabuoy in Wasim"""
#!/usr/bin/env python
from WasimHandler import WasimJob, WasimJobList # Required for running fourier,
    harmonic2sif etc...
from Rules import *
import sys, time
import numpy
from scipy.stats import norm

#
    ================================================================

#   W A S I M J O B S   B A S E   C A S E S
#
    ================================================================



run_0kn = RuleBasedJob(  linear, speed( 0.0,'kn'), mass(type='pnt',massfile=False)
    )
run_0kn_nl = RuleBasedJob(  nonlinear, speed( 0.0,'kn'), mass(type='pnt',massfile=
    False) )
"""Calculates Tz"""
def tz(tp,gamma):
    return tp*(0.6673+0.05037*gamma-0.006230*gamma**2 + 0.0003341*gamma**3)

periods     = [9.0, 9.8, 10.4, 13.0, 11.4, 15.4, 14.9, 15.8, 17.2]
wave_heights = [4.2, 3.9, 5.6, 10.0, 6.7, 15.8, 15.2, 17.0, 19.8]
titles = ['1 year 1', '1 year 2', '10 year 1', '10 year 2', '100 year 1', '100
    year 2','100 year 3','100 year 4', '1000 year 1']
gamma = 2.2
def generate_irregular():



    for tp,h  in zip(periods,wave_heights):
        job = RuleBasedJob()
        a = {
        'var.wavegen.irregular.PM.Hs'       : h,
        'var.wavegen.irregular.PM.Tz'       : tz(tp,gamma),
        'var.wavegen.irregular.PM.gamma'    : gamma,     # 1.0: PM spectrum    <=7:
            JONSWAP spectrum

         # Frequency spacing ( 1 and 2 are without signal repetition )
        'var.wavegen.irregular.PM.spacing'  : 2,     # 0: Constant  1: Faltinsen
            2: Pastoor

        'var.wavegen.irregular.PM.shift.t'  :  0.0,
        'var.wavegen.irregular.PM.shift.x'  :  0.0,
        'var.wavegen.irregular.PM.shift.y'  :  0.0,
```

```
        'var.wavegen.irregular.PM.nregion'          :  1,
        'var.wavegen.irregular.PM.region(1).nfreq' :  400,
        'var.wavegen.irregular.PM.region(1).Tmin'  :  4.0,
        'var.wavegen.irregular.PM.region(1).Tmax'  :  40,#     ! math expressions
            inside {}

        'var.wavegen.irregular.PM.heading.n'          : 1,
        'var.wavegen.irregular.PM.heading.npowcos'    : 0,#      ! 2, 4, 6, 8, 10,
            ....
        'var.wavegen.irregular.PM.heading.beta_main' : 180.0,
        'var.wavegen.output.format'                     : '3',
        'var.wavegen.output.file.wave'                  : 'Hs%.3f_Tp%.3f_Beta180
            .0.sea'%(h,tp)
        }
        job.update(a)
        job.GenerateWaves()



def run_irregular_sea():

    jobTemplate = {
              'dir.project'       : dir_project,
              'exe.setup'         : os.path.join(dir_exe,'wsetup_20080523.exe'),
              'exe.solve'         : os.path.join(dir_exe,'wsolve_07052008.exe'),
              'exe.mesh'          : os.path.join(dir_exe,'WASIM_MESH.EXE'),
              'exe.dformd'        : os.path.join(dir_exe,'DFORMD.DLL'),
              'import.wasim.inp'  : os.path.join(dir_project,r'input/inp_template/
                  template.inp'),
              'exe.wave_generator': os.path.join(dir_project,r'exe/
                  wave_generator_061215.exe'),
              }


    bases = [run_0kn, run_0kn_nl]


    jobs = WasimJobList()
    for base in bases:
        for tp,h,title  in zip(periods,wave_heights,titles):
            title = title.replace('␣','-')
            job=WasimJob(base,jobTemplate)
            job.delete(['var.wasim.period',
                        'var.wasim.ampltd',
                        'var.wasim.phase'])
            job.update({'var.wasim.iwave_model' : 3,
                        'var.wasim.iwave_file'  : os.path.join(os.getcwd(),'input
                            ','sea','Hs%.3f_Tp%.3f_Beta180.0.sea'%(h,tp)),
                        'var.wasim.nomega'      : 0,
                        'dir.case' : title
                        })
            jobs.append(job)
    jobs.install()
    jobs.enque()

""" test() preforms statistical operations to the time series"""
def test():
```

```
from matplotlib import pyplot as plt
import numpy as np
jobTemplate = {
      'dir.project'        : dir_project,
      'exe.setup'          : os.path.join(dir_exe,'wsetup_20080523.exe'),
      'exe.solve'          : os.path.join(dir_exe,'wsolve_07052008.exe'),
      'exe.mesh'           : os.path.join(dir_exe,'WASIM_MESH.EXE'),
      'exe.dformd'         : os.path.join(dir_exe,'DFORMD.DLL'),
      'import.wasim.inp'   : os.path.join(dir_project,r'input/inp_template/
          template.inp'),
      'exe.wave_generator': os.path.join(dir_project,r'exe/
          wave_generator_061215.exe'),
      }


bases = [run_0kn, run_0kn_nl]


jobs = WasimJobList()
for tp,h,title  in zip(periods,wave_heights,titles):
    print '-'*20
    heaves = []
    pitchs = []
    legends = []
    for base in bases:
        title = title.replace('_','-')
        job=WasimJob(base,jobTemplate)
        job.delete(['var.wasim.period',
                    'var.wasim.ampltd',
                    'var.wasim.phase'])
        job.update({'var.wasim.iwave_model' : 3,
                    'var.wasim.iwave_file'   : os.path.join(os.getcwd(),'input
                        ','sea','Hs%.3f_Tp%.3f_Beta180.0.sea'%(h,tp)),
                    'var.wasim.nomega'       : 0,
                    'dir.case' : title
                    })
        jobs.append(job)
        paths = job.paths()
        mot = paths['file.run.mot']
        t,surge,sway,heave,roll,pitch,yaw,wave = np.loadtxt(mot,skiprows=3,
            unpack=True)
        """Calculates MPL and STD"""
        print title, base['id'], 2*(2*np.std(heave)**2*np.log(10800/tz(tp,
            gamma)))**0.5, 2*(2*np.std(pitch)**2*np.log(10800/tz(tp,gamma)))
            **0.5
        print np.std(heave), np.std(pitch)
        plt.figure()
        plt.hist(heave,100)
        plt.savefig(os.path.join(os.path.split(mot)[0],'Heave.png'))

        plt.figure()
        plt.hist(pitch,100)
        plt.savefig(os.path.join(os.path.split(mot)[0],'Pitch.png'))

        heaves.append(heave)
        legends.append(base['id'].split()[0])
        pitchs.append(pitch)
```

```
"""Makes QQ plots"""
heave1 = heaves[0]
heave2 = heaves[1]

heave1.sort()
heave2.sort()

plt.figure()
plt.plot(heave1, heave2)
plt.xlabel(legends[0])
plt.ylabel(legends[1])
plt.savefig(os.path.join(os.path.split(mot)[0],'QQ_heave.png'))

F_H = numpy.arange(len(heave1), dtype=float) / len(heave1)
heave_norm = norm.ppf(F_H)

plt.figure()
plt.plot(heave_norm, heave1)
plt.plot(heave_norm, heave2)
plt.legend(legends, loc='best')
plt.xlabel('Standard normal')
plt.ylabel('Data')
plt.savefig(os.path.join(os.path.split(mot)[0],'QQ_norm_heave.png'))

pitch1=pitchs[0]
pitch2=pitchs[1]

pitch1.sort()
pitch2.sort()

plt.figure()
plt.plot(pitch1, pitch2)
plt.xlabel(legends[0])
plt.ylabel(legends[1])
plt.savefig(os.path.join(os.path.split(mot)[0],'QQ_pitch.png'))

F_P = numpy.arange(len(pitch1), dtype=float) / len(pitch1)
pitch_norm = norm.ppf(F_P)

plt.figure()
plt.plot(pitch_norm, pitch1)
plt.plot(pitch_norm, pitch2)
plt.legend(legends, loc='best')
plt.xlabel('Standard normal')
plt.ylabel('Data')
plt.savefig(os.path.join(os.path.split(mot)[0],'QQ_norm_pitch.png'))

plt.figure()
plt.plot(pitch_norm, pitch1)
plt.xlabel('Standard normal')
plt.ylabel('Data')
plt.savefig(os.path.join(os.path.split(mot)[0],'QQ_norm_pitch1.png'))
plt.figure()
plt.plot(pitch_norm, pitch2)
plt.xlabel('Standard normal')
plt.ylabel('Data')
```

```
        plt.savefig(os.path.join(os.path.split(mot)[0],'QQ_norm_pitch2.png'))

    for job in jobs:
        job.trend()


#
# ============================================================================


def main():
    tasks = sys.argv[1:]
    out = open('task.log','a')
    for task in tasks:
        if not '(' in task: task+='()'
        date = time.ctime()
        exec task
        out.write('%s # %s # %s\n' % (date, task, __file__))
    out.close()
    logScript(tasks,__file__)

if __name__ == "__main__":
    main()
```

A.6.2 Python Script Octabuoy in Waqum

```
""" Script for analysing the Octabuoy in Waqum"""

 """ Importing different functions needed"""
from __future__ import division
from tictoc import tic, toc
import numpy, os
from math import pi
from filelib.waqum_db import open_run_file
from Waqum import Input, Analysis
import matplotlib.pyplot as plt
import matplotlib

#########################################################
# Open run file (WDB or Wadam SIF)

"""Function "Tic-Toc" measures time used for analysis"""
tic('Read_SIF_file')
""" Reads .SIF file with hydro coefficients"""
f = open_run_file('G1.SIF', helper_file='WADAM1.LIS')
f.read_data()
run = f.runs[-1]
toc()

"""Add critical damping"""
coeff = run.add_coefficients('viscous-damping-fraction-of-critical')
coeff.critical_damping_matrix[2,2] = 0.015
coeff.critical_damping_matrix[4,4] = 0.02

"""Defines coefficients"""
displacement = run.geometry.displacement
water_plane_area = run.geometry.water_plane_area
zb = run.geometry.center_of_bouyancy[2]
zg = run.center_of_gravity[2]
rho = run.rho
g = run.g

#########################################################
# Define Input
"""Defines wave heading"""
input = Input()
input.heading = 180

#input.wave_spectrum = 'JONSWAP'
#input.wave_spectrum_parameters = {'periods': [22.5], 'amplitudes': [6], 'gamma
    ':[2]}
""" Defines duration and timestep"""
input.wave_spectrum_seed = 42
input.dt = 0.1
input.ramp_time = 30
input.transient = 30
input.tmax = 10800

input.dw = 100 # ????
input.verbose = False
input.log = 'mylog.txt'
```

```
"""Chooses solver, here Runge Kutta 4"""
input.solver_method = 'Runge-Kutta 4'
input.initial_position = numpy.zeros((6,), float)

#########################################################
# Define Force
"""Non linear damping added"""
class NonLinearDamping(object):
    def __init__(self, B):
        self.B = B

    def set_system(self, system):
        self.system = system
""" Example of added non linear damping, unfortunately not finished in the master
    thesis"""
    def excitation(self, t, vel, pos):
        forces = numpy.zeros(6, float)
        forces[2] = - vel[2]**2 * self.B
        return forces*0

"""Mooring line restoring added"""
class Mooring(object):

    def set_system(self, system):
        self.system = system

    def excitation(self, t, vel, pos):
        forces = numpy.zeros(6, float)
        forces[0] = -(-0.0029*pos[0]**6 + 0.4995*pos[0]**5 - 33.281*pos[0]**4 +
            1084.1*pos[0]**3 - 17752*pos[0]**2 + 138714*pos[0])
        forces[1] = -(-0.0029*pos[1]**6 + 0.4995*pos[1]**5 - 33.281*pos[1]**4 +
            1084.1*pos[1]**3 - 17752*pos[1]**2 + 138714*pos[1])
        return forces

""" Run Analysis """
"""Defines decay analysis"""
def decay():
    """ Need to insert a spectrum, otherwise default spectrum is applied"""
    input.wave_spectrum = 'PM'
    input.wave_spectrum_parameters = {'Hs': 0.0, 'Tz': 22.5}
    working_dir = 'Decay-'
    cwd = os.getcwd()
    """Choosing which DOF(s) to preform decay for"""
    for dof in [4]:
        print 'Solving for DOF',dof
        if not os.path.isdir(os.path.join(cwd,working_dir+'%d'%dof)):
            os.makedirs(os.path.join(cwd,working_dir+'%d'%dof))
        os.chdir(os.path.join(cwd,working_dir+'%d'%dof))
        input.initial_position[dof] = 5*numpy.pi/180
        plt.figure()
        """adding damping to the motion control springs"""
        for damp in (0.05,0.05):
            analysis = Analysis(input, run)
            analysis.setup()
            system = analysis.system

            """Adds non linear damping"""
```

```
            nl_excitation = NonLinearDamping(0)
            system.add_excitation(nl_excitation)

            """Adds non linear restoring"""
            nl_restoring = NonLinearRestoring()
            system.add_excitation(nl_restoring)

            """ Mooring lines taken into account"""
            mooring=Mooring()
            system.add_excitation(mooring)
            """ Motion control springs, not used when mooring lines are added"""
            system.add_spring(dof=0, spring_period=320, damping_ratio=damp)
            system.add_spring(dof=1, spring_period=320, damping_ratio=damp)
            system.add_spring(dof=5, spring_period=320, damping_ratio=damp)


            tic('Run analysis')
            analysis.simulate()

            """FFT analysis, generates power spectrum distribution"""
            pxx,freqs = matplotlib.mlab.psd(system.pos_hist[:,dof],Fs=10,NFFT
                =2**20)

            """Plotting FFT results"""
            max_pxx = -1e10
            max_freq = 0
            for _pxx, freq in zip(pxx,freqs):
                if _pxx > max_pxx:
                    max_pxx = _pxx
                    max_freq = freq
            print 'Decay dof', dof, max_freq, 1/max_freq
            plt.plot(freqs, pxx, label='Damping %.2f'%damp)
            toc()
            last_pxx=0
            eps=1e-11
            x=[]
            for f,p in zip(freqs,pxx):
                if (p>eps and last_pxx<eps) or (p<eps and last_pxx>eps):
                    x.append(f)
                last_pxx=p

#             plt.axis([x[0], x[-1], 0, max_pxx*1.05])
#             plt.savefig('fft of dofnr%d.png'%dof)
        plt.legend()
    plt.show()

""" Run Analysis"""
"""Defines JONSWAP analysis"""
def jonswap(wave_period, significant_waveheight, gamma):
    working_dir = os.path.join('HS-%.2f'%significant_waveheight,'Period-%.2f'%
        wave_period)
    cwd = os.getcwd()
    if not os.path.isdir(working_dir):
        os.makedirs(working_dir)
    os.chdir(os.path.join(cwd,working_dir))
    input.wave_spectrum = 'JONSWAP'
```

```
    input.wave_spectrum_parameters = {'Hs': significant_waveheight, 'gamma': gamma
        , 'Tp': wave_period}

    analysis = Analysis(input, run)
    analysis.setup()
    system = analysis.system

    """Adds non linear damping"""
    nl_excitation = NonLinearDamping(0)
    system.add_excitation(nl_excitation)
    """Adds non linear restoring"""
    nl_restoring = NonLinearRestoring()
    system.add_excitation(nl_restoring)
    """ Mooring lines taken into account"""
    mooring=Mooring()
    system.add_excitation(mooring)
    """Adds motion control springs, not used when mooring lines are added"""
    system.add_spring(dof=0, spring_period=320, damping_ratio=0.05)
    system.add_spring(dof=1, spring_period=320, damping_ratio=0.05)
    system.add_spring(dof=5, spring_period=320, damping_ratio=0.05)
#
    tic('Run_analysis')
    analysis.simulate()
    toc()


    plot_force = []

    """ Plots results"""
    plt.figure()
    plt.subplot(2,1,1)
    plt.plot(analysis.t, system.pos_hist[:,2], label='Heave')
    plt.legend()

    plt.subplot(2,1,2)
    plt.plot(analysis.t, system.pos_hist[:,4]*180/pi, label='Pitch')
    plt.legend()

    gamma=2.2
    heave=(system.pos_hist[:,2])
    pitch=(system.pos_hist[:,4])
    """Calculates Tz"""
    tz = wave_period*(0.6673+0.05037*gamma-0.006230*gamma**2 + 0.0003341*gamma**3)
    """Calculates MPL and Standard Deviation"""
    print 2*(2*numpy.std(heave)**2*numpy.log(10800/tz))**0.5, 2*(2*numpy.std(pitch
        *(180/numpy.pi))**2*numpy.log(10800/tz))**0.5
    print numpy.std(heave), numpy.std(pitch*(180/numpy.pi))


    os.chdir(cwd)
"""Prints different features of the analysis for control"""
def info():
    print 'g', g
    print 'rho', rho
    print 'displacement', displacement
    print 'water_plane_area', water_plane_area
    print 'zb', zb
```

```
    print 'zg', zg

info()
"""Runs the above defined analyses with different inputs"""
#decay()
periods = [9.0, 9.8, 10.4, 13.0, 11.4, 15.4, 14.9, 15.8, 17.2]
HS = [4.2, 3.9, 5.9, 10.0, 6.7, 15.8, 15.2, 17.0, 19.8]
gamma =[2.2]
for wave_period,significant_waveheight in zip(periods, HS):
    print '-'*20
    jonswap(wave_period,significant_waveheight,gamma)
plt.show()
```

A.6.3 Python Script LSQ

```
""" Least Square Solver"""

 """ Importing different functions needed"""
from __future__ import division
from numpy import zeros, cos, sin, complex, array, asarray, reshape
""" Importing least square solver from numpy"""
from numpy.linalg import lstsq
from math import pi
import numpy as np


""" Defining constants"""
omega = 2*pi/22.6
phase = 0
ampl = 6
rho = 1025
g=9.81
r=18.75



 """Shifts between which signal to apply the LSQ to."""
# Read signal
t, signal = np.loadtxt('total_6.txt', unpack=True)
#t, signal = np.loadtxt('pressure_6.txt', unpack=True)
#t, signal = np.loadtxt('visc_data_4m.txt', unpack=True)

""" Filter, removes the first 30 seconds to ensure a stabilized signal"""
sieve = t > 30
t2 = t[sieve]
signal2 = signal[sieve]

"""Makes Matrix with four columns, 1. const, 2. velocity, 3. acceleration"""
N = len(t2)
Mx = zeros((N, 4), float)

""" Heave displacement """
etta_3=-ampl*cos(omega*t2 + phase)
""" Water plane area """
Aw =pi*r**2

""" Restoring force"""
res =rho*g*Aw*etta_3
""" Removing the restoring signal, keeping only damping and mass terms"""
signal3=signal2+res
""" Defining speed"""
v = ampl*omega*sin(omega*t2 + phase)
""" Defining acceleration"""
a = ampl*omega**2*cos(omega*t2 + phase)

Mx[:,0] = 1
Mx[:,1] = v
#Mx[:,2] = v*np.abs(v)
Mx[:,2] = a
#Mx[:,4] = a*np.abs(a)
```

```
"""Perform least square fit. Return the least-squares solution to a linear matrix
    equation."""
(p, residuals, rank, s) = lstsq(Mx, signal3)

print p

# Best fit signal
const = p[0]
res = np.dot(Mx, p)


 """ Plotting the results"""
import matplotlib.pyplot as plt
plt.plot(t, signal, 'k', lw=2, label='Original')
plt.plot(t2, res, label='Best fit')
for i in range(4):
    plt.plot(t2, Mx[:,i]*p[i], label='Column %d' % i)
plt.plot(t2,p[1]*v+p[2]*a,label='Refit')
print p[1], p[2], p[3]
plt.legend()
plt.show()
```